

**Dottorato di Ricerca in
Biologia Cellulare, Molecolare e Industriale
Progetto n. 2: Biologia Funzionale dei Sistemi Cellulari e Molecolari**

Ciclo XXIV

**Settore Concorsuale di afferenza: 05/I1
Settore Scientifico disciplinare: BIO19**

**GENETIC ENGINEERING AND PRECLINICAL
EVALUATION OF ONCOLYTIC
HERPES SIMPLEX VIRUSES RETARGETED
TO CANCER-SPECIFIC RECEPTORS**

Presentata da: Dott.ssa VALENTINA GATTA

Coordinatore del Dottorato:

**Chiar.mo Prof
VINCENZO SCARLATO**

Relatore:

**Chiar.ma Prof.ssa
GABRIELLA CAMPADELLI-FIUME**

Table of contents

1. INTRODUCTION	4
1.1 THROUGH THE AGES OF HERPES SIMPLEX VIRUS	4
1.2 HERPESVIRIDAE FAMILY AND ITS CLASSIFICATION	5
1.3 EPIDEMIOLOGY OF HSV INFECTION	6
1.4 HERPES SIMPLEX VIRUS 1	8
1.4.1 <i>Virion Structure overview</i>	8
1.4.2 <i>HSV-1 genome organization</i>	9
1.4.3 <i>Functional organization of HSV genome</i>	10
1.4.4 <i>Overview of viral replication</i>	11
1.4.5 <i>Latency</i>	12
1.4.6 <i>Entry</i>	13
1.5 GLYCOPROTEINS OF HSV-1 INVOLVED IN ATTACHMENT AND ENTRY	14
1.5.1 <i>Glycoprotein C</i>	14
1.5.2 <i>Glycoprotein D</i>	15
1.5.3 <i>Glycoprotein B</i>	18
1.5.4 <i>gH/gL complex</i>	19
1.6 GLYCOPROTEIN D RECEPTORS	21
1.6.1 <i>Nectins</i>	21
1.6.2 <i>HVEM</i>	22
1.6.3 <i>3-O-sulfated Heparan sulfate</i>	23
1.7 VIRUSES AS ONCOLYTIC AGENTS	24
1.7.1 <i>Virus retargeting</i>	24
1.7.2 <i>Arming viruses</i>	25
1.7.3 <i>Shielding viruses</i>	26
1.8 ONCOLYTIC HSV	27
1.9 TUMOR SPECIFIC RECEPTORS	33
1.9.1 <i>HER2 receptor</i>	33
1.9.2 <i>PSMA receptor</i>	36
1.9.3 <i>EGFRvIII receptor</i>	38
2. OBJECTIVE	40
3. MATERIAL AND METHODS	41
3.1 CELLS	41
3.2 CONSTRUCTION OF CELL LINES EXPRESSING HETEROLOGOUS RECEPTORS	42
3.3 PLASMIDS	42
3.4 VIRUSES	43
3.5 RECONSTITUTION OF VIRAL PROGENY FROM BAC-DNA AND VIRUS CULTIVATION	50
3.6 VIRAL YIELD ASSAY	51
3.7 INFECTION ASSAY	51
3.8 INHIBITION OF VIRUS INFECTION	51
3.9 IN VITRO CYTOTOXICITY	52
3.9.1 <i>Erythrosin B assay</i>	52
3.9.2 <i>Alamar Blue Assay</i>	52
3.10 IN VIVO EXPERIMENTS	52
3.10.1 <i>Tumor growth</i>	52
3.10.2 <i>In vivo infection</i>	53
3.10.3 <i>Antitumor activity</i>	53
3.10.4 <i>Statistical analysis</i>	53
4. RESULTS	54
4.1 R-LM249	54
4.2 R-LM113	64

4.3	R-LM291	74
4.4	O-HSV RETARGETED TO ADDITIONAL TUMOR SPECIFIC RECEPTORS (PSMA AND EGFRVIII).....	80
5.	DISCUSSION	88
5.1	GENERAL CONSIDERATIONS AND PERSPECTIVES	91
6.	BIBLIOGRAPHY.....	94

1. Introduction

1.1 *Through the ages of herpes simplex virus.*

The first descriptions of lesions that resembled those caused by herpes simplex virus (HSV), have been found on a Sumarian Tablet (third millennium BC) and on the Ebers Papyrus (1500 BC). Nevertheless, the first time we came across knowledge of HSV was with the ancient Greeks, where lesions that seemed to creep and crawl along the skin were described by Hippocrates with the term “herpes” (1). Through the centuries, investigators have described this pathological skin condition with a variety of terms and meanings up to the 17th and 18th centuries when a more rigorous definition of herpes emerged. Bateman described a recurrent HSV infection as “*a restricted group of localized vesicles with a short, self-limited course*” (see (1) refs therein). The research has progressed from the simple classification of lesions to a description of disease, epidemiology of infection and nowadays to the molecular characterization of the virus. For many years, the virus was considered to be a troublesome childhood disease and an affliction of a few unfortunate individuals. The experimentation and recognition of the aetiological agents started between the 19th and 20th centuries.

In the first half of the 20s, Gruter conducted several animal experiments that confirmed the infectious nature of HSV, showing how the virus could be transmitted serially from rabbit to rabbit. It is to him that the virology community attributes the merit for the isolation of HSV.

It is noteworthy that in the 1930s Andrews and Carmicheal laid the foundation of HSV biology by observing that only adults carrying neutralizing antibodies were affected by recurrent infections.

In the first part of the 50s, there was a big development in herpesvirology with the advent of culture protocols allowing isolation of other members of the human herpesvirus family. During the 1970s, genital herpes was recognized as a serious sexually transmitted infection that could threaten the life of a fetus if the virus was contracted shortly before or at delivery. The public took into account the problem when newspaper articles were written on the subject, with sexual freedom and increase in incidence of sexually transmitted disease. The awareness grew even more with the advent of the first cases of HIV.

The first antiviral therapy developed at the end of the 70s was vidarabine, that reduced the fatality of HSV encephalitis, but the real therapeutic advance was the discovery of acyclovir and the demonstration of its mechanism of action by Dr Gertrude Elion (1), who was awarded Nobel Prize in Physiology and Medicine in 1988.

The vaccines against herpesvirus have been of great interest since the early 20th century but their history has been uncertain. Two vaccines have been evaluated for prophylaxis and therapy, both based on viral glycoproteins and an adjuvant. They gave difficult to interpret results e.g. decrease of the incidence of HSV-2 infection in women but not in men, so their efficacy has still to be proven.

The beginning of modern research on HSV can be placed between the 1960s and 1970s. During this period the size and complexity of the structure of HSV DNA were discovered, as well as the large number of proteins that make up HSV particles. This could be called the golden age of

research on HSV where a great amount of information on the function of viral genes and virus-cell interactions was collected.

In the last twenty years research focused on the therapeutic potential of HSV besides its pathogenic properties. HSV has been taken into account as a promising viral vector to be used in immunoprophylaxis and gene therapy. In particular, there are two potential therapeutic uses for HSV: 1) delivery of missing, damaged or modified genes to the CNS and 2) engineering of the virus to destroy cancer cells. The latter is the topic of my PhD thesis.

1.2 *Herpesviridae* family and its classification

A common feature of the family *Herpesviridae* is the architecture of the virion. A typical herpes virion is composed of: a core containing linear double-stranded DNA, a 100-110nm diameter icosahedral capsid, an amorphous and asymmetrical tegument around the capsid, and the exterior lipid envelope with surface glycoprotein spikes (2, 3).

The herpesviruses are highly widespread in nature and several animal species are the natural host of at least one herpesvirus. Nine herpesviruses have been isolated from humans and they are listed in the table below (Table 1.1).

Table 1.1 - Viruses belonging to the human *Herpesviridae* family (4).

Designation	Vernacular name	Subfamily	Genome Size (bp)	Abbreviation
<i>Human herpesvirus 1</i>	Herpes simplex virus 1	α	152	HHV-1 (HSV-1)
<i>Human herpesvirus 2</i>	Herpes simplex virus 2	α	152	HHV-2 (HSV-2)
<i>Human herpesvirus 3</i>	Varicella-zoster virus	α	125	HHV-3 (VZV)
<i>Human herpesvirus 4</i>	Epstein-Barr virus	γ	172	HHV-4 (EBV)
<i>Human herpesvirus 5</i>	Cytomegalovirus	β	229	HHV-5 (HCMV)
<i>Human herpesvirus 6A</i>		β	162	HHV-6A
<i>Human herpesvirus 6B</i>		β	162	HHV-6B
<i>Human herpesvirus 7</i>		β	153	HHV-7
<i>Human herpesvirus 8</i>	Kaposi's sarcoma associated virus	γ	230	HHV-8 (KSHV)

The known herpesviruses share four basic biological traits:

- i) Production of a large amount of enzymes engaged in nucleic acid metabolism (e.g.

thymidine kinase, thymidylate synthetase, dUTPase), DNA synthesis and possibly, processing of proteins.

- ii) Synthesis of viral DNA and assembly of capsids in the nucleus.
- iii) Generation of infectious viral progeny associated with the lysis of the infected cell.
- iv) Latency in the natural hosts with expression of only a small subset of viral genes.

There are three subfamilies of the Herpesviridae family classified by the Herpesvirus Study Group of the International Committee on the Taxonomy of Viruses (ICTV) on the basis of biological features.

Alphaherpesvirinae: viruses in this subfamily share efficient destruction of infected cells in a wide variety of hosts, rapid spread in culture, short reproductive cycle, and the ability to start a latent state infection primarily but not only in sensory ganglia. In this subfamily are the genera Simplex viruses HSV-1, HSV-2, Varicellovirus (VZV, pseudorabies virus and equine herpesvirus 1), circopithecine hepersvirus 2, and bovine mammillitis virus.

Betaherpesvirinae: the majority of its members has a restricted host range. The reproductive cycle takes a long time, a growth in culture is slow and the nuclei of infected cells become larger (cytomegalia). The virus establishes latency in several cells type like secretory glands, lymphoreticular cells, kidneys and other tissues. The genera *Cytomegalovirus* (HCMV) and *Muromegalovirus* (murine cytomegalovirus) belong to this subfamily.

Gammaherpesvirinae: all members replicate in lymphoblastoid cells, and some cause lytic infections in some types of epithelioid and fibroblastic cells. These viruses are specific for either T or B lymphocytes and establish latent infections in lymphoid tissue. The Gammaherpesvirinae family contains two genera, Lymphocryptovirus (e.g. EBV) and Rhadinovirus (4). This thesis will focus on HSV-1.

1.3 Epidemiology of HSV infection

HSV replicates in many cellular types, including neurons where it carries out a lytic cycle and is capable of aggressive spread and tissue destruction. The initial HSV infection requires contact between the virus and mucosal surfaces or abraded skin. The two viral serotypes (type 1 or 2) are transported in a retrograde manner along the axons of neurons that innervate the portal of entry to the cell body's nuclei in sensory ganglia. In the nuclei they ultimately establish a latent infection characterized by persistence of viral DNA in the absence of viral protein synthesis. Viral replication occurs in a small number of neurons; the viral genome then remains in a latent state for the life of the host. In a large fraction of individuals carrying latent HSV, various stimuli (damage to nerve endings, hormonal imbalances or emotional stress) result in re-activation of virus replication (5). The virus is then transported in an anterograde flow to mucosal membranes at or near the portal of entry into the body, and visible sores become active for transmission to uninfected individuals (Fig. 1.1).

The host immune system condition influences the type of HSV infection. Seronegative individuals contract primary infection at their first exposure to HSV-1 (*facial*) or HSV-2 (*genital*). This is different from an "initial infection" where a person with antibodies against HSV-1 contracts HSV-2 or vice versa. The clinical manifestations caused by the two serotypes are similar although they are usually transmitted by different routes and localize at different areas

of the body. These viruses have worldwide distribution with different impacts depending on the socio-economic situation of the individuals concerned, no seasonal changes and naturally infect only humans. HSV infection is seldom fatal, except for newborns, particularly in the pre-acyclovir era.

The incubation period of HSV-1 or HSV-2 is about 4 days and ranges from 2 to 12 days.

The diagnostic assessment is based on virus isolation in cell culture and PCR detection of viral DNA. Symptomatic oropharyngeal disease by HSV-1 is characterized by sores of the buccal and gingival mucosa (lasting 2-3 weeks) and by fever between 38 to 40°C. Intraoral ulceration lesions indicate primary infection whereas lip lesions suggest recurrent infection.

Primary genital herpes by HSV-2 appears as macules and papules, followed by vesicles, pustules and ulcers. During pregnancy the infection is rarely transmitted to the fetus (5% in utero), in fact the most transmissions occur during vaginal delivery (80%) or after birth. The infected babies frequently die owing to encephalitis and disseminated infection. To prevent mother-to-baby transmission, caesarian section is applied.

Complications in men are rare; aseptic meningitis and urinary retention are more common in women. Non primary initial genital infection cause milder symptoms than primary infection (fewer lesions, less pain and less like hood of complications).

Immunocompromised patients are at increased risk of severe HSV infection, they can develop progressive disease involving respiratory tract, esophagus or gastrointestinal tract (5, 6). The cure for initial or recurrent HSV infection is the topical, oral or intravenous administration of acyclovir, a purine-nucleoside analogue prodrug. It is activated by viral thymidine kinase and when it is incorporated into viral DNA, it acts as a chain terminator. This treatment keeps symptoms under control symptoms and has been successfully employed to treat other HSV infection such as encephalitis, hepatitis, pulmonary infection, proctitis or eye infection (6).

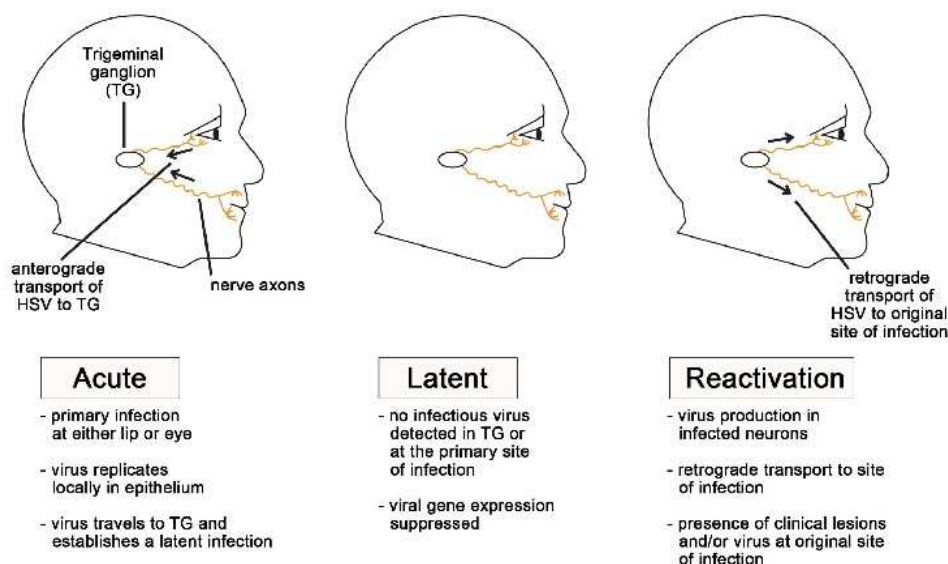


Figure 1.1 - Progression of HSV-1 infection *in vivo*. HSV-1 primary infection occurs in the mucosa of the lips or eye. Here, virus replicates actively in cells and enters in the sensory neurons near the portal of entry. The virus then is transported to the nerve cell bodies in the trigeminal ganglia. During latent phase the viral gene expression is turned off in ganglia, except for LAT gene. Periodically, various stimuli cause virus reactivation. In this phase virions travel in anterograde manner through the axons of neurons toward the primary site of infection (7).

1.4 *Herpes simplex virus 1*

The first human herpes virus discovered was HSV-1 and it is considered the prototype virus in the family, and is still one of the most investigated herpes viruses (8). The biological properties which make it an interesting research subject are that a) it remains latent in the human host for life, b) it reactivates causing lesions and c) it causes several infections. This virus is used as tool and model to study translocation of proteins, synaptic connections in the nervous system, membrane structure, gene regulation, gene therapy, cancer therapy and many other biological problems (9).

1.4.1 **Virion Structure overview**

As mentioned earlier in the text the HSV virion consists of four elements (6, 9): a core, an icosadeltahedral capsid surrounding the core, a tegument surrounding the capsid, and an envelope.

A study conducted with cryo-electron tomography on HSV-1 described the virion structure in great detail (Fig 1.2) (10). The virion consist of a pleiomorphic membrane-bound particle. It is generally spheric in shape, although some moved away from sphericity which appears to be a genuine feature. The bilayer membrane was seen as a continuous smoothly curved surface (5 nm thick). Its diameter ranges from 170 to 200 nm, averaging 186 nm and an array of spikes protrude from each virion, making the full diameter on average, ~ 200 nm.

The core contains densely coiled and complex DNA, with spermidine and spermine proteins that neutralize the DNA's negative charges, conferring a toroidal shape (9).

The capsid consists of 162 capsomers arranged in a T=16 icosahedral symmetry and an intermediate layer organized in a T=4 lattice. The outer and the intermediate layers are organized so that channels along their icosahedral twofold axes coincide, forming a direct pathway and potential channel between the DNA layer and the exterior of the virion (11). The non-central location of the capsid inside the virion allows for proximal pole identification where the capsid is near the envelope and distal pole where it is not.. The tegument occupies about two-thirds of the volume enclosed within the membrane and at 7 nm of resolution it appears to consist of a reticulum of particulate density. Some tegument components appear polymeric; some cellular filaments resembling actin were incorporated (10).

The process which HSV acquires its lipid envelope has given rise to disputes. Some studies suggested that virion lipids are similar to those of cytoplasmic membranes and different from those of nuclear membranes of uninfected cells (12). The envelope acquisition and the subsequent viral egress have been proposed to follow different mechanisms (9):

- a) single nuclear envelopment model: the capsids are enveloped at the inner nuclear membrane and exit the perinuclear space by means of perinuclear vesicles which bud from the outer nuclear membrane. Vesicles are transported, interact with Golgi apparatus and virions are then released to the plasma membrane.
- b) the dual envelopment pathway (de-envelopment-re-envelopment pathway): capsids

acquire a primary envelope at the inner nuclear membrane and lose it through fusion with the outer nuclear membrane. The capsid is then released into the cytoplasm. The de-enveloped capsids acquire tegument in the cytoplasm and undergo a secondary envelopment at other membranes in the cytoplasm including Golgi stacks and multivesicular bodies;

- c) single cytoplasmatic envelopment: capsids exit from nucleus through enlarged nuclear pores. They acquire the envelope budding into cytoplasmic vesicles and are transported to the plasma membrane.

At present, the single cytoplasmatic envelopment (c) is the most popular model of HSV maturation and exit.

The envelope surface contains numerous spikes. The spikes arrangement is not random, they usually are few and scattered at the proximal pole and densely packed around the distal pole. This distribution could reflect functional associations such as local clustering of glycoproteins destined to serially make contact with different receptors during cell entry (13). At least 15 different viral transmembrane proteins have been identified in HSV-1 particles (14).

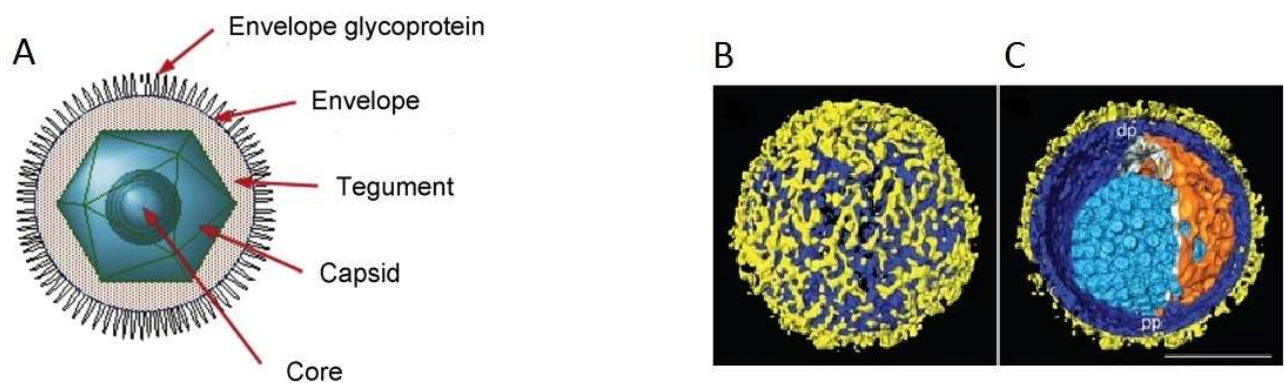


Figure 1.2 - Structure of a HSV1 virion A) A HSV-1 virion has a diameter of about 200 nm. The viral particle consists of an icosahedral capsid, which contains the viral DNA with a genome of 152 kbp. Around the capsid, there is an amorphous tegument, which contains viral structural and regulatory proteins and is surrounded by an external envelope containing glycoproteins (8). **B-C Virion segmented surface rendering tomogram.** B) Virion outer surface with glycoproteins (yellow) protruding from the membrane (blue). C) Virion section. The capsid (light blue), the tegument (orange) and the envelope (blue and yellow). Scale bar, 100 nm. (10).

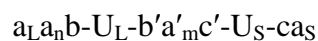
1.4.2 HSV-1 genome organization

The HSV-1 genome contained in the virion core consists of linear, double stranded DNA wrapped as a toroid or spool (15). *In vivo*, the HSV-1 genome has been found to exist in at least three different states: linear, circular, and concatemeric. In the virion, genomes are linear, but within hours after infection, end joining has been found to occur, resulting in “endless genomes” that have been interpreted to represent circles (15, 16). Thus, genome circularization has been

thought to be a prerequisite for viral DNA replication, although there is no direct proof for circular replication intermediates. Some experimental results evidence that genome circularization is not a characteristic of a productive infection but instead may take place during the establishment of latency (17).

The entire HSV-1 genome consists of 152,000 bp, with a G+C content of 68%. These numbers include only single copies of the *a* sequence at the ends of the L component and do not take into account their variation in size (200 to 500 bp each) and number.

The HSV-1 genome consists of two unique sequences covalently joined, referred to as U_L (long) and U_S (short); each region is flanked by inverted repeats: the repeats of the L component are designated *ab* and *b'a'*, whereas those of the S component are *a'c'* and *ca*. The number of *a* sequence repeats at the L-S junction and at the L terminus is variable and their sequences are highly conserved. The HSV genome can then be represented as follows:



where *a_L* and *a_S* contain direct repeats (18). In the viral genome three origins of replication are present: *ori_L* located in U_L, and two copies of *ori_S* located in the flanking region of U_S. Furthermore, the HSV-1 genome undergoes inversions that result from recombination events mediated by the viral DNA replication machinery. These events generate four genomic isomers with L and S sequences inverted relative to one another (prototype) in equimolar amounts (9, 17).

Herpes simplex virus DNA contains about 90 unique transcriptional units, at least 84 encode proteins, several stable non coding RNAs and miRNAs (19). Each viral transcript encodes a single protein except for the single transcript of ORF P that also serves as the template for the ORF O protein; U_L26 which encodes for a transcript cleaved into two proteins, and the mRNA of U_L3 which contains the ORF of U_L1,2 and 3. Many clusters of transcriptional units are 3' co-terminal (arranged either head-to head, head-to-tail, or tail-to-tail), several examples exist of transcriptional units wholly embedded in the coding sequence contained in the larger transcript, some of the expressed ORFs are antisense to each other and several transcripts appear not to encode proteins. Those best known are the latency associated transcripts (LAT)(9).

1.4.3 Functional organization of HSV genome

HSV-1 genes fall into at least three kinetic classes, expressed sequentially in a coordinated fashion: α or immediate early; β or early and γ or late. The α genes map near the termini of the L and S components and are expressed very soon after infection, approximately from 2 to 4 hours post infection. The expression of α genes does not require prior protein synthesis. The viral tegument protein VP16 promotes their transcription interacting in the nucleus with host cell octamer binding protein 1 (Oct1) and host cell factor (HCF1) at the G_nTAATGAR_nTTC response element in the promoters of α genes. Moreover the transcription initiation of α genes requires the demethylation of histones by lysine specific demethylase 1 (LSD1) that belongs to the dynamic repressor complex CoREST/REST. The protein is recruited by the VP16/Oct1/HCF1 complex

(20). The α genes encode six proteins designated as infected cell protein (ICP) ICP0, ICP4, ICP22, ICP27, ICP47 and U_S1.5. Their task is to silence the cellular machinery by inhibiting transcription, immune response e.g. block of interferon pathway, RNA splicing, RNA transport out of the nucleus and protein synthesis. Some of them also act by promoting the transcription of β and γ genes. This process facilitates the transition from cellular to viral gene expression. With few exceptions β and γ genes are distributed in the unique sequences of both the L and S components. The exceptions are the ICP34.5 and ORF P genes located in the repeated sequences flanking the L component. The expression of the β genes takes place from 4 to 8 hours post infection and requires at least the presence of functional ICP4. This protein acts as a repressor and as a transactivator involved in replication of the viral DNA and nucleotide metabolism. The β genes are U_L30, U_L42, U_L29, U_L9, U_L5, U_L8 and U_L52. Among β genes, two subgroups have been identified: β 1 genes are expressed within a short time after, or concomitantly with ICP8 (U_L29 single strand binding protein) and ICP6 (U_L39 the large subunit of ribonucleotide reductase) protein synthesis. The β 2 genes are expressed later after α protein synthesis. When the β proteins are expressed, most of them localize into the nucleus and assemble onto the parental viral DNA molecules in structures called *prereplicative sites* located near ND10 structures. These structures attract a variety of histones, histone-modifying enzymes, coactivators and corepressors. The ND10 bodies are dynamic structures consisting of a large number of proteins (20).

The γ genes expression occurs after the onset of viral DNA synthesis. They are subgrouped into γ 1 and γ 2 genes. Neither β 2 nor γ 1 genes require viral DNA synthesis for their expression. They differ because inhibitors of DNA synthesis reduce γ 1 but not β 2 gene expression. The products include structural proteins of mature virions and tegument components required to prepare newly infected cells for an efficient infection. γ 1 genes (ICP5, glycoproteins gB, gD and ICP34.5) are expressed early in infection and are stimulated by viral DNA synthesis whereas the γ 2 genes are expressed late in infection and are not expressed in the presence of effective concentrations of viral DNA synthesis inhibitors.

1.4.4 Overview of viral replication

HSV can follow two alternative pathways to enter cells. One is binding to cell membrane receptors, followed by fusion at the plasma membrane, the other involves endocytosis of the enveloped capsid and receptor-dependent fusion of the enveloped virus with the membranes of the endocytic vesicle (21, 22). The fusion of the virus to the cell membrane or to the endocytic vesicle causes the release of the virion into the cytoplasm. The capsid and some of the tegument proteins are transported to the nuclear pore. The interaction of pore components with the capsid-tegument structure results in the release of viral DNA into the nucleus. In this compartment the transcription of the viral genome takes place as well as its replication and new capsid assembly. The viral DNA is transcribed by a host RNA polymerase with the participation of viral factors in all stages of infection.

The synthesis of viral gene products are tightly regulated as already described above. Assembly occurs in several stages. After the γ capsid protein synthesis, the capsid assembly occurs in the

infected cell nucleus. At the initial stages, some capsid proteins are located in the cytoplasm. In particular the major capsid protein VP5, VP26 and VP23 are not able to localize to the nucleus without the help of pre VP22 scaffolding proteins and VP19C. When the complex enters the nucleus, the capsid proteins are added as hexons and pentons to form a partial capsid together with scaffolding proteins. Empty shells containing an internal scaffolding are assembled first and the scaffolding is lost in DNA encapsidation. In particular the encapsidation is a process that requires HSV DNA concatemer cleavage into monomers and their packaging. The viral DNA has signals for cleavage and packaging in the α sequences, named *pac1* and *pac2*. The process is not well defined but the insertion of viral DNA is concomitant to the displacement of scaffolding proteins like VP22a. The assembled capsid can then proceed to the egress from the cell.

1.4.5 Latency

When HSV virions enter the nucleus, they can either start lytic replication or enter the latent state. This is a particularly successful form of accommodation with the host. Latently infected neuronal cells stay alive, and HSV-1 latency sometimes lasts the lifetime of the host. In the latent state the viral DNA is circular in shape, bound to histones, and maintained in a repressed state with the exception of the latency-associated transcripts (LATs) and a set of microRNAs (miRNAs) derived from LAT or its precursor RNA (20). In a fraction of neurons harbouring latent HSV, the virus can be reactivated; assembled virion move anterogradely near the initially infected site (9). During the establishment of latency, VP16 /HCF1 complex is not translocated to the nucleus, and the transcription of α viral genes is prevented. At the beginning the LAT promoter and 5' LAT exon are associated with acetylated histones, markers of active chromatin whereas the lytic gene promoters are not associated with acetylated histone H3 (9). The LAT gene localization is within the inverted repeat component that encloses the unique long segment. Its product is an 8.3 kb precursor present at low copy (minor LATs) and, upon splicing, it generates a series of stable unpolyadenylated RNAs (major LATs, 2 kb and 1,5 kb in size) that accumulate to high levels within the nuclei of latently infected neurons (23). The LAT promoter is 3' and antisense to the ICP0 gene, a protein highly involved in a transactivation of several viral genes. ICP0 is able to start both viral gene transcription from quiescent genomes in cells in culture and viral reactivation from latently infected sensory neurons *in vivo* (23). This protein might thus play a key role in the balance between latency and viral reactivation.

LATs and miRNAs have a role in the maintenance of latency but not in its onset. No viral product expressed from LAT has been identified nor its role in HSV-1 latency. It has been observed that Δ LAT mutant viruses can establish a lytic state, but the yields of virus recovered from the ganglia may be reduced relative to those infected with wild type virus; furthermore these mutants exhibit increased expression of viral genes (18). The number of neurons in murine ganglia infected with a LAT deleted virus is lower than that of ganglia harbouring wild-type virus. For these reasons LAT has been proposed to “protect” neurons from apoptosis (24).

HSV microRNAs derive at least in part from LATs. It is not clear whether miRNAs are synthesized from LAT or its precursor or from independent transcription. Their functions seems to be related to establishing or maintaining latent infection. Alternatively they could also play a role in the regulation of the synthesis or function of some essential α proteins(20).

Several findings show that HDAC-1 or HDAC-2/CoREST/LSD1/REST repressor complex also have a role in silencing HSV DNA in neurons. It has been reported that HDAC inhibitors increase reactivation of virus *in vivo* and *in vitro* and that inhibitors of LSD1 (histone demethylase) block viral replication and reactivation from the latent state. The repressor complex is required for activation of α genes and to block the expression of β and γ genes; it works in a manner that is easily overcome in productive infections but not in infections leading to the establishment of the latent state (20).

1.4.6 Entry

HSV is considered as the prototype for the *Herpesviridae* family. It encodes a multipartite entry machinery with essential distinct glycoproteins (gB, gC, gD, gH/gL), each one with a specialized activity, whereas smaller enveloped viruses possess only one or two fusion glycoproteins for entry and fusion functions. The multistep process of fusion that characterizes HSV entry prevents the indiscriminate activation of the fusion apparatus (25).

HSV enters cells by fusion of the envelope with the plasma membrane or after endocytosis through neutral or acidic compartments, insensitive or sensitive to bafilomycin A (BFLA), respectively. The entry route of HSV differs from cell to cell. The cell is responsible for choosing the entry pathway for the virus, routing HSV to the appropriate site on the cell membrane. For example, HSV virions are routed to cholesterol-rich rafts and a dynamin2 dependent acidic compartment by $\alpha V\beta 3$ -integrin. In general, it has also been reported that cellular factors other than the glycoprotein D (gD) receptors may address HSV to acidic endosomes or a neutral compartment (26).

The process of viral entry consists of four steps: attachment, recognition of cellular receptor by a viral glycoprotein, triggering of fusion and fusion execution.

First, the virus interacts with the cell plasma membrane through the binding of gC and gB to glycosaminoglycans (GAGs) moieties of heparan sulfate (HS) or chondroitin sulphate (22, 27, 28). This non-essential binding enhances HSV infectivity but lacks specificity and likely serves to create multiple points of adhesion, tethering and concentrating virions at the cell surface. This binding is reversible, and the detached virus is still infectious (25). In some cellular types it has been observed that virions accumulate near cell membrane projections, named filopodia through the interaction of gB with HS. From there, virions travel with a lateral movement along the length of filopodia to arrive closer to the cell body. This phenomenon was called viral surfing and it has been reported to increase infection efficacy directing the virus to cell membrane regions enriched in receptors. After viral attachment, gD binds in an irreversible manner to one of its specific receptors. gD is able to bind to at least three alternative receptors: nectin-1, herpesvirus entry mediator (HVEM or HveA, herpesvirus entry mediator A) and O-sulphated (3-O-S) moieties of HS. Many of the receptors are broadly expressed in a wide variety of human cell types and tissues (24). It is unknown why HSV binds to alternative receptors. The gD affinity to nectin-1 and HVEM is of the same order of magnitude (10^{-6} M); hence, affinity is not a basis for preferential usage (29). Likely this serves to increase the chance of a successful infection and spread in the human host. When gD binds to its receptor a protein conformational change occurs resulting in the triggering of the fusion process (24). The gD binding signals the receptor-recognition and thus triggers fusion, by recruiting the other three glycoproteins – gB,

gH, gL. The trio of gB, gH, gL, executes fusion with the plasma membrane or endocytic vesicle of the target cell (Fig. 1.3). The trio appears to constitute the conserved fusion machinery across the herpesvirus family with the highest degree of sequence conservation seen in gB (30). The complex nature of the entry machinery that has no other example in viruses, and has made the complete understanding of the fusion triggering mechanism difficult. Due to the number of proteins working on the entry pathway a fine communication is necessary among them. The gH and gB proteins have created an intriguing scenario about which of the two proteins could be the fusion executor. gH has been considered for a long period as a potential HSV-1 fusogen but structural studies on its crystal found no homology with any known fusion proteins (31); the structure of gB has already been solved and exhibits a remarkable homology to that of VSV fusogen, gG. Considering the structure of the gH-gL complex, it is likely that they may activate gB for fusion rather than having a direct role in the mechanism of fusion. Exactly how the two glycoprotein cooperate to execute fusion is still unclear (32).

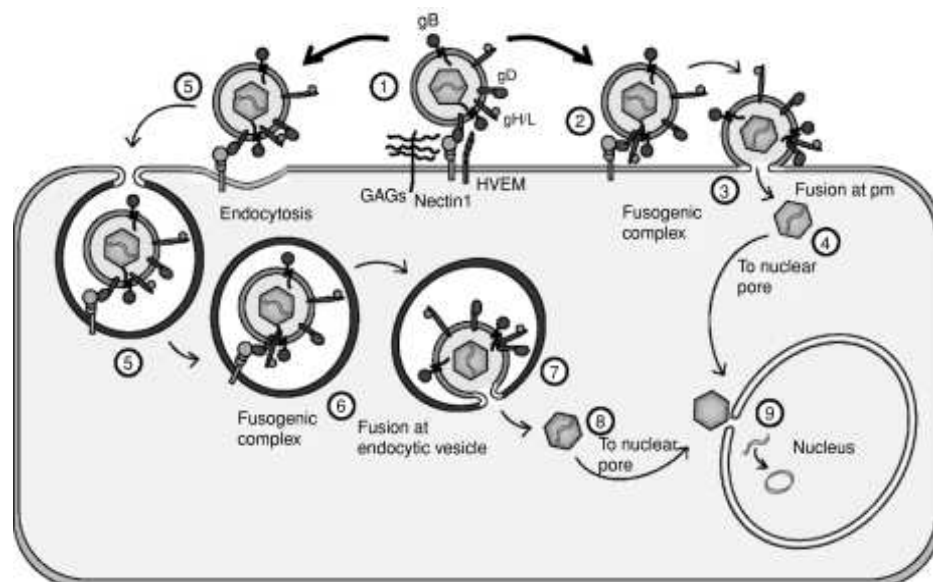


Figure 1.3 - Attachment and entry of herpes simplex into cells. On the top is the pathway associated with HSV endocytosis. Below is the pathway related to HSV-1 fusion at the plasma membrane. Initially HSV binds in an aspecific manner to glycosaminoglycans on the cell surface (1). In the second step, gD binds to one of its cellular receptors (2) and after a conformational change is able to recruit glycoprotein gB, gH and gL triggering fusion at the plasma membrane (3). The naked capsid is transported to the nucleus (4,9). Depending on the cell line the virus can also enter by endocytosis (5-9). After acidification and maturation of the vesicles, the fusogenic complex may form (5-6) and fusion between the virion envelope and the vesicle occurs (7). The naked capsid is then releases into the cytoplasm and is transported to the nucleus (8-9) (30).

1.5 Glycoproteins of HSV-1 involved in attachment and entry

1.5.1 Glycoprotein C

Glycoprotein C (gC) is encoded by the UL44 gene (33). It is a 511aa mucin-type glycoprotein heavily N- and O-glycosylated and its gene belongs to the γ class of HSV genes. gC contains a 25

aa signal sequence at the N-terminus, a 453 aa extracellular domain, a 23 aa transmembrane anchoring domain and a short 10 aa C-terminal cytoplasmic tail. gC facilitates the adsorption of virions into cells by binding to heparan sulphate's glycosaminoglycans or to a chondroitin sulphate (30). In fact, several observations revealed its importance in virus attachment: first, gC projections are long and slender and they are the most externally exposed structures of the virion (34). Second, albeit gC is not essential for virus production in cell cultures, mutant virions deleted in gC, unlike the negative mutant gB, are not able to bind to the cells. Furthermore, some data showed that monoclonal antibodies for gB, gD, and gH inhibited HSV-1 penetration but had little or no effect on attachment. HSV-1 virions with this glycoprotein deleted are defective in penetration but bind to cells normally (27, 34, 35). gC serves multiple accessory functions, it has the ability to bind to the C3b component of the complement and is also a major viral antigen which elicits a strong humoral and cellular immune response during infection (36). It plays an important role in the induction of herpetic eye disease in animal models of herpesvirus keratitis (33).

1.5.2 Glycoprotein D

Glycoprotein D serves as the entry receptor-binding protein and is the main determinant of viral tropism (37). Recently it has been reported that the interaction of gD with its receptors is not only required to activate the HSV fusion machinery but, in some cell types, also to target the virus to the endocytic pathway (38). The structure of gD has been solved for gD alone, encompassing amino acids up to 259, and bound to HVEM (up to aa 285 of gD) or nectin-1 (up to aa 285 of gD) (39-41). gD is a type 1 membrane glycoprotein 369 aa long after the cleavage of the signal sequence of 25 aa (42). Its structure consists of an ectodomain of 316 aa, a transmembrane domain located between aa 317 and 399, and a cytoplasmic tail. The protein has six cysteines that form three disulfide bonds (Cys 66-Cys 189, Cys 106-Cys 202, and Cys 118-Cys 127) and has three N-linked oligosaccharide attachment sites.

gD is essential to mediate HSV entry. Its ectodomain is organized in three regions with different structural and functional characteristics: the N-terminal, the core and the C-terminal (Fig. 1.4 A). The first 20 aa of the N-terminal are disordered, flexible and extended when gD is not bound whereas they fold back to form a hairpin when gD is bound to HVEM. This region, that contains all residues involved in HVEM receptor binding, pack to the core of the protein which it is connected to through a short flexible proline-rich region, encompassing aa 45-54 (25). No electron density resulted for residue 1 to 22 in the gD/nectin-1 complex. The first 32 amino acids are also involved in binding 3-OS-HS but are dispensable for nectin-1 binding and usage (41, 43).

The core includes an Immunoglobulin Variable (IgV) folded region (aa 56 to 184) and a helix (α -helix 3) of 17 aa that ends at aa 240. In the crystal, helix 3 is positioned between IgV and the N-terminus (Fig. 1.4 B,C). Downstream of the helix 3 is a long flexible proline rich region, spanning aa 244-312. From studies presented by Zhou and Roizman (37) residues 61-218, encompassing almost entirely the Ig core, do not execute a function required for HSV-1 entry into cells. Indeed, it was hypothesized that the Ig core can serve as a scaffold, and to connect the functional C- and N-terminal regions. This consideration was further confirmed because its removal and substitution with a heterologous ligand such as a scFv to HER2 does not impair the functionality of the protein (44).

The C-terminus of the ectodomain (aa 250/260-310), designated as pro-fusion domain (PFD), carries a region required for the trigger of fusion and for the interaction with other viral glycoproteins (45). It has a flexible conformation that has made it impossible to determine the structure in receptor bound gD whereas in unbound gD it folds back around the core towards the N-terminus. The PFD is essential for virus entry, in fact the insertions or deletions in the segment 250-310 impair infection and cell-cell fusion (25). Furthermore, it has been reported that the soluble form of gD, as gD285 and gD306, rescue the infectivity of a gD null virus whereas gD260 lacks this ability.

PFD is also responsible for the “switch-on” mechanism that allows activation of the virion near the cell surface. In the receptor free complex, the C-terminal region is in an auto-inhibited conformation where PFD folds back around the core stabilized by contacts that include Trp294 outside of PFD. In particular, amino acids 280 to 306 are located in the position which is occupied by the first 20 aa of D in the gD/HVEM complex. This is consistent with the increased receptor affinity of the C-terminal truncated form of gD compared to the full length molecule (41). The Trp294 side chain is located toward a groove on the gD surface anchoring the PFD in proximity of the N-terminal region. The PFD of gD has been supposed to stay in balance between this closed state and a partially open state, with the side chain of Trp294 in and out of the groove respectively. The receptor binding may change this equilibrium and lock gD in the open conformation.

gD residues involved in Nectin-1 binding, different from those in HVEM, are not in the same confined region but resulted independent and located downstream of residue 32. The recent gD/Nectin-1 solved structure definitively identified the contact region between the two molecules and show key residues (Y38, D215, Q132, L220, R222, F223) that make contact with the receptor (Fig 1.4 D). In the glycoprotein/receptor surface contact there are several residues that previously have been shown to affect nectin-1 binding when mutagenized (Y38, H39, Q132, D215, L220, P221, R222, R223) whereas others have been proposed for the first time. Most of the residues identified are in the gD C-terminal of the ectodomain while Y38 and Q27 are located in the N-terminal portion (41).

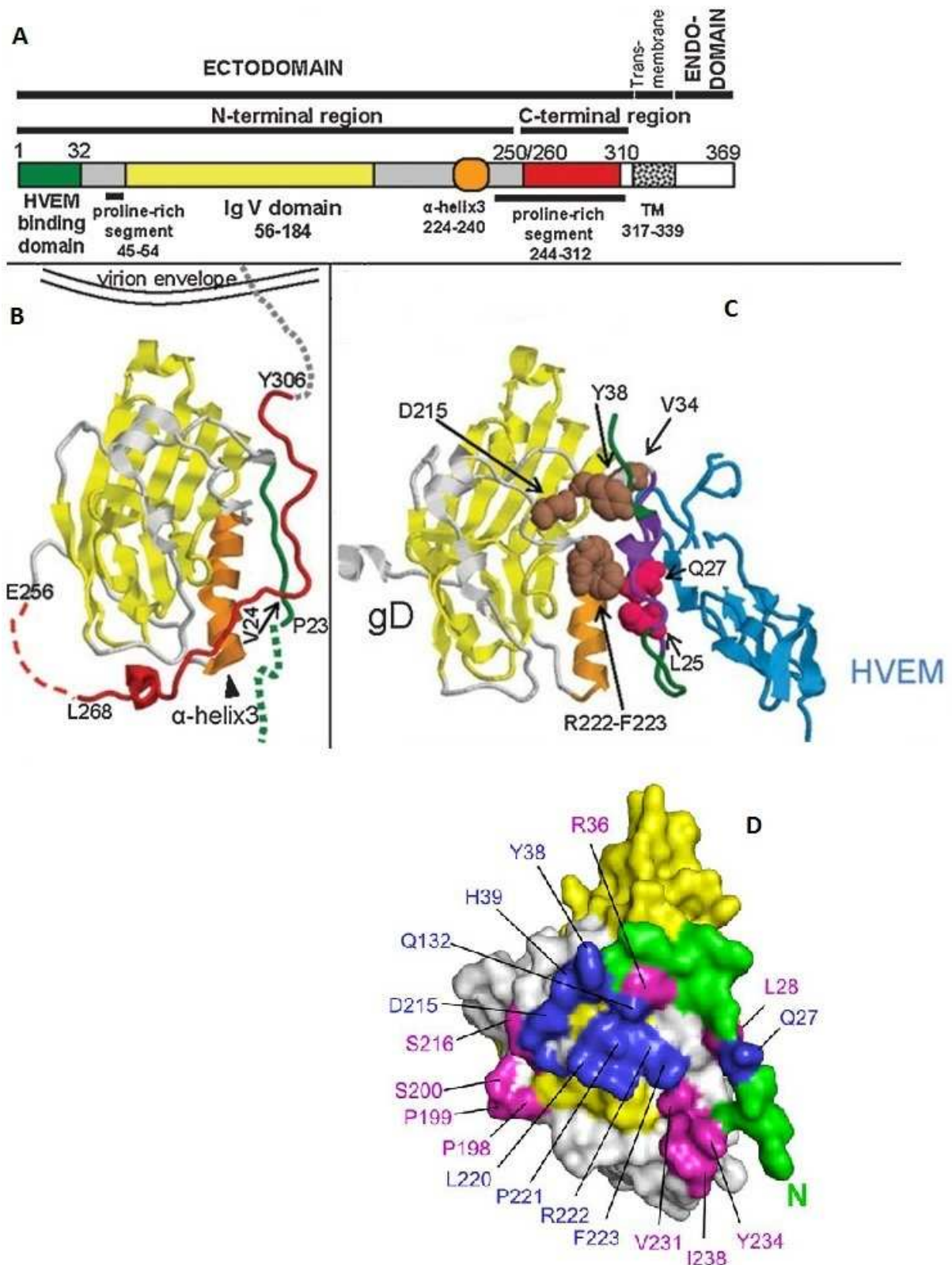


Figure 1.4 - Structure of gD in HSV-1. **A)** Linear representation of domains in mature gD. The colors are the same in panel A, B and C. **B)** Crystal structure of gD ectodomain in a free conformation, HVEM binding site is unstructured. **C)** Crystal structure of gD/HVEM (light blue). The N-terminal region of gD forms a hairpin that contacts the receptor. Critical residues for nectin-1 binding are represented as brown space fill. Q27 and L25 are residues involved in HVEM binding, Ig core in yellow, HVEM binding residues in green, residues 185 to 250 from C-terminus of ectodomain in light gray (25). **D)** gD surface representation located in gD/nectin-1 interface. Nectin-1 contact area is colored in blue and magenta. Residues in blue have been shown to impair nectin-1 binding while magenta residues have been proposed for the first time (41).

1.5.3 Glycoprotein B

Glycoprotein B (gB) is a 904 amino acid trimeric protein encoded by the U_L27 gene. gB's main functions are associated with two steps in HSV entry. A non-essential function is attachment of the virus to the cellular membrane through the binding to a modified heparan sulphate. The second, essential, function is the fusion of the virus with the host membranes. The non specific interaction between gB and the cells occurs via a binding site located between aa 68-76 of the protein, whereas the fusion is executed not by gB alone but require in addition of gH and gL. To further complicate herpes entry mechanism it has been demonstrated that gB interacts with its own receptors, other than heparan sulfate (46). It has been reported that a soluble form of gB binds to cells lacking HS and this inhibits HSV-1 infection in some cell lines (47). To date, three possible gB receptors have been identified. Satoh and coworkers demonstrated that the paired immunoglobulin like-type 2 receptor (PILR α) interacts with gB mediating HSV-1 infections. (48) Furthermore, their experiments showed that anti-PILR α or anti-HVEM antibody inhibits HSV-1 infection of monocytes, which constitutively express both PILR α and HVEM. However, interaction between gB and PILR α alone does not mediate membrane fusion in the absence of HVEM and gD. So PILR α acts as an essential co-receptor for viral entry (49). Another receptor for gB was identified in myelin-associated glycoprotein (MAG), expressed in neural tissue. Indeed, gB is able to cause cell-cell fusion interacting with MAG in the presence of gH/gL (48). Recently, an intriguing discovery of a third gB receptor has been made (50). The non muscle myosin heavy chain IIA (NMHC-IIA) has been found to interact with gB, functioning as an HSV entry receptor. An antibody against NMHC-IIA blocks infection in susceptible cells and moreover the knockdown of the putative receptor inhibits the infection in the presence of the HSV entry machinery (gB, gD, gH/gL). The protein is normally localized in the cytoplasm where it is known to perform its function. During HSV absorption there is a marked enrichment of NMHC-IIA at the plasma membrane.

gB consists of an ectodomain of 696 amino acids, a transmembrane of 69 aa and a cytoplasmatic tail of 109 aa (51). The ectodomain of gB is needed for fusion and some identified mutations confer temperature sensitivity entry (52).

The cytoplasmatic tail carries two alpha helices that negatively regulate the fusogenic process. The carboxyl-terminal helix contains two endocytosis domains, named YTQV 889-892 and LL871, and one mutation in the aminoterminal confers a syncitial phenotype (R858H, *syn 3*). Deletion of the two alpha helices blocks gB internalization as demonstrated by the increase of fusion assay efficiency and the appearance of a *syn* phenotype.

gB is the most conserved entry glycoprotein across the *Herpesviridae* family and its crystal structure shows a surprising similarity with the postfusion conformation of protein G from vesicular stomatitis virus (VSV G) ectodomain (53, 54). This similarity suggests that gB is the fusion executor in HSV. Although both proteins do not show a typical fusion peptide they are able to trigger the fusion between viral and cellular membranes.

The crystal structure of gB ectodomain shows that it is a trimer stabilized by several points of contact. 10 cysteins residues to create 5 disulfide intramolecular bonds (32). Each subunit of the trimer consists of five domain (Fig. 1.5). Domain I, the *base*, is a continuous polypeptide chain folded like a pleckstrin homology (PH) domain. Generally, this fold serves to proteins as a scaffold mediating cytoplasmatic signaling pathways such as phosphoinositide binding.

Monoclonal antibodies against this domain are able to block HSV-1 entry (55). Uchida et al. found the substitution D285N associated to A549T (domain III) to enhance virus entry. Maybe the two mutations hypersensitize gB to respond more promptly to signals from gD therefore the authors speculated that this includes the possibility that the mechanism involves a change in the yet unknown region of gB-gD contact (56). Domain II, designed as *middle*, consists of two discontinuous fragments (142-153 and 364-459) in which a six-strand β barrel similar to a PH domain is present. Domain III, named as *core*, comprises three discontinuous segments (117-133, 500-572 and 661-669) and shows a long α helix of 44 residues that form with the other protomers essential contacts for the oligomerization. Domain IV is the crown of the molecule and does not seem to be related to other known structure. It encompasses two discontinuous fragments linked by a disulfide bond. The last domain (V) is the arm and extends from the crown to the bottom of the monomer. The long α helix forms a central coiled coil structure with other protomers which is the responsible for the trimer stability (32).

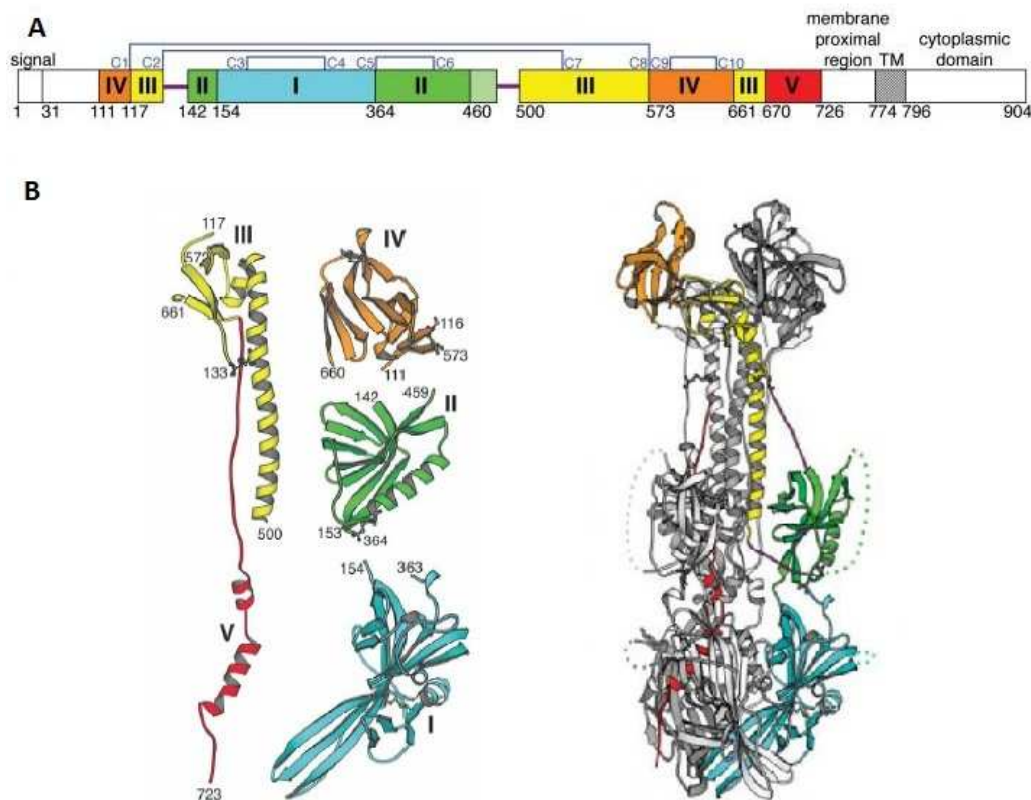


Figure 1.5 – Crystal structure of HSV-1 gB ectodomain – A) Linear representation of gB domains. B) On the left: ribbon diagram of single domains in one protomer. The five domains are highlighted. On the right: structure of the gB trimer (32).

1.5.4 gH/gL complex

The heterodimer gH/gL is highly conserved among Herpesviridae family and both gB and gH/gL are required for efficient viral entry and cell fusion in all herpesvirus (31). Numerous neutralizing antibodies are directed to gH, stressing its importance in virus infection. The role of

gH in fusion has been confirmed by experiments where neutralizing antibodies to gH block virus entry but not the binding to the host cell surface (57). A receptor for this protein has not yet been found, but indirect evidence points to the existence of a receptor (26). It was reported that a soluble form of gH/gL immobilized on plastic facilitates the adhesion of CHO cells transiently overexpressing a number of integrins, in particular, $\alpha V\beta 3$ integrin (58).

gH, encoded by U_L22 gene, is a protein of 838 residues with a signal peptide of 18 aa, a large ectodomain of 785 aa, only one transmembrane domain and a short cytoplasmatic domain. gL is 224 amino acid long and is devoid of a transmembrane region. In the mature virions the two proteins are always found in a stable 1:1 complex (31). Recently the three-dimensional crystal structure of the complex has been resolved for HSV-2 gH/gL showing a “boot like” conformation (Fig. 1.6) (31). gH consists of three domains which are located as continuous segments. Domain H1 is placed in the upper part of the boot and is divided in two subdomains (H1 and H2) connected by a short linker. This is the only domain that makes contact with gL forming a mixed β sheet with four strands coming from gL. Three short helices are also preset in H1 domain. Domain H2 is globular consisting mainly of 13 alpha helices and corresponds to the terminal part of the boot. It is composed by a β sandwich of 10 strands with five strands for each part.

Most of gL has not a regular conformation, only 30% of the protein has a secondary structure with three helices and two β sheets. The protein contains two disulfide bonds essential for the function of the complex and to fold gL in the proper shape. gL activity is needed for the correct folding and trafficking of gH, but it cannot be defined as a chaperone protein because it remains closely attached to gH also after the folding phase. It is more likely a scaffold that creates with gH wide complementary contact surfaces. Thus, it was proposed that gH and gL need each other to stabilize their conformation.

In the past it was proposed that gH/gL exerted the function of a fusogen. On the basis of the recent crystal structure of HSV-2 complex, gH/gL do not resemble any known viral fusogen. Moreover, the putative fusion peptides inside the structure are buried and involved in sheets. Their removal would affect complex stability. So it has been proposed that gB is the real fusogen and the complex works as a positive regulator coordinating the transition of gB into its fusion active state (31).

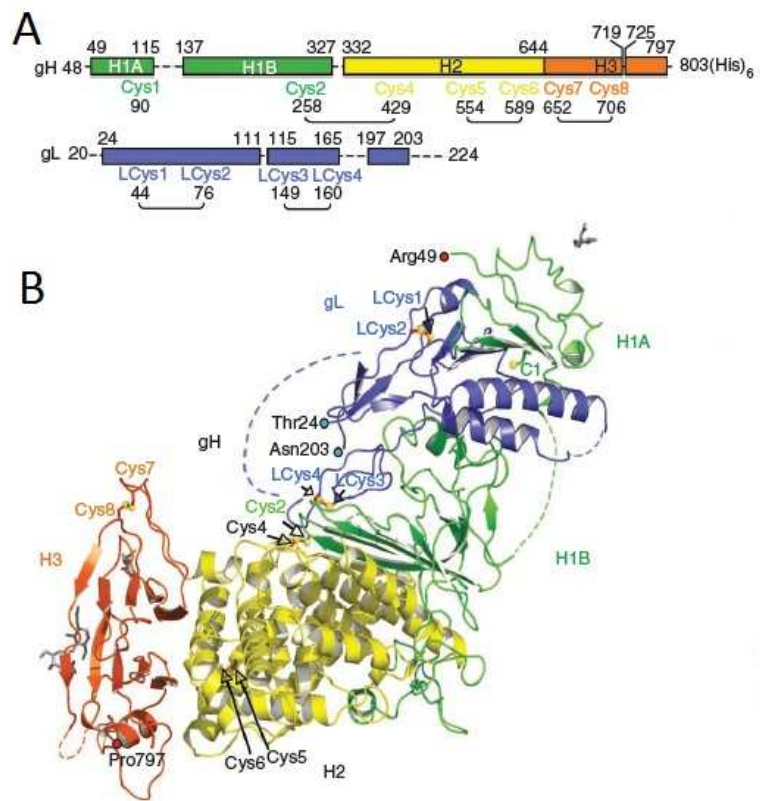


Figure 1.6 –Structure of gH/gL complex in HSV-2. **A**) Linear structure of gH and gL showing domain arrangements: domain H1A and H1B (green), domain H2 (yellow), domain H3 (orange), gL (blue). Unsolved structures are indicated as dashed lines. **B**) Three dimensional side view of gH/gL. Dotted lines show unsolved fragments. Sugars, cysteins and disulfide bond are indicated in grey, yellow spheres and red stick respectively (31).

1.6 Glycoprotein D Receptors

1.6.1 Nectins

Nectins are immunoglobulin (Ig)-like Ca²⁺ dependent cell adhesion molecules (CAMs) essential for several cellular activities like cell-cell adhesion and polarization, differentiation, movement, proliferation and survival. The family includes four members (Nectins-1, -2, -3, -4). They are expressed in different cell types including epithelial cells, neurons and fibroblasts and have two or three splicing variants designated with Greek letters (30). Nectins are involved in the creation of cell-cell junctions like adherent junctions between neighbouring epithelial cells and fibroblasts and in the establishment of apical-basal polarity at cell-cell adhesion sites. They also are implied in the formation of tight junctions in epithelial cells. Nectins form homo-*cis*-dimers, but non hetero-*cis*-dimers. Each protein then forms homo-*trans*-dimers.

Nectin1 and Nectin-2 were initially isolated as receptors for α -herpesvirus and were called PRR1 and PRR2 respectively. All the members, except Nectin-1 γ , have an extracellular region with one Ig V-like domain, two C-like Ig domains and 8 potential sites for N-Linked oligosaccharides, a single transmembrane region, and a cytoplasmatic tail region (59-61). The second Ig-like loop of

the protein is involved in the formation of the cis-dimers, whereas the formation of the trans-dimers needs of the first Ig like loop (59).

In this region the proteins bind the filamentous (F)-actin binding protein afadin, through its PDZ domain, and the cell polarity protein partitioning defective 3 (PAR3) (60). The interaction with afadin is not necessary for the formation of the cis dimers or the trans-dimers. The C-terminal conserved domain, which is absent from nectin-1 β , activates a signalling that involve several extracellular and intracellular molecules like Ras, CDC42 and Rac small G proteins (59).

gD binds physically nectin-1 and crystal structure of gD bound to Nectin-1 have been recently solved. The binding site of gD spans from aa 1 to 250 and requires exclusively the β sheets of the V domain of nectin-1 (41) (Fig. 1.7). The highest affinity was found for the truncated form of gD at residue 250 (30). An important interaction involves Phe 129 of Nectin-1; in the complex this residue is inserted in the pocket formed by residue between the α 3 helix and the side chain of Phe 223 of gD. The mutation of Phe 129 impairs the binding to gD. There are similarities in the structures of the nectin-1 dimer and the gD/nectin-1 complex. The crystal structure of the complex gD/nectin-1 showed that binding of gD contacts many of the same residues involved in nectin-1 dimerization. This finding demonstrates that gD binding impair nectin-1 dimerization and thus interferes with nectin-1 mediated cell adhesion. Other non- enveloped adenovirus, reovirus and measles interact with a similar regions of their receptors which are also Ig-like cell-adhesion receptor CAR, JAM-A and SLAM (41).

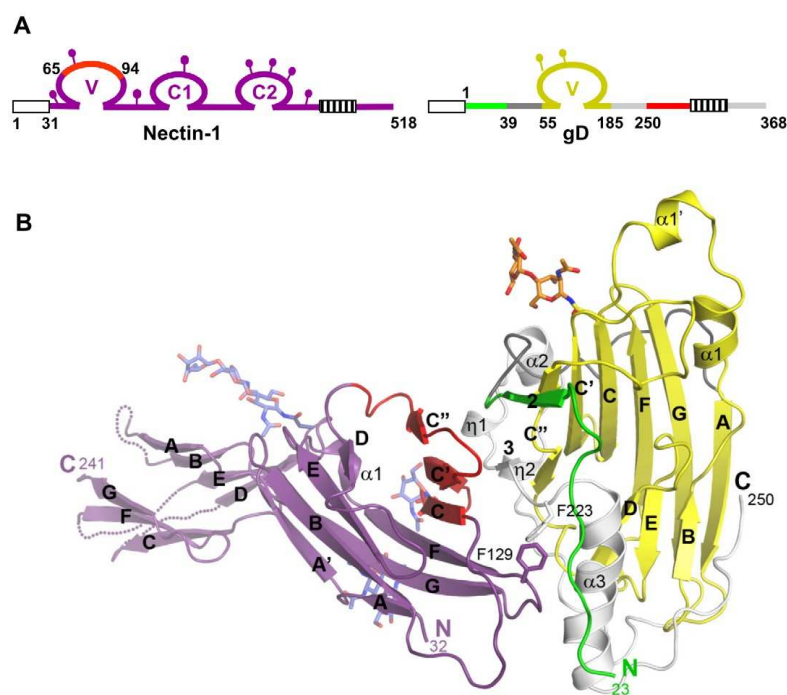


Figure 1.7 - Structure of the gD/nectin-1 complex. A) Linear representation of human nectin-1 and HSV-1 gD. N-glycosylation sites are drawn as lollipop. Signals peptides are shown as white boxes and the transmembrane segments as hatched boxes. B) Ribbon representation of the gD/nectin-1 complex. Dotted lines represents unsolved loops (41).

1.6.2 HVEM

Herpes virus entry mediator A (HVEM, HveA) is a member of the tumor necrosis factor receptor superfamily (TNFR) (62). Its members are molecules that transmit signals for the regulation of

cell proliferation, differentiation and for apoptosis (30). HVEM is mainly expressed on activated T-lymphocytes where it mediates HSV entry, however its distribution may be wider considering its presence in several cultured cells line together with nectin-1 (30, 63). The receptor consists of an ectodomain with four typical cystein-rich domains (CRD) of ~40 residues each and a cytoplasmic tail with sequences that signals the ligand binding (Fig. 1.8) (25, 39). In particular the cytoplasmatic tail interacts with several members of TRAF family (TNFR-associated factor) and leads to the activation of NFκB, Jun N-terminal kinase, and AP-1 (64). HVEM binds directly to gD and mediates entry of most HSV-1 and HSV-2 strains (65). HSSV entry and gD binding are blocked by a monoclonal antibody that binds CRD1, but biochemical studies showed that both CRD1 and CRD2 are necessary and sufficient for gD binding (66). The gD-HVEM interface focalized on the hot spot HVEM-Y23 phenol ring that protrudes into a crevice on the surface of gD and site-directed mutagenesis showed that this residue is essential for gD binding (39, 65). Mutagenic studies have also showed that several residues in the contact surface between gD and HVEM are clustered near an intermolecular antiparallel β-sheet formed by HVEM residues 35 to 37. These residues, such as residues in CRD2 contributed to gD binding (65).



Figure 1.8 - Linear structure of HveA – Black circles identified glycosylation sites where TM indicates the transmembrane region (65).

Comparison between gD/HVEM and gD/nectin-1 complex

The binding site of nectin-1 and HVEM on gD are different. Only the first 32 N-terminal residues of gD folded as a hairpin interacts with HVEM and the binding involves hydrogen bonds through main and side chain atoms. Indeed, several disperse gD residues, between N-terminal and C terminal extension of its ectodomain, take contact with the V domain of nectin-1. The structural superimposition of the two receptors shows that the most part of amino acids of nectin-1 involved in gD binding are deeply hidden by gD-N-terminal residues in the gD/HVEM complex. It can be concluded that likely the binding to one receptor interferes with binding of the other (41). A soluble form of nectin-1 is able to block virus entry in HVEM expressing cells (67).

1.6.3 3-O-sulfated Heparan sulfate

The third class of HSV-1 receptors are 3-O-sulfated heparan sulfates (3-OS HS). They are a modified form of HS created by the enzymatic activity of 3-O sulfotransferases (3-OSTs). This type of non proteic receptors are polysaccharides, containing specific sulfated motifs that

specifically mediate HSV-1 entry (68).

Heparan sulphate are expressed in a great variety of cell types (69). Interestingly, although both HSV-1 and HSV-2 use HS during the attachment phase in viral entry, HSV-1 can bind to distinct modification sites on HS that HSV-2 is unable to, which could explain some of the differences in cell tropism exhibited by the two viruses (68). Heparan sulphate chains consist of repeating uronic acid (d-glucuronic acid or l-iduronic acid) and d-glucosamine disaccharide units (69).

1.7 Viruses as oncolytic agents

Some viruses have an intrinsic cytolytic activity and since their discovery, at the beginning of the nineteenth century, they were considered attractive agents against tumors (70). The idea that a virus could be employed as a drug to treat cancer disease stemmed from the observation that some cancer patients affected by natural viral infections, showed a brief period of clinical remission. This was true especially for hematological malignancies like leukemia (71, 72). This observation laid the groundwork for the birth of oncolytic virotherapy whose aim is to exploit the ability of virus to infect and kill cells in order to obtain the selective elimination of cancer cells. The purpose of this strategy is twofold: (i) to limit the growth of the tumor mass and (ii) to treat tumors and metastases for which there are no current effective therapies (73). Oncolytic virotherapy offers several advantages. First, it is possible to kill selectively only mitotically active neoplastic cells through the genetic engineering of viruses. Second, it can make use of replication competent viruses to obtain a spread of infection to tumor cells distal from the injection site. In this way tumor cells lysis is not confined to the initially targeted cells. Third, some viruses can be “armed” to potentiate their oncolytic activity through the introduction of heterologous genes, e.g. boosting the antitumoral immunity with IL-12 cytokine introduction-. Lastly oncolytic virotherapy can be combined with standard clinical therapy (74). From the first evidence of a viral antitumor activity, several attempts have been made to use viruses as therapeutic agents coupling them with new advances in surgical radiotherapy, chemotherapy, and immunotherapy.

1.7.1 Virus retargeting

For viruses with either a natural or partial tropism for the target cancer cells the challenge with viral tropism is to introduce mutations that make the virus able to enter and replicate only in cancer cells and to preserve its oncolytic activity. The approaches were: virus retargeting to specific cancer surface molecules, virus activation by cancer-specific proteases, control of viral transcription and replication by tissue-specific promoters and exploitation of cancer cell defects (75).

Some of the viruses belonging to the retargeted class have their surface glycoproteins engineered in order to recognize only specific cancer receptors or to be activated by molecules present in the cancer environment. In measles virus (MV), the epidermal growth factor (EGF) or the insulin-like growth factor 1 (IGF1) were inserted in MV hemagglutinin by Schneider and coworkers and the resulting viruses could infect cells expressing EGR and IGF-1 receptor that were not

susceptible to infection before (76). Recent years the use of single chain antibodies to retarget viruses has been widely applied. These molecules overcome the problem of the large size of an entire antibody tetramer and maintain the specificity for the target cells. Several viruses have been engineered to express scFv like anti-EGFRvIII or anti-prostate specific membrane antigen (PSMA) for MV (77), anti-vascular endothelial growth factor (VEGF) for vaccinia virus (78) or human epidermal growth factor receptor 2 (HER-2) for HSV (79, 80).

Another approach was to exploit the fact that nearly all cancer cells express matrix metalloproteinases (MMPs) at high levels conferring viral cancer specificity to viruses. MV has been engineered to express its fusion protein F with an hexameric sequence recognized by an MMP instead of furin, the natural activator of MV fusion protein. The modified virus was rescued and strongly restricted on primary human hepatocytes (75, 81, 82), whereas it was unable to infect cells that did not express MMP in the extracellular matrix.

However, the greatest challenge in retargeting viruses to cancer specific receptors is to deprogram the virus from its natural receptor recognition. This result can be achieved either through mutagenesis of several residues known to be responsible for the virus receptor binding or through retargeted molecules on a virus surface that can mask the normal site of virus attachment.

Another strategy considered here is that in order to control the specificity of viral replication, essential gene products can be controlled by cancer specific promoters. DNA viruses are the most suitable candidates for this approach because they can tolerate large DNA insertions. In adenoviruses, E1A gene that normally transactivates viral promoters to initiate the replication cycle has been put under the prostate specific membrane antigen to reach cancer type specificity (83). Other adenoviruses have been engineered to be controlled by the survivin promoter, active only in cancer cells (84).

Oncolytic virus design can also exploit some cancer specific defects in order to reduce viral toxicity to normal tissue. For example, many α -HSV are deleted in the neurovirulence gene or in genes related to nucleotide metabolisms in order to obtain viruses able to replicate only in cancer dividing cells (see below in the text). ONYX-015, a derivative of adenovirus type 5 (dl1520 strain), is a conditionally replicating virus deleted in the E1B gene and it was the first tumor-selective OV to show antitumor activity in a clinical setting (85, 86). E1B gene interacts directly with a cellular p53 blocking apoptosis in infected cells, so its deletion makes the virus able to replicate only in cells with a non functional p53 (87). However, ONYX-015 possesses insufficient antitumor potency as a single agent because, after intra venous administration, it is not able to infect efficiently tumor metastases, exhibits slow replication and spread in solid tumors (24). Nowadays it is administered in combination with chemotherapy and the results are encouraging in patients with head and neck cancer. H101, an E1B-55k mutant adenovirus has passed successfully a phase III clinical trial in China and has been approved by the Chinese FDA for its use in patients with head and neck cancer in combination with chemotherapy (87).

1.7.2 Arming viruses

Although the retargeting approach has been proven to be effective in specifically directing viruses against cancer cells, other strategies have been evaluated to potentiate viral oncolysis and

to increase the clearance of tumor masses through the stimulation of the immune system. The arming can be achieved for example (i) through the insertion of transgenes that convert a prodrug into a harmful compound, (ii) the insertion of immunomodulatory molecules able to recruit the immune system cells, (iii) the introduction of pro-apoptotic transgenes that force the cell to commit suicide only at a late stage of infection.

An example of arming through an immune stimulating protein is the vaccinia virus that has recently been used as an armed replication competent oncolytic virus that selectively infects tumors. Vaccinia virus is suitable as oncolytic agent because it has evolved mechanisms that facilitate intravenous stability and circulation to distant tissues. JX-594 is an engineered vaccinia oncolytic virus with the deletion of viral thymidine kinase gene and expression of granulocyte-macrophage colony stimulating factor (GM-CSF) and LacZ. Recently the first phase I dose escalation trial of JX-594 with a single intravenous infusion in human metastatic solid tumors was reported. The virus has been generally well tolerated (88).

An example of proapoptotic transgenes is an adenovirus modified to express the TNF-related apoptosis inducing ligand (TRAIL). This molecule leads to apoptosis in a wide set of tumor cells without dependence on p53 status. The virus was effective both *in vitro* and *in vivo*: mice tumor models revealed efficient replication of this vector and the elimination of preestablished liver metastases (75).

1.7.3 Shielding viruses

The systemic route of administration for the treatment of tumor metastases is still an open issue for oncolytic virotherapy. Preexisting immunity against a specific viral agent can preclude its spread in the tumor due to its inactivation by the host immune system. To overcome this problem some strategies have been designed to permit the co-existence of the OV and the host immunity (75). On the other side the injected OV itself can induce a local innate immune response that facilitates the elimination of tumor masses. The first preclinical studies are normally conducted on immunodeficient mice that do not represent the real state of the final patient.

The combined use of virotherapy and chemotherapy can help to limit the action of neutralizing antibodies in the blood stream. Cyclophosphamide (CPA) is normally administered as chemotherapeutic but at the same time it causes the immune-suppression state of the patient. For this reason it was used in combination with different OVs and it has already shown enhanced viral delivery and efficacy through a decrease of neutralizing antibodies or depletion of T cells (89). In a recent study however, it has been shown that vesicular stomatitis virus (VSV) used in combination with CPA caused a loss of chemotherapeutic functions, impairing the oncolysis. This was likely the result of the viral-induced activation of immune suppressive components (90). Another approach to tricking the immune system lays in the construction of chemical shields with polymers such as polyethylene glycol (PEG). The polymer coated virus can get around the immune system avoiding the macrophages' attack and having time to reach the tumor. So far adenovirus has been modified in this way and the method has proved satisfactory (91).

The last strategy for virus shielding is the use of carrier cells that delivery the virus through the blood stream to the tumor mass. The cells, chosen as vectors, must have some characteristics: they should be highly susceptible to virus infection, not be rapidly lysed by the virus, and spread

the infection to the cancer cells (92).

1.8 *Oncolytic HSV*

HSV offers several advantages for cancer therapy as compared to other viral vector systems. In addition to its natural neurotropism, (i) HSV has a broad host range that allows it to infect and replicate in many cell lines; (ii) a distinct benefit compared to other α -viruses is the availability of specific anti HSV therapy for the treatment of undesired infections (Acyclovir, Ganciclovir etc.); (iii) it also has a large genome size of about 152 kbp, part of which consists of non essential genes that can be replaced with novel mutagenesis technologies (e.g. GalK recombineering) of up to 30 kbp. The adenovirus, whose genome any way is five times smaller, shares this last characteristic with HSV, whereas the genome of MV and adeno-associated virus (AAV) do not have space to additional genes. Other advantages are that (iv) the viral DNA does not integrate into the cellular genome, eliminating the concern of insertional mutagenesis (8, 24, 73); (v) the glycoproteins of the entry apparatus are well known and tolerate the insertion of heterologous ligands and modifications (80, 93, 94); (vi) clinical trials have highlighted that it is possible to construct attenuated, replication competent HSVs that show efficacy in several tumor types; (vii) HSV completes its replication cycle in 20 h, in contrast to adenovirus whose replication cycle typically lasts 48-72 h (95). Finally, (viii) a good characteristic is HSV's ability to spread cell to cell directly through cell junctions and to disseminate in the extracellular space, allowing an efficient viral penetration within solid tumors (24).

The original pioneering research on HSV as oncolytic viruses was conducted by Martuza and coworkers and in 1991 they published the first evidence that an oncolytic mutant HSV-1 prolonged survival time of nude mice bearing intracranial human glioma (96). The virus had been deleted in the thymidine kinase (TK) gene, encoded by U_L23. TK cooperates in the synthesis of deoxyribonucleotides to facilitate viral DNA replication in non dividing cells and it plays a protective role converting non-toxic prodrugs such as ganciclovir and acyclovir into toxic metabolites (24, 96). However, it was so neurotoxic at high titers and insensitive to antiherpes treatments that its use in clinical trials was stopped (97). However, this constituted the proof of principle that the strategy could be followed. Today, with regard to safety, TK genes must be maintained to stop undesired infections due to potential HSV mutations (73).

Further knowledge about cancers and virus biology has allowed the design of OV combining different strategies as the modification of viral tropism, the arming of viruses to enhance antitumoral immunity or the shielding of viral particles to escape host immunity (Cattaneo 2008).

The first and second generation of α -HSV share the attenuation of the virulence and are conditionally replicating viruses (single or double mutants) with the deletion of some nonessential genes to avoid replication in normal cells. The third generation includes attenuated viruses with enhanced antitumor immunity (e.g. G47 Δ). Subsequently the third generation developments were focused on arming viruses with cytokines like IL-12 and GM-CSF incorporated in an attenuated backbone. The last generation includes the tropism retargeted viruses whose aim is to enter cells through tumor specific receptors other than their own.

Conditionally replicating HSV: A rapid cellular division is a main characteristic of tumor cells and this implies a large availability of nucleotide precursors for DNA synthesis. In this regard early attempts to use o-HSV focused on genes involved in nucleotide metabolism to force engineered viruses to replicate only in mitotically active cells (97). So the first conditionally replicating virus was a thymidine kinase-negative mutant of HSV-1 (*dlsp_{tk}*) (96). Other viruses were developed with mutations in viral enzymes involved in nucleotide metabolism as ribonucleotide reductase (RR) and uracil deglycolyase (UNG) or DNA polymerase (97). Subsequent viruses have been developed taking into account the deletion of protein ICP34.5, found to be a neurovirulence factor, determines a high grade of attenuation and causes the block of viral replication and spread in CNS with a low replication in peripheral tissue. The ICP34.5 deleted viruses are avirulent on intracerebral inoculation of mice and are unable to establish latent state after infection due to removal of part of LATs (73, 98). ICP34.5 maps in the inverted repeats flanking the long unique sequence of HSV DNA and therefore it is present in two copies in the viral genome. Its product blocks the shut-off of host cell protein synthesis induced by viral infection and counteracts the protein kinase R (PKR) that is responsible for phosphorylation of the eukaryotic translation initiation factor 2 (eIF2 α). ICP34.5 antagonizes PKR by recruiting the protein phosphatase 1 that dephosphorylates eIF2 α and restores late viral protein synthesis (73). HSV γ_1 34.5 mutants include 1716, in strain 17, and R3616 based on strain F. A potential drawback is that they replicate less efficiently with lower viral yield compared to wt (97).

HSV 1716 was developed by MacLean and coworkers (99) on the wild type strain 17 backbone. It carries the deletion of both copies of γ_1 34.5 gene and replicates only in actively dividing cells. *In vitro* and *in vivo* studies have shown its selective replication and cytolytic activity in a variety of tumor types including glioma, medulloblastoma, melanoma, human embryonal carcinoma, mesothelioma and non small cell lung carcinoma.

Intratumoral injection of HSV-1716 at a dose of 10^5 pfu or 5×10^5 into an oral squamous cell carcinoma (SCC) is safe but with little biological activity (100). To date, there are four cancer types in which HSV-1716 is used in clinical trials (73). In general, the virus is well tolerated but shows little viral replication due to the low doses used. An upcoming trial will include increasing doses or repeating treatments (73).

Double mutated o-HSV

NV1020 (named also R7020) carries the deletion of a 15-kb region at the UL/S junction encompassing one copy of the diploid genes $\alpha 0$, $\alpha 4$, and $\gamma 134.5$ encoding the proteins ICP0, ICP4, and ICP34.5, respectively, and one copy of *UL56*, the protein product of which has not been fully characterized but is thought to be involved in neuroinvasiveness of HSV-1. It was originally designed to be a vaccine against HSV-1 and HSV-2 infection but it provided unsatisfactory results. The removed region was replaced with a fragment of HSV-2 *U_S* DNA (*U_S2*, *U_S3*, *gJ* and *gG*) creating an intertypic recombinant (97). NV1020 has been used as an oncolytic agent against various non CNS tumors like prostate and head and neck (97, 101). The virus is replication competent but highly attenuated (101). It is the first engineered HSV administered through vascular infusion for treatment of human cancer in a phase I trial. Using an intra arterial pump (hepatic artery), NV1020 was injected in 12 HSV seropositive patients with liver metastases derived from a primary colorectal tumor (three cohorts 3×10^6 , 1×10^7 and 1×10^8 pfu). All the enrolled patients had previously failed chemotherapy. One month after virus administration they started an intra arterial chemotherapy (floxuridine plus dexamethasone). The

virus was well tolerated, made the tumors responsive to chemotherapy again and show biological activity with tumor size reduction, decrease in carcinoembryonic antigen (CEA, colorectal tumor marker) and lack of immunoreactivity (101). The results of a phase II study on liver metastases has been reported by Geevarghese et al., (102). Patients treated with NV1020 showed hepatic metastases stabilization and have become sensitive to chemotherapy again. After one month from the first virus infusion it is noteworthy that a considerable increase in NV1020 neutralizing antibody occurred without significant adverse effects.

G207 derives from strain F and is deleted in both copies of ICP34.5 and has a LacZ insertion within U_L39 (ICP6) locus causing its inactivation. U_L39 encodes the large subunit of ribonucleotide reductase that is required for nucleotide synthesis in quiescent cells like neurons while its enzymatic function is balanced by its cellular enzyme counterpart in rapidly dividing cells (73, 103). The intracerebral inoculation of G207 in murine and simian primates was not pathogenic. It was the first oncolytic HSV admitted to clinical trials in the United States (104). The safety of G207 has been documented in a phase I trial involving 21 patients with recurrent glioma, treated with stereotactic administration up to the highest possible dose (3×10^9 pfu). No acute, moderate or severe toxicity were observed and the maximum tolerated dose could not be determined (104). The first clinical study had some limitations (e.g. single site of inoculation, no *in vivo* assessment of viral replication) that were overcome in a phase Ib clinical trial in recurrent malignant glioblastoma. The study aimed to confirm virus safety after direct cerebral injection adjacent to the tumor or the resected tumor, and after multiple-injections as well as the virus spread into the tumor and the degree of patient immune response (105). The study was conducted on six patients with recurrent glioblastoma. The virus was administered through a catheter stereotactically implanted into the tumor. First, 13% of a total dose of 1.15×10^9 pfu was injected; second, either 2 or 5 days later the tumor mass was resected and the remaining part of G207 was injected in the brain surrounding tumor cavity. G207 infected and replicated and the patient who showed the highest grade of replication had the longest survival. Seroconversion of three seronegative patients occurred and there was immunohistochemical evidence of lymphocyte infiltration into the tumor following G207 administration (93, 105).

G47 Δ derives from G207 and carries an additional deletion in the α 47 gene. The protein ICP47 is responsible for inhibiting the transporter associated with antigen presentation (TAP). In infected cancer cells, ICP47 deletion induces an increased expression of MHC class I and consequently enhanced antitumor immunity through antigen presentation (24). The deletion places the late U_S11 gene under control of the immediate-early α 47 promoter. U_S11 product suppresses the reduced growth properties of γ 34.5-deficient mutants, precluding the shutoff of protein synthesis (9, 106). In most of the cell lines tested, G47 Δ replication is better than G207 with an increased viral yields and a greater cytopathic effect (104). G47 Δ efficacy was seen in different animal models of several tumors (breast, prostate, brain) (104). Recently the combination of G47 Δ and the alkylating agent temozolomide (TMZ) has been seen acting synergistically in killing glioblastoma stem cells (GSCs) in mice with GSC-derived intracranial tumors (107). Moreover systemic administration of G47 Δ by tail vein injection was effective in inhibiting the growth of established breast cancer lung metastases in Balb/c nude mice (108). In Japan, a clinical trial of patients with recurrent glioblastoma is ongoing (104).

A limitation of $\Delta\gamma$ _{134.5} HSV is that protein synthesis and replication are limited, and a concerning situation is the heterogeneity of the tumor. $\Delta\gamma$ _{134.5} HSV is effective in tumor with a

low PKR activity but certain type of tumor present high activity of this enzyme. The expression of PKR has been seen to correlate inversely with MAPK/ERK kinase (MEK) expression.

Cell lines transduced with a constitutively active MEK were susceptible to R3616 that carries the deletion of both copies of $\gamma_134.5$ in strain F backbone. The virus, administered by systemic delivery (intra-peritoneum), showed greater oncolytic activity in xenografted tumors with higher level of MEK compared to tumors with low expression of MEK (109).

To overcome the problem of MEK expression, two recombinant HSV (C130 and C134) were generated carrying inhibitors of PKR activity *TRSI* and *IRSI* respectively in place of $\gamma_134.5$ gene. The two viruses were able to restore late viral protein synthesis and did not show neurovirulence. Their antitumor activity was greater than in parental virus at lower doses; improved survival was demonstrated in a human malignant glioma in severe combined immune deficient (SCID) mice and a syngeneic immunocompetent murine neuroblastoma model (110).

Armed HSV: as mentioned before, HSV has the advantage of being able to host large transgenes in its genome. The introduction of cytokines into HSV should augment the antitumor immunity induction and potentiate cancer clearance. Viruses with IL4 in place of $\gamma_134.5$ gene showed higher antitumor activity and increased survival of mice with intracranial tumors. Immunohistochemical analyses for tumor revealed infiltration by macrophages and CD4+ and CD8+ T cells (73, 104, 111).

IL-12 is another cytokine employed for boosting local immune response. It is expressed by cells that present antigen, lymphocytes B and monocytes. One of its properties is to enhance oncolytic activity, recruiting natural killer cells and cytotoxic T lymphocytes, as much as the development of a TH-1-type immune response mediated. A likely second mechanism for its antitumor activity is its antiangiogenic properties (74). Two HSV have been engineered to express and secrete IL-12.

M002 is a conditionally replication competent virus generated through the deletion of both copies of $\gamma_134.5$ which were replaced with murine IL-12 (74). It was tested in murine brain tumors (neuroblastoma) through stereotactic injection and it showed an increase of the median survival time of mice compared to controls. The immunostaining of explanted brain tissues revealed a great infiltration of CD4+ lymphocytes as well as CD8+ cells and macrophages (74).

NV1042 was generated from NV1020 with the introduction of murine IL-12 in the deletion of the joint region of the long and short sequence (112). It was evaluated in preclinical studies of several cancer types e.g. murine model of prostate cancer, colorectal cancer, colorectal metastatic liver cancer and prostate cancer that creates metastasis in the lung (113-115). The results of experiments in transgenic TRAMP mice, that develop primary tumor spontaneously or metastatic prostate cancer, showed the efficacy after intravenous (i.v.) administration. In particular the virus was able to reduce the frequency of tumor growth and the formation of lung metastases (113). Compared to NV1034, a virus that shares the same backbone but expresses GM-CSF, NV1042 has higher oncolytic activity at low doses for intratumoral injections in colorectal cancer (115).

Another cytokine used in arming HSV has been the granulocyte-macrophage colony-stimulating factor. It acts as a differentiation promoter in monocytes, macrophages, neutrophils and eosinophils from myeloid precursors cells and stimulates the proliferation of dendritic cells. It also acts as a vaccine adjuvant by stimulating the expression of IL-1 and acting as a growth factor for antigen presenting cells (116). Thus, in oncolytic virotherapy GM-CSF may contribute in enhancing the immune response induced by cells lysed after infection.

Oncovex is an attenuated HSV 1 derived from a fresh clinical isolate (JS-1) to avoid the use of laboratory strains that after many passages may have lost some of their oncolytic potential (24). The virus carries the deletion of ICP47 and both copies of $\gamma_134.5$ replaced with GM-CSF (117). Oncovex has already been tested in phase I clinical trials in several tumor types (breast, melanoma, colorectal, head and neck cancer) showing significant antitumor effect (117). The phase II studies have been completed in metastatic melanoma with many injections (about 10^8 pfu up to 24 administrations in some cases). In general, virus administration showed increased survival percentage of patients with low side effects. The most important result was the efficacy in sites distant from virus injection pointing out a systemic anti tumor immunity (118). Considering the results obtained, the phase III clinical trial has been promoted.

Retargeted α -HSV: A correlated problem to attenuated HSV vectors has been their low replication in dividing cells as well as their poor ability to kill tumor cells at low doses(119). The viral spread is also reduced and because these viruses cannot overcome host defenses in normal cells their activity depends in large part on the tumor genotype. A different approach has been to create replication competent non attenuated viruses targeted to tumor specific receptors. A selective tropism should make viral attenuation not as necessary (73). This goal has been achieved through modifications that impaired the first viral step of life cycle like attachment and binding to cellular receptors. Deletion of HS binding sites on gC (N-terminal) and gB (polylysine tract) removes the ability of HSV to bind glycosaminoglycans on cell surfaces. The first attempt to retarget HSV in this way was obtained through the deletion of an HS binding site followed by the fusion of N-terminal of gC with erythropoietin (EPO) (120). The resulting virus KgBpK⁻gC⁻ was not able to make a productive infection but showed a reduced ability to bind GAG, a specific binding to EPO receptor and an acquired ability to stimulate EPO dependent cell lines (FD-EPO) (24, 121). However, gD of EPO retargeted virus could still interact with its cognate receptors.

Retargeting through genetic engineering of gD fused to a heterologous molecule was used to modify the spectrum of HSV receptors. The IL13 α R is expressed in malignant glioma and can be a good target for oncolytic virotherapy. R5111 is a non attenuated replication-competent virus that carries IL-13 between aa 24-25 of gD (119). The virus is able to enter cells that express IL13 α 2R but it still retains the ability to infect through HSV receptors. R5141 is a further modification of R5111 in which the ability to use nectin-1 and HVEM has been ablated by the deletion of the signal peptide of gD, the deletion of its first 32 aa, and the introduction of the amino acid substitution V34S. The retargeting was achieved introducing the sequence of IL13 in 1-32 deletion. R5141 was able to infect cells expressing IL13 α 2R and not cells expressing nectin-1 or HVEM separately (122). R5181 was another virus engineered according to the same strategy through the insertion of urokinase-type plasminogen activator and no deletion in gD gene. UPAR is expressed in glioma cells and differently from IL13 receptor has not a transmembrane domain but binds to membranes through a GPI anchor. The virus can interact with cells expressing only uPA receptor, but retains its natural tropism. However, these were proof of the principle that the retargeting of HSV is feasible and can be applied to retarget HSV to a number of tumor specific receptors (with or without transmembrane and cytoplasmatic domain). R5181 was further modified to make it similar to the IL13 recombinant virus R5141. In this attempt it was discovered that the 61-218 sequence do not execute a function required for

HSV-1 entry into cells. Based on these demonstrations Menotti et al. constructed fourth generations of HSV retargeted to HER2 receptor through a scFv anti HER2 (44, 80, 123). The characteristics of this receptor will be discussed in the next chapter. The first recombinants obtained were R-LM11 and R-LM11L (123), carrying the scFv against HER2 between aa 24-25 of gD. They were able to infect cells expressing HER2 as a sole receptor but retained the ability to enter in J-nectin-1 cells. The first recombinants demonstrated that it is possible to exploit the characteristic of antigen-antibody binding to retarget HSV. In addition, it surprisingly demonstrates that gD is able to tolerate large insertions as the scFv is as large as gD itself. The second and third generation of retargeted HSV consist of viruses carrying single or multiple mutated residues responsible for binding to nectin-1, in particular D215G, R222N, F223I and V34S substitutions (R-LM39). The mutations did not work in ablating the binding to nectin-1, in fact R-LM39 was still able to infect cells expressing the receptor. The fourth generation engineering was based on knowledge inferred by the 3-dimensional structure of gD: it was supposed that the insertion of a large insert such as scFv in the deletion of aa 6-38 of gD could sterically mask the nectin-1 binding site better than the previous position (between 24-25) which was lateral to the site of interaction. Moreover, the scFv size could make the interface between virus gD and nectin-1 inaccessible. The resulting virus R-LM113 confirmed the hypothesis, in fact it was completely retargeted to cells expressing HER2 as sole receptor (80). Furthermore, it showed to be fully detargeted from both nectin-1 and HVEM.(37, 44)

Table 1.2 - O-HSV generated and applications in oncolytic virotherapy

<u>Oncolytic HSV</u>	<u>Engineered mutation(s)</u>	<u>Tumor type</u>	<u>Clinical trials</u>	<u>Ref</u>
dlsp _{tk}	tk			(96)
HSV1716	γ_1 34.5 gene deletion (both copies in strain 17)	Recurrent glioblastoma	<u>Completed: I and I/II.</u>	(124)
		Metastatic melanoma Oral squamous cell carcinoma	<u>Completed pilot</u> <u>Completed: II</u>	(125) (100)
<u>R3616</u>	γ_1 34.5 gene deletion (both copies in strain F)	Pancreatic cancer		(126)
<u>NV1020</u>	15 kbp region in U _L /U _S junction (deletion of α_0 , α_4 , γ_1 34.5 and U _L 56 genes)	Prostate Head and Neck Colorectal cancer liver metastases failing the first-line chemotherapy	<u>Completed:I and II</u>	(102, 127)
<u>G207</u>	γ_1 34.5 gene deletion (both copies in strain F), U _L 39	Recurrent glioblastoma	<u>Completed: I and Ib/II</u>	(105, 128)

	deletion			
<u>G47Δ</u>	γ_1 34.5 gene deletion (both copies in strain F), U _L 39 and α 47 genes deletion	Glioblastoma	<u>Ongoing</u>	<u>(104)</u>
M002	γ_1 34.5 gene deletion replaced by mIL-12	Glioma		<u>(129)</u>
NV1042	15 kbp region in U _L /U _S junction (deletion of α 0, α 4, γ 134.5 and U _L 56 genes) replaced by mIL12	Prostate, colorectal, colorectal cancer liver metastases and prostate cancer lung metastases		<u>(97, 113, 115)</u>
<u>Oncovex</u>	ICP47 deletion and both copies of γ_1 34.5 gene deletion replaced by GM-CSF	Solid tumors with cutaneous and s.c. tumor deposits Head and Neck cancer Unresectable stage IIIc/IV melanoma	<u>Completed: I</u> <u>Completed: I/II</u> <u>Completed: II</u>	<u>(130)</u> <u>(131)</u> <u>(132)</u>

1.9 Tumor specific receptors

1.9.1 HER2 receptor

The human epidermal growth factor receptor 2, called also ERBB2, HER2/neu or c-erbB2, is a type 1 transmembrane tyrosine kinase belonging to a closely related family of 4 cell surface receptors (ERBB 1, ERBB 3, ERBB 4). HER2, as all other members of the ERBB family, consists of an extracellular ligand binding domain, a single α -helical transmembrane portion and a cytoplasmic tyrosine kinase domain. The extracellular portion is in turn subdivided into four domains (Fig. 1.9). Domain I and III are normally involved in peptide binding whereas the domain II is essential in homo- or heterodimerization that triggers the internal signaling cascade. The HER2 distinctive feature is how the domains are spatially organized in the ectodomain. In absence of ligands, ERBB1, ERBB3 and ERBB4 take on a close conformation where domain II, located near domain IV, is not available to take contact with other receptors. Conversely, HER2 exists in a fixed open conformation that is similar to ligand-activated receptor state: the interaction between domain I and III is present while the domain II–IV interaction does not occur. In this way domain II results constitutively exposed (Fig. 1.9) (133). This arrangement

makes HER-2 unable of binding to a ligand and a suitable partner for heterodimerization with other family members. ERBB3 receptor seems to be the favorite.

HER2 has the strongest catalytic kinase activity and HER2-containing heterodimers have the strongest signaling activity (134). The HER2 dimerization activates signaling cascade that regulate cell proliferation, survival, invasion and angiogenesis (Fig. 1.10) (135). In particular, HER2 activation and signaling play an essential role in embryogenesis of the heart demonstrated by the fact that embryos lacking of HER2 receptor die for the onset of myocardium dysfunction in the maintaining of blood flow (136). HER2 is poorly expressed in normal adult tissues with the exception of the heart.

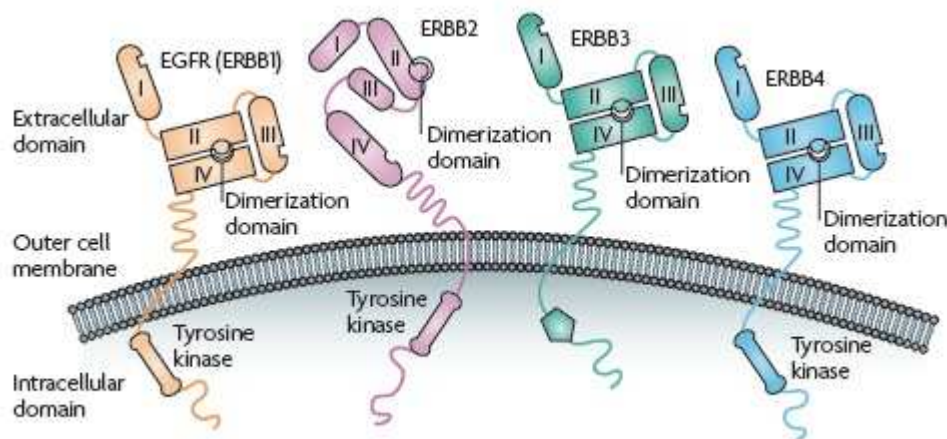


Figure 1.9 – Domain organization of ERBB receptor family. ERBB1,ERBB3 and ERBB4 exist in a closed conformation where in absence of ligand the domain II is not exposed and not available for the interaction with other receptor. ERBB2 exist in an open conformation permanently available for dimerization (137).

A potent mitogen signal is associated with HER2 receptor activation. The receptor is able to bind to a great amount of phosphotyrosine-binding proteins such as the growth-factor-receptor bound-2 (GRB2) and Src-homology-2-containing (Shc) (Fig. 10). These adaptor proteins mediate in turn the recruitment of Ras and activation of the mitogen-activated protein kinase (MAPK) cascades. This signaling lead to activation of transcription factors which regulate genes that affect various cellular function (Fig. 10) Furthermore, heterodimers containing HER-2 show an enhanced affinity and specificity to several ligands (133).

HER2 receptor was found to be overexpressed in about 18-25% of human breast cancers and its amplification occurred also in ovarian cancers, gastric carcinoma, a small proportion of non-small cell lung tumors and salivary gland tumors (137). HER2 amplified breast cancer are characterized by an increasing in proliferation rates, more aneuploidy, tendency to metastasize to CNS and viscera, resistance to endocrine therapy as well to a poor prognosis (134). Breast cancers can arrive up to 25 to 50 copies of the HER2 gene and up to a 40 to 100 fold increase in HER2 protein. The difference in expression between tumor and healthy tissues makes this receptor an ideal target for cancer therapy. Early experiments showed that mAb against the receptor extracellular domain were able to inhibit tumor growth in cancer cells overexpressing HER2 (137).

Two drugs are currently FDA-approved for treatment of HER2-positive cancers.

Trastuzumab is a humanized monoclonal antibody that recognizes the domain IV of HER-2 extracellular domain. It seems to affect highly tumors with increased HER2 homodimer. The mechanism of action is still unclear but it seems to inhibit the receptor signaling, to disrupt HER2/Src interaction as well as to cause the internalization and downregulation of the receptor. This antibody was used in combination of chemotherapy with promising cytotoxic results. For example doxorubicine is more effective in combination with trastuzumab because of coamplification with HER2 of its target topoisomerase 2 (134). Several large clinical trials have shown that administration of trastuzumab in the initial adjuvant (post-surgical) setting in combination or sequentially after chemotherapy results in an improvement in disease-free survival with a 50% reduction of the risk of relapse as well as overall survival (137).

Lapatinib is an oral small inhibitor of tyrosine kinase activity of HER1 and HER2. It is effective in tumors resistant to trastuzumab as showed by a phase III study in which patients who had previously failed therapy with anthracycline, taxane and trastuzumab had a significant improvements after lapatinib administration in combination with capecitabine (135).

Trastuzumab and lapatinib are also synergistic in preclinical models, suggesting that these agents could be combined in the clinic (138).

Other monoclonal antibodies against HER2 are under investigation to be used as therapeutic agent. Pertuzumab (Genentech/Hoffmann-La Roche) is a humanized monoclonal antibody that binds to an epitope in domain II. It acts through the inhibition of signaling cascade and has shown excellent activity *in vitro* against several breast cancer cell line that express ERBB ligands and *in vivo* against human breast cancer xenograft tumors (137).

One of the last therapeutic approach for HER2 positive tumor is the use of scFv antibody that bind specifically to the receptor. Recently recombinant immunotoxins, consisting of single-chain variable fragments (scFv) anti-Her2/neu fused to recombinant gelonin (rGel) were evaluated for the effect on antitumor efficacy and off-target toxicity *in vitro* (139).

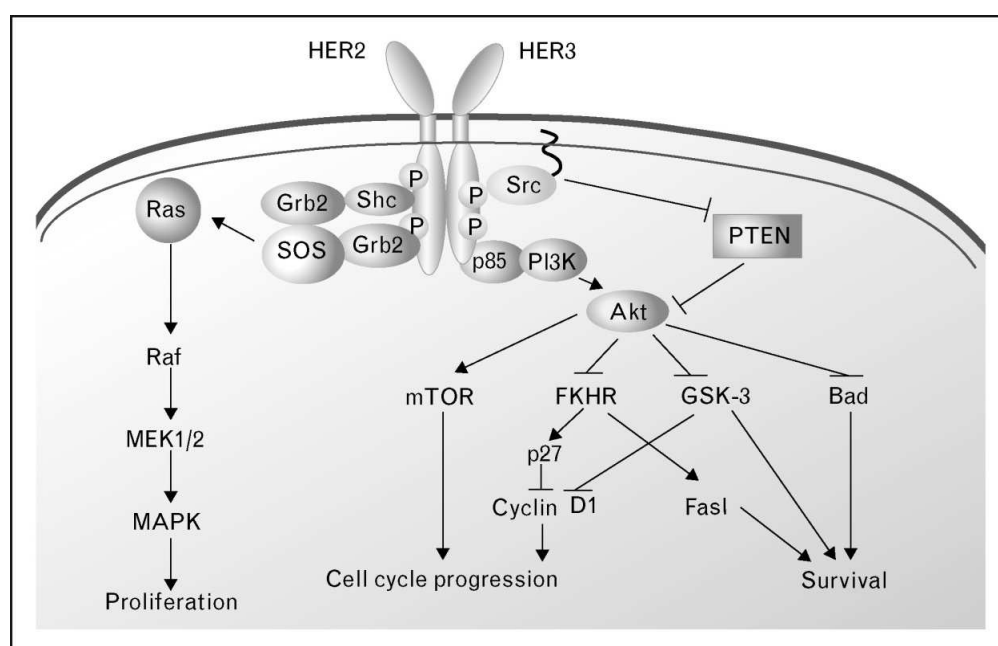


Figure 1.10 - Signaling cascade after HER2 dimerization. After ligand binding, dimerization occurs leading to activation of the intracellular tyrosine kinase. HER2 can create homo or heterodimers with other members of HER family. FKHR, forkhead in

rhabdomyosarcoma; Grb2, growth factor receptor- bound protein 2; GSK-3 glycogen kinase synthase-3; MAPK, mitogen-activated protein kinase; mTOR, molecular target of rapamycin; PI3K, phosphatidylinosito 3-kinase; PTEN, phosphatase and tensin homologue deleted on chromosome 10; SOS, son- of sevenless guanine nucleotide exchange factor (135).

1.9.2 PSMA receptor

The prostate specific membrane antigen (PSMA) is a 100 kDa type II membrane glycoprotein. Human PSMA gene was cloned by means of the 7E11mAb from human LNCaP cell line and was found to be located in chromosome 11p11-12. The protein consists of an extensive extracellular domain, spanning from amino acids 45 to 750, a single hydrophobic transmembrane domain (aa 20-44) and a short NH₂ cytoplasmatic tail (aa 1-19). The extracellular domain is glycosylated contributing to 25% of the protein molecular weight (Fig. 1.11). The short cytoplasmatic tail carries a short internalization motif MXXXL. The receptor undergoes internalization and recycling at high rate especially when it is bound by antibody J591(140). The PSMA endodomain interacts with actin binding Dilamin a (FLNa) that maintain the receptor anchored to plasma membrane decreasing the internalization rate of 50% (140). PSMA is expressed as a non covalently linked homodimer on the cell surface. And was demonstrated that the dimerization is critical to maintaining the conformation and enzymatic activity of PSMA (141). PSMA has different names that reflect its role in several cellular pathway as in prostate carcinogenesis and progression, glutamatergic neurotransmission and folate absorption (140). PSMA name derived from its strong expression in the prostate, NAALADase is due to its ability to metabolized the N-acetyl-aspartyl-glutamate neurotransmitter in the brain, folate hydrolase FOLH1 because it removes glutamates form poly-g-glutamated folate in the small intestine and is also named glutamate carboxypeptidase II, GCPII as a carboxypeptidase (140). PSMA is mainly expressed in glandular cells of the secretory acinar epithelium in normal prostate and immunohistochemical analysis revealed its expression also in kidney, brain, skeletal muscle, colon heart or breast(142), even if the staining is much less intense than in prostate. The amount of PSMA in these tissues was estimated three orders of magnitude less than in prostate (141).

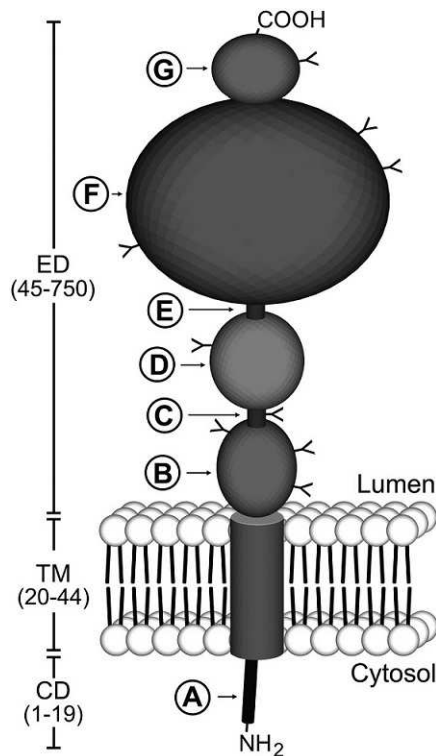


Figure 1.11 – Schematic PSMA structure The type 2 transmembrane protein consists of a small intracellular domain (CD), a single hydrophobic transmembrane domain (TM) and a large ectodomain (ED). A- endocytic targeting motif and filamin A (FLNa) binding site. Y- nine predicted ectodomain N-glycosylation sites. B-D- domains of unknown function that encompass aa 44-150 and 152-274 respectively. C-E proline and glycine rich regions. F-G- catalytic domain aa 274-587 and a final domain of unknown function from 587 to 750 with a helical dimerization domain (141).

The receptor has been described several times upregulated in prostate cancer and its increase correlates with more aggressive tumor forms (143). The analysis of resected tumors showed that high expression of PSMA matched with high relapse percentage in short time. PSMA is also expressed in the tumor-associated neovasculature of solid tumors while it is absent in normal vascular endothelium. The anti PSMA antibody J591 has successfully employed to targeting neovasculature of solid tumors *in vivo*. In a recent paper Wrenicke et al. reported that 32 specimens from GBM patients exhibited positive staining for PSMA (144).

PSMA expression was found to be suppressed by androgen (145). This feature makes it a good target as a therapeutic agent because normally patients undergo androgen deprivation therapy.

PSMA has been exploited as antigenic target for a variety of clinical application because of its large ectodomain and specific tissue expression. ProstaScint[®] (Citogen) was the first mAb FDA approved as imaging molecule. It binds to an intracellular epitope highlighting only dead or necrotic cell and this feature was used to reach viable cells in proximity to dying tumor cells in soft tissues (143). It is less effective in identifying bone metastases because low dead cell percentage is present (141). The second generation of antibodies is still under investigation.

J591, a humanized monoclonal antibody against the extracellular domain of PSMA was conjugated with radionuclides and cytotoxic drugs (146, 147). The scFv to PSMA derived from J591 has been employed as targeting agent in measles virus. scFv was inserted as a C-terminal extension on the MV attachment protein. The PSMA virus induced tumor regression of LNCaP and PC3-PSMA tumor xenografts (148). It has recently been reported that J591 linked to the

saporin toxin of *Saponaria officinalis* shows a potent and selective antitumor effects on PSMA-positive cells *in vitro* and *in vivo* (149). Moreover, this antibody labeled with a 177 Lu is still in phase II trials (150).

PSMA likely has a role in cell adhesion in fact PSMA expressing cells are resistant to proteolytic disassociation when grown on bone marrow matrix. This feature could explain why bones are the preferential site of prostatic metastases (151).

1.9.3 EGFRvIII receptor

As mentioned in 1.9.1 paragraph, epidermal growth factor receptor (EGFR, ErbB1 or HER1), a 170-kDa transmembrane glycoprotein belongs to a closely related family of 4 cell surface receptors. EGFR is involved in cellular proliferation pathway and has a trophic effect on several cells. Wt EGFR gene amplification occurs with 36% to 40% of frequency in GBM and its expression at high levels correlates with various types of cancer (152). Of this 36% - 40% more than a half has rearrangements of the EGFR gene. The specific mutant form of EGFR receptor, EGFRvIII, is highly expressed on many glioblastomas, breast carcinomas, and other tumors and is associated with increased invasiveness and growth rate of tumors. This mutated receptor forms resulted in the deletion of exons 2 to 7. The result is an in frame deletion of 26 amino acids from the ectodomain of the receptor (Fig. 1.12). In place of the deletion a glycine codon, absent in the protein wt form, is generated. This transcript arises from an aberrant splicing explains why the sequence is the same despite the variable sequence losses in the amplified genes (153). Several antibodies have been described that are specific to EGFRvIII and do not cross-react with wild-type EGFR (154). EGFRvIII expression has no effect on survival of GBM patients but is predictive of GBM-like clinical behavior. The deletion in EGFRvIII ectodomain results in a constitutive tyrosine kinase activity because the receptor is unable to bind any known EGFR ligand (155).

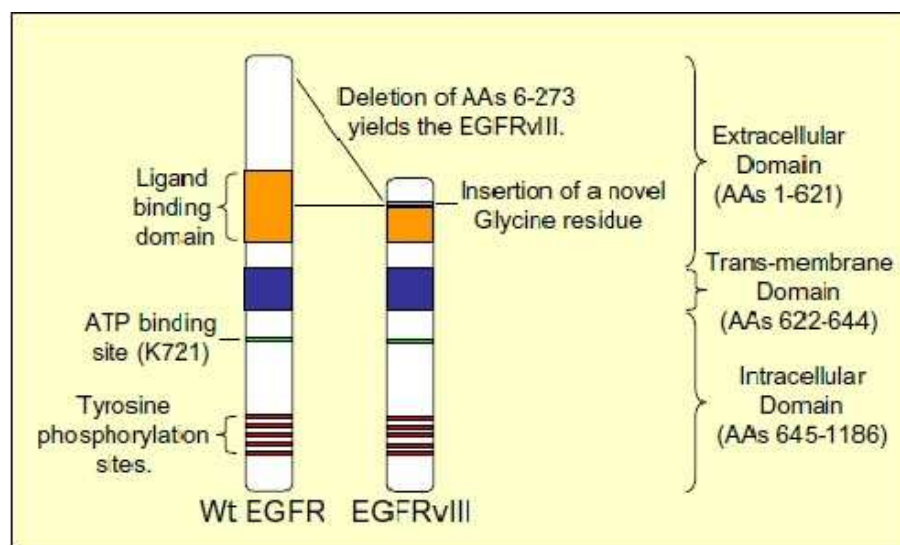


Figure 1.92 - Comparison of the structures of the EGFR and EGFRvIII. The EGFRvIII variant receptor is characterized by a deletion of exons 2–7 of the wild type (Wt) EGFR gene. A new glycine residue is inserted at the fusion junction.

EGFR does not appear to be ever present in not transformed tissues, appearing as a completely specific tumor marker, expressed in high quantities enough to be a potential therapeutic target. The ectodomain deletion abolishes the receptor ability to interact with the ligands but makes it able to dimerize stably. The constitutive activation resulting in activation of the kinase domain resulting in stable phosphorylation of tyrosine residues on the C-terminal tail.

The internalization of EGFRvIII is reduced compared to the wt form of the receptor probably due to the absence of the ligand. In this way, the mutated receptor has a longer residence time on the cell surface, prolonging its effect signaling. *In vivo* it was highlighted that EGFRvIII confers a greater proliferation capacity and a cellular resistance to apoptosis. This ability seems to result from preferential activation and signaling mediated by PI3K, as regards the resistance to apoptosis appears to be involved the Bcl-XL activation (member of the Bcl-2) (155) (Fig 1.13).

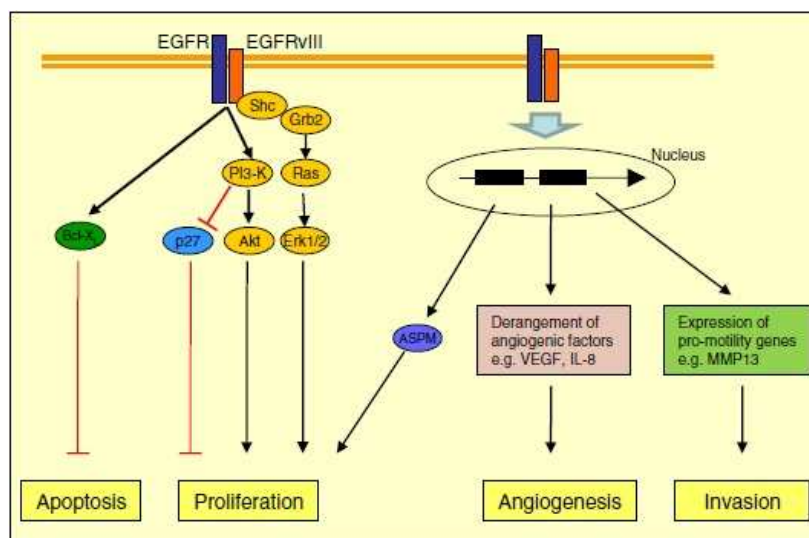


Figure 1-13 - The epidermal growth factor receptor (EGFR)vIII confers enhanced glioblastoma multiforme (GBM) tumorigenicity through several key mechanisms. The EGFRvIII receptor increase cell proliferation through promotion of PI3K/Akt signalling; Shc and Grb2 association and Ras activity while inhibiting cell cycle regulators such as p27KIP1 and upregulating abnormal spindle-like microcephaly-associated (ASPM) expression. Furthermore, EGFRvIII promotes survival in cells by increasing expression of anti-apoptotic proteins such as Bcl-XL, and enhances angiogenesis and cell invasion by un-regulating vascular endothelial growth factor (VEGF), interleukin-8 (IL-8) and matrix metalloproteinase 13 (MMP13) expression. Red lines with blunt ends indicate inhibitory effects; black lines with arrow heads indicate stimulatory effects.

2. Objective

The aim of this thesis has been the genetic engineering, characterization and anti-tumor efficacy *in vitro* and *in vivo* of oncolytic HSVs retargeted to tumor specific receptors. Retargeting implies the modification of viral tropism in order to make HSV-1 able to recognize and bind only to the cancer receptors for which it was engineered. At the same time the HSV-1 was rendered unable to recognize its natural receptor (detargeting), HVEM and Nectin-1 (Fig. 2.1). In particular, three tumor cancer-specific receptors were selected: HER-2 receptor, highly expressed in ovarian, breast cancer and in glioma multiforme (viruses R-LM249 and R LM113 and R-LM291); PSMA receptor (virus R-LM593), over-expressed in prostate cancer and neovasculature of solid tumors; and EGFRvIII (virus R-LM613), expressed in gliomas.

The devised strategy has made use of (i) in-depth knowledge of glycoprotein gD of HSV, which determines viral tropism, (ii) the availability of single chain antibodies against the examined receptors and (iii) technology for o-HSV-1-BAC engineering.

Receptor specific single chain antibody was inserted in gD in two positions: N-terminus (deletion 6-38) in R-LM249 and R-LM291 or in place of the immunoglobulin core (deletion 61-218) in R-LM113, R-LM593 and R-LM613.

I describe:

- (i) R-LM249 genetic engineering to HER2 retargeting and its efficacy against ovary and breast tumor *in vivo*;
- (ii) R-LM113 (HER2 retargeted) efficacy against glioblastomas;
- (iii) R-LM291 (HER2 retargeted) genetic engineering to introduce two mutation in gB for the purpose of improve rate of entry in HER2 positive cancer cells;
- (iiii) R-LM593 genetic engineering to prostate specific membrane antigen (PSMA) and *in vitro* characterization;
- (iiiii) R-LM613 genetic engineering to epidermal growth factor receptor variant III (EGFRvIII) and *in vitro* characterization.

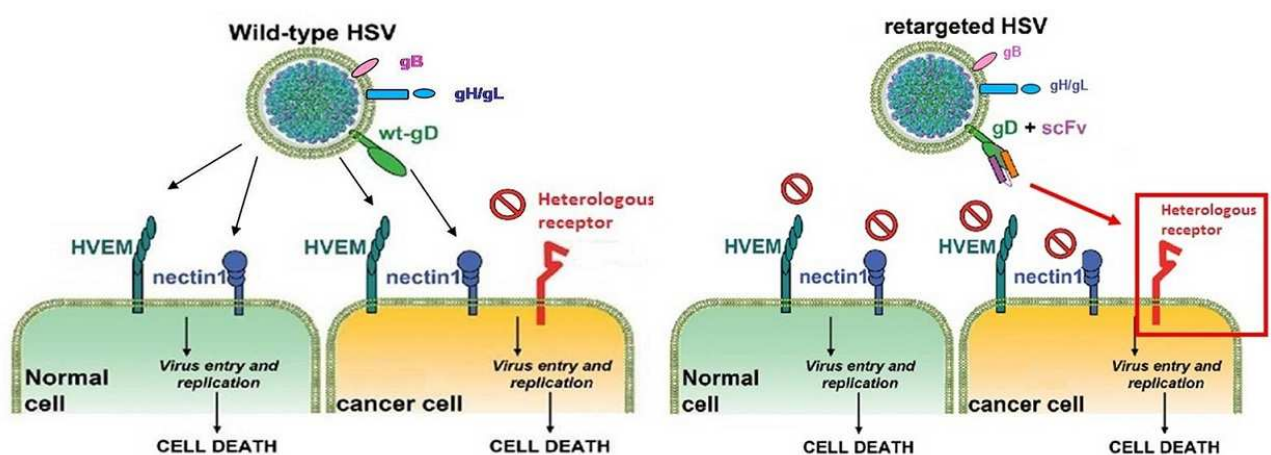


Figure 2.1 - Tropism of an oncolytic HSV detargeted from its natural receptors , HVEM and Nectin-1 and retargeted to a cancer specific receptor, as compared to the tropism of wt HSV (156).

3. Material and Methods

3.1 Cells

In this research these cells have been used:

HER2 positive cells

Human: SK-OV-3 (human ovarian adenocarcinoma), SK-BR-3, BT-474 and MDA-MB-453 cells (human mammary adenocarcinoma) express HER2 at high levels. MCF-7 cells (human mammary adenocarcinoma) have an intermediate HER2 expression level.

Murine: D2F2/HER2 cells are BALB/c mouse mammary tumor cells transduced with the huHER2 gene and 1E-huHER2 cells are a murine mammary carcinoma cell line transduced with the huHER2 gene. FVB 6443.0 cells derived from explanted tumor of a FVB/N HER-2/neu transgenic mouse (Genentech). TT12E2 (mammary carcinoma of rat HER-2/neu transgenic mice) express high levels of rat HER2/neu and were use a negative control.

Hamster: J-HER2 cells derived from J cell stably transfected with plasmid encoding HER2 receptor (79).

PSMA positive cells

LNCaP-FGC (human prostate carcinoma) have a high level of PSMA expression. J-PSMA cells derived from J cell stably transfected with pIRES-PSMA plasmid.

EGFRvIII positive cells

U251-EGFRvIII is a human glioblastoma cell line transfected with pcDNA-EGFRvIII
J-EGFRvIII cells are derived from J cell transfected with pcDNA-EGFRvIII

Other control cells

Human: HEP-2 (human epithelial cells), U251 (human glioblastoma cells), I-143tk- (human) was a derivative the thymidine kinase (tk) positive cell lines R970-5 by selection with BrdUrd (157). SJ-Rh4 (human rhabdomyosarcoma) do not express HER2 and were used as negative control.

Murine: L (mouse fibroblasts), NIH3T3 (mouse fibroblasts).

Hamster: BHK (baby hamster kidney), J cells are derived from BHK tk-. They lack of Nectin-1 and HVEM receptors and are resistant to HSV infection (61).

The following cell lines were generated from J cells after transfection of single receptors: J-Nectin-1, J-HVEM, J-EGFR. They are maintained under constant selection with G418 (400 μ g/ml).

Rabbit: Rabbit skin (RS), RGDp6 (RS expressing glycoprotein D under the control of HSV late promoter γ U_L26.5) (80).

Simian: Vero (green monkey kidney cells).

Cells were grown in Dulbecco's modified Eagle medium (DMEM) supplemented with 5-10% FBS (Gibco), PenStrep (1%; Euroclone) except for SK-OV-3, BT-474, MDA-MB-453 that were grown in RPMI 1640 Ultraglutamine (Lonza) supplemented with PenStrep and 10% FBS heat inactivated at 56°C for 30 minutes. All cells were maintained at 37°C in 5% of CO₂ atmosphere.

3.2 Construction of cell lines expressing heterologous receptors

J cells were transfected with pIRES-PSMA, pcDNA EGFR and pcDNA EGFRvIII to generate J-PSMA, J-EGFR and J-EGFRvIII respectively. Cells were selected with neomycin G418 at a concentration of 400 to 800 µg/ml for 5 days. Single clones were obtained by limiting dilution and were checked for membrane expression of heterologous receptor by indirect immunofluorescence (IFA) with mAb 9G6 (Santa Cruz) for HER2, mAb PMSA cl 1071A4 (MBL), mAb sc-120 for EGFR and EGFRvIII (Santa Cruz) diluted 1:50 in 20% newborn calf serum (NCS) in phosphate-buffered saline (PBS), followed by fluorescein isothiocyanate (FITC)-conjugated anti-mouse IgG (Jackson Immunoresearch).

3.3 Plasmids

pGalK carries the coding sequence of galK enzyme and is described in ref. (158).

pMR1-ENV1 carries the nucleotide sequence of scFv to EGFRvIII. The plasmid was kindly provided by Ian Lorimer, Ottawa Health Research Institute and was described in (159).

pSL1180-scFv-PSMA contains the nucleotide sequence of scFv (J591) to PSMA. The plasmid was kindly provided by Micheal Sadelain, Memorial Sloan-Kettering Institute (160).

pIRESneo-PSMA was kindly provided by Angelo Baccala, Cleveland Clinic.

pcDNA-EGFR I isof a was generated by amplification of EGFR receptor coding sequence from genomic DNA of CHO-EGFR cells (kindly provided by Steve Russell (161) and subcloned in pcDNA 3.1(-) vector (Invitrogen). A 4000 bp PCR fragment was obtained with primers T7 (5'-TAA TAC GAC TCA CTA TAG GG_3') and BGHrev (5'_TAG AAG GCA CAG TCG AGG_3'). The fragment was sequenced with the same primers and aligned with submitted sequence NM_005228 on GeneBank database. The XbaI and HindIII site were used to subclone in pcDNA 3.1(-). Sequence positive EGFR clones were transfected in RS cells and tested for cell surface expression of the EGFR receptor by immunofluorescence.

The EGFRvIII variant receptor is characterized by a deletion of exons 2–7 of the wild type EGFR gene. This results in an in-frame truncation of amino acids 6 to 273 in the extracellular domain of the full length protein EGFRvIII.

pcDNA-EGFRvIII was generated from pcDNA-EGFR. The EGFRvIII coding insert was amplified by PCR using a synthetic oligonucleotide to generate the truncated N-terminal region of EGFRvIII and to insert a XbaI site. These primers were used: Xba_EGFRvIII_f (5'_TGT GCT CTA GAT GCG ACC CTC CGG GAC GGC CGG GGC AGC GCT CCT GGC GCT GCT GGC TGC GCT CTG CCC GGC GAG TCG GGC TCT GGA GGA AAA GAA AGG TAA TTA TGT GGT GAC AGA TCA CGG) and BGH rev (5'_TAG AAG GCA CAG TCG AGG). The fragment of about 3200 bp was subcloned into pcDNA 3.1 (-) in XbaI and HindIII sites.

Sequence EGFRvIII positive clones were transfected in RS cells and tested for cell surface expression of the EGFR receptor by immunofluorescence with mAb anti-EGFR Santa Cruz sc-120 diluted 1:50 in 20% NCS in PBS followed by fluorescein isothiocyanate (FITC)-conjugated anti-mouse IgG (Jackson Immunoresearch).

gB D285N A549T was obtained through mutagenesis of wt gB cloned in pcDNA 3.1(-). The amino acid substitutions D285N and A549T described in (56) and EcoRI (nt 856-861), NheI (nt 1651-1656) as silent sites for clone screening were inserted by means of Quick Change XL Site Directed Mutagenesis Kit® of wt gB in pcDNA3.1 (-) with primers gB_D285N_EcoRI_f (5'_GCT CGG TGT ACC CGT ACA ACG AAT TCG TGC TGG CGA CTG GC_3'), gB_D285N_EcoRI_r (5'_GCC AGT CGC CAG CAC GAA TTC GTT GTA CGG GTACAC CGA GC_3'), gB_A549T_NheI_f (5'_GCA AGC TGA ACC CCA ACA CGA TCG CTA GCG CCA CCG TGG GCC GGC GGG_3'), gB_A549T_NheI_r (5'_CCC GCC GGC CCA CGG TGG CGC TAG CGA TCG TGT TGG GGT TCA GCT TGC_3').

3.4 Viruses

All recombinant HSV-1-BACs in this research were derived from pYEbac102, which carries pBeloBAC11 sequences inserted between U_L3 and U_L4 (162).

R-LM5 was described in (80) and derived from gD⁻-EGFP-HSV-BAC (Fig 3.3.1 A). R-LM5 is a recombinant virus carrying wild-type (wt) gD and an EGFP reporter under the viral promoter α 27 and was generated by homologous recombination in mammalian cells (Fig. 3.3.1 B).

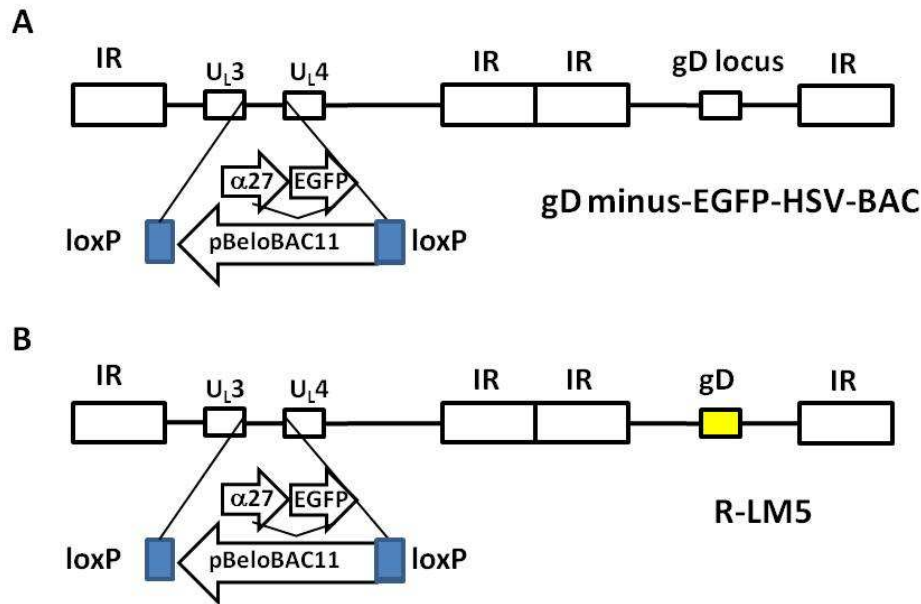


Figure 3.3.1 – Schematic representation of (A) gD minus-EGFP-HSV-BAC and (B) R-LM5 (80).

R-LM113 was described in (80) (Fig. 3.3.2). It was generated from gD minus EGFP-HSV-BAC (Fig. 1 A) and carried scFv to HER2 in place of the deletion aa 6-38 of gD.

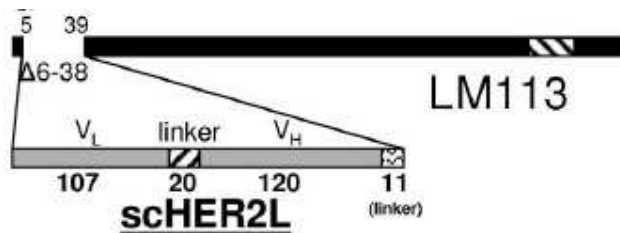


Figure 3.3.10 – gD in R-LM113. scFv HER2 with a 11aa glycine serine linker was inserted in deletion aa 6-38 of gD. V_L and V_H, light and heavy-chain variable domains of the anti-HER2 antibody 4D5 (80).

R-LM249

R-LM249 was obtained by means of 2-step replacement recombination in *Escherichia coli* DH10B strain as described in (44, 163). The pS249 shuttle vector carries the sequence coding for a chimeric glycoprotein gD engineered with a single chain antibody (scFv) anti HER-2 flanked by serine-glycine linkers (upstream 8 aa residues: HSSGGGSG; downstream 12 aa residues: SSGGGSGSGGSG) in place of gD amino acid residues 61 to 218. Mutagenesis and cloning was performed on pLM5, a plasmid containing WT-gD plus 500 bp upstream and downstream flanking sequences (80). First, 2 NdeI sites were inserted in the coding sequence for gD amino acid residues 61–62 and 218–219 of mature gD with mutagenic primers gD_61/62_NdeI_f (5'_ACG GTT TAC TAC GCC CAT ATG GAG CGC GCC TGC C_3') and gD_218/219_NdeI_f (5'_GAC GGT GGA CAG CAT CCA TAT GCT GCC CCG CTT C_3'). Next, an oligo encoding a 9 aa serineglycine linker was inserted in place of the sequence encoding amino acid 61–218 of gD by annealing and ligating into the NdeI cut vector the 2 phosphorylated oligos

P-SG9Bam7/Nde_f (5'_TAG TAG TGG CGG TGG CTC TGG ATC CGG_3') and P-SG9Bam7/Nde_r (5'_TAC CGG ATC CAG AGC CAC CGC CAC TAC_3'), containing a silent BamHI site. The scFv to HER-2 was amplified from pS2019a (164) with primers scFv_Bam_f (5'_GGC TTA TGG ATC CGA TAT CCA GAT GAC CCA GTC CCC_3') and scFv_SG_x37_BamH_r (5'_CGG AGG ATC CAC CGG AAC CAG AGC CAC CGC CAC TCG AGG_3') and inserted into the BamHI site of the serine-glycine linker. Last, the cassette containing the engineered gD, plus gD genomic upstream and downstream flanking sequences was subcloned to pST76KSR shuttle vector to obtain pS249 for homologous recombination in *E. coli* (Fig. 3.3.3). The recipient genome gD⁻-EGFP-HSV-BAC, carrying EGFP as reporter gene, was described in ref. (80). The recombinant virus, designated R-LM249, was reconstituted as described in ref. (44).

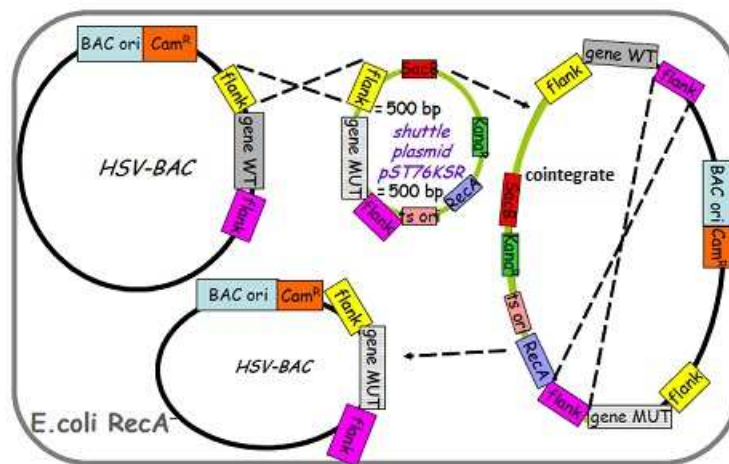


Figure 11.3.3 - Schematic representation of two-step replacement in *Escherichia coli* DH10B.

R-LM291, R-LM593 and R-LM613 construction

GaIK recombineering technology

All the other recombinant HSV-1-BAC viruses reported in this thesis were generated by the gaIK recombineering technique, an efficient galactokinase-based positive/negative selection system (gaIK), that makes it possible to modify BAC DNA via homologous recombination (158). It exploits a modified *E. coli* strain (SW102) deleted for gaIK that makes bacteria unable to grow in medium with galactose as only carbon source. However, the gaIK function can be added in *trans* restoring the ability to metabolize galactose. Further to this, SW102 strain carries λ prophage RED recombination system under the control of a temperature sensitive λ repressor, cI857, that inhibits the expression of recombinases at 30°C. When bacteria are shifted to a temperature of 42°C recombinases are actively expressed and can mediate the recombination between the HSV-1-BAC backbone and the insert carrying transgene flanked by homology sequence arms to the target.

The technology consists of two steps: first, the gaIK gene, amplified from pGalk plasmid, is inserted in the target site on HSV-1-BAC backbone in bacteria via homologous recombination (Fig. 3.3.4A). Bacteria are plated on medium supplemented with chloramphenicol (antibiotic

resistance carried by HSV-1-BAC) and galactose as only carbon source, where only positive galK clones are able to grow (positive selection) (Fig. 3.3.4B). Second, through a second homologous recombination the galK cassette is replaced by a cloned fragment or PCR product carrying the transgene of interest (Fig. 3.3.4C). Electroporated bacteria are plated on medium plates supplemented with chloramphenicol the toxic analogue of galactose 2-deoxy-galactose (DOG) and glycerol as the sole carbon source. DOG is not toxic for bacteria unless phosphorylated by galK. The resulting resistant colonies will be positive for transgene although some background is present consisting of bacteria that have lost galK not introducing the new transgene (Fig. 3.3.4D).

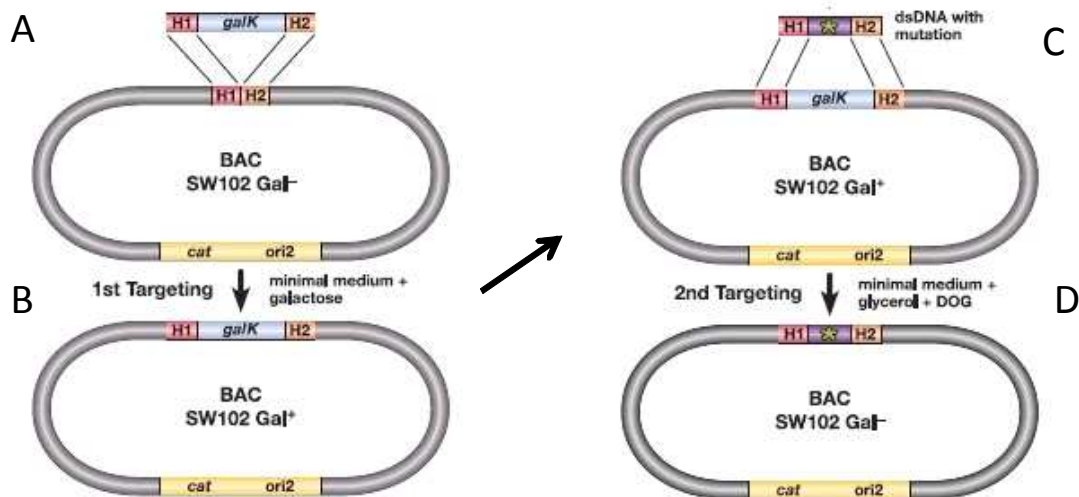


Figure 3.3.12 – GalK recombinering technology. A) Knock-in of galK cassette in BAC recipient and B) selection on galactose plates. C) Knock out of galK cassette and insertion of DNA fragment of interest. D) Counterselection of recombinants on DOG-glycerol plates. *cat*: chloramphenicol acetyltransferase as BAC selection marker. H1 and H2: homology arms in BAC and DNA fragments for homologous recombination. Modified by (158).

GalK protocol

galK knockin

Briefly, the *galK* gene is amplified with primers: forward: 5'-50bp-homology CCT GTT GAC AAT TAA TCA TCG GCA-3' and reverse: 5'-50bp-homology-compl-strand-TCA GCA CTG TCC TGC TCC TT-3' following this PCR protocol: 94°C 15 sec, 60°C 30 sec, 72°C 1 min for 30 cycles. For each 50 µl PCR reaction, 2 µl of DpnI are added, mix and incubate at 37°C for 1 hour in order to remove any plasmid template. The PCR product is gel extracted with Wizard® SV Gel and PCR Clean-Up System (Promega). A single SW102 colony containing the recipient BAC is inoculate in 5 ml of LB low salt with chloramphenicol 12.5 µg/ml at 30°C.

The next day 2 ml of SW102 culture are diluted in 100 ml of LB low salt and chloramphenicol and shaken at 32°C to an OD₆₀₀ of about 0.55-0.6. The culture is then divided in two bottles and left to shake in waterbath at 30°C or 42°C respectively for 15'. The two samples, hereafter called induced and un-induced, are transferred in pre-cooled 50 ml conical tubes and centrifuge at 3000 rpm for 8 minutes at 0°C. The supernatant is poured off from both tubes and the pellet are resuspended in 5 ml of sterile H₂O by gently swirling in ice/waterbath slurry. After resuspension H₂O is added to 50 ml and tubes are centrifuge again. The last step of resuspension is repeated.

After the second washing, the supernatant is completely removed and 50µl of cells are electroporated with 30 ng of galK amplificate in a 0,2 cm cuvette (BioRad) at 25 mF, 2,5 kV and 200 ohms. Bacteria from both induced and un-induced are recovered in 1 ml of LB low salt for 1 hour at 30°C. Then, bacteria are washed twice with M9 salt 1x and plated on M63 minimal media plates supplemented with chloramphenicol 12,5 µg/ml and galactose as carbon source. Plates are left at 30°C.

After about 5 days colonies should be visible only in induced bacteria plates. Single colonies are streaked into McConkey agar plates, supplemented with 1% of galactose and chloramphenicol 12,5 µg/ml, to assess the presence of galK (background colonies will be white/colorless). Red galK⁺ colonies are however screened by colony PCR for galK gene presence with primers galK_129_f (5'_ACA ATC TCT GTT TGC CAA CGC ATT TGG_3') and galK_417_r (5'_CAT TGC CGC TGA TCA CCA TGT CCA CGC_3').

galK knock out

Before starting it is necessary to amplify, digest with DpnI and purify from agarose gel the insert for galK substitution.

Then, red galK⁺ colonies from McConkey agar plates are inoculated in 5 ml of LB low salt and chloramphenicol 12.5 µg/ml and grown overnight at 30°C. The protocol continues in the same manner as the galK knock-in step until electroporation. Then, 50 µl of electrocompetent cells induced and un-induced are electroporated with 200 ng of the amplified insert. The recovery occurs by shaking in 10 ml of LB low salt at 30°C for 4 hours. After two washes with M9 salts, the bacteria are plated on M63 minimal media plates with chloramphenicol 12.5 µg/ml, glycerol as carbon source and DOG 0.2%.

After 5 days colonies are visible both in induced and un-induced plates with or without a great difference in number. This second selection step is less stringent in fact some colonies are background bacteria that have lost galK no introducing the transgene of interest. About 30 colonies are picked up, screened by colony PCR for the desired insert and confirmed by sequence analysis.

Adjustments to galK recombineering protocol

Considering the size of inserts used (scFv of about 800 bp), some changes were made to the original protocol in order to increase recombination efficiency:

- Homology arms between insert and target sequence were lengthened to 400 bp instead of 50 bp.
- DOG concentration was increased to 0.3% to make the selection of the second recombination more stringent
- In the second recombination step 400 ng of template were used instead of 200 ng.

Minimal media and the indicator plates were prepared using following solutions:

Luria-Bertani medium (low salt)

1% Tryptone

0.5% Yeast Extract
 0.5% NaCl
 for agar plates 0.15% of Agar is added.

M9 washing solution (1x)

0.6% Na₂HPO₄
 0.3% KH₂PO₄
 0.1% NH₄Cl
 0.05% NaCl

M63 solution (5x)

1% (NH₄)₂SO₄
 6.8% KH₂PO₄
 0.0025% FeSO₄·7H₂O
 adjust to pH 7 with KOH

Gal positive selection:

1xM63 + agar (15 g/l) + D-galactose (0.2%; Sigma) + D-biotin (1 mg/l; Sigma) + L-leucine (45 mg/l; Sigma) and chloramphenicol (12.5 µg/ml; Sigma).

Gal counterselection:

1xM63 + agar + glycerol (0.2%; Sigma) + D-biotin (1 mg/l) + L-leucine (45 mg/l; Sigma) + DOG (0.2%; Sigma) and chloramphenicol (12.5 µg /ml).

Gal indicator plates: MacConkey agar (Difco, BD Biosciences) + D-galactose (1%) and – chloramphenicol (12.5 µg /ml).

BAC-LM291, BAC-LM593 and BAC-LM613 were generated through galK recombinering technology (Fig. 3.3.5 and 3.3.6).

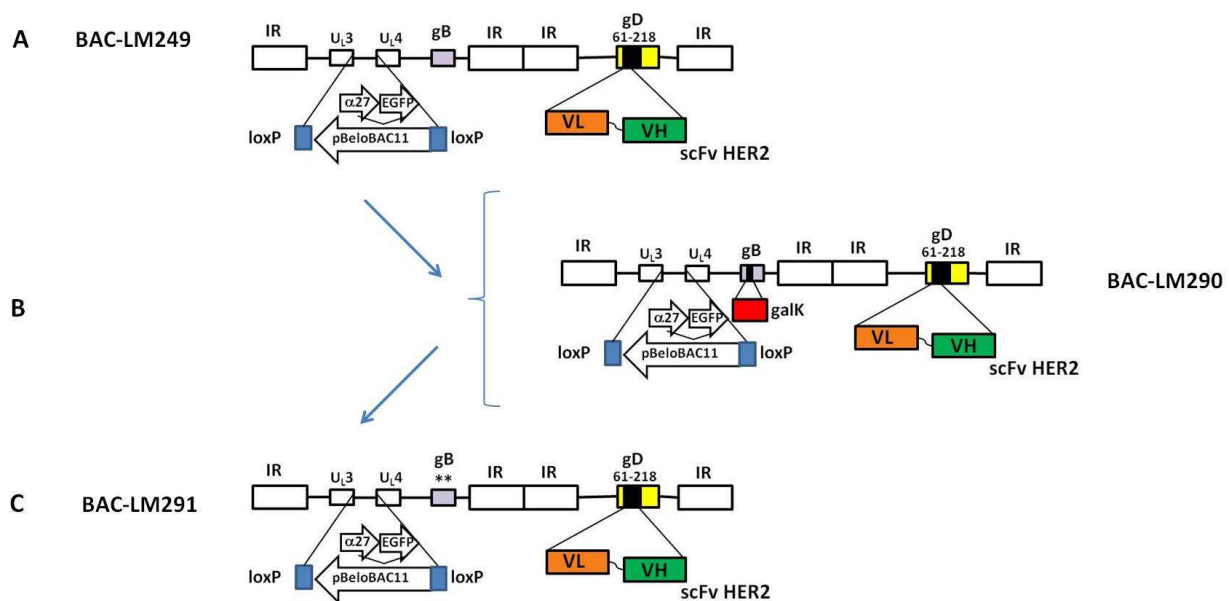


Figure 3.3.13 - Schematic representation of BAC-LM291 generation. A-B) GalK cassette was inserted in gB of R-LM249 (44) between nucleotides 852-1648, generating the intermediate BAC-LM290. C) BACL290 becomes BAC-LM291 after second step of galK recombineering where galK gene was replaced by D285N-A549T insert (primers in table 2).

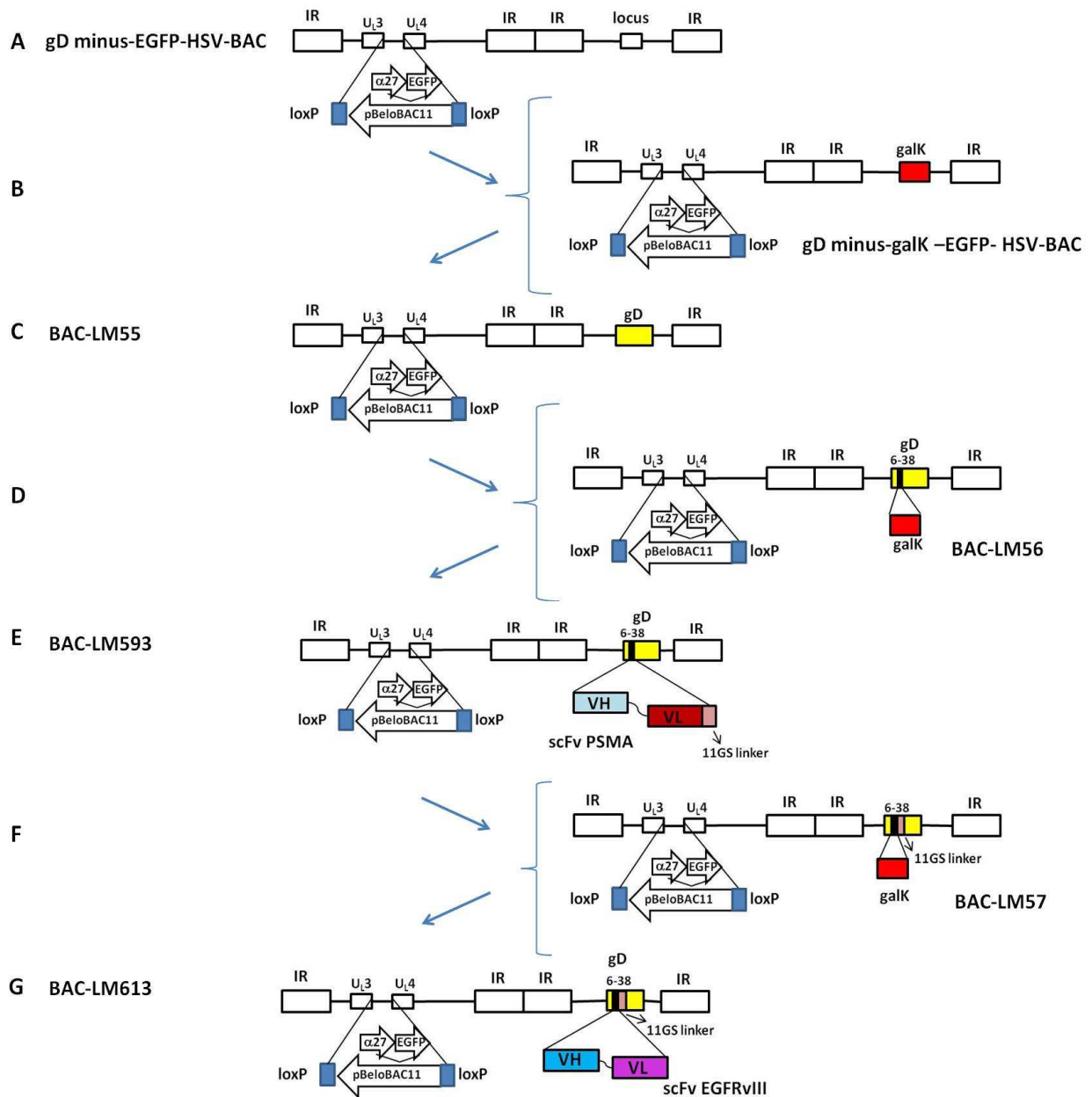


Figure 3.3.14 – Schematic representation of BAC-LM593 and BAC-LM613 generation. A-B) GalK gene was inserted in place of gD locus in gD minus-EGFP-HSV-BAC (80), generating the intermediate gD⁻galK-EGFP-HSV-BAC. C) BAC-LM55 carries the repaired wt-gD after second step of galK recombineering on gD minus-galK-EGFP-HSV-BAC. D-E) In order to insert scFv anti-PSMA in gD, first galK cassette was inserted between amino acids 6-38 of wt-gD in R-LM56 and subsequently the insert was replaced by scFv PSMA in R-LM593 followed by 11GS linker. F-G) In R-LM57, galK gene was inserted in place of scFv PSMA leaving the 11GS (glycine-serine)linker inside gD sequence. Then, galK was replaced by scFv anti-EGFRvIII to generate R-LM63.

Primers used for generation of recombinant viruses in this research are summarized below (Table 3.3.1 and 3.3.2).

Table 3.3.3- Primers for knock in of galK cassette (DNA template is pGalK (158)).

Primer name	Sequence	HSV-1 BAC
gDup_GalK_f	TAAGCTTCAGCGCGAACGACCAACTACCCCGATCATCAGTTATCCTTAAGCCTGTTGACAATTAATCATCGGCA	gD ⁻ galK BG53
gDdown_GalK_r	TGTCCACCTTCCCCCTTCCAGACTCGCTTTATATGGAGTTAAGGTCCTCAGCACTGTCTGCTCCTT	gD ⁻ galK BG53
gD5_galK_f	TTGTCGTCATAGTGGGCTCCATGGGGTCCGCGGCAAATATGCCTTGGCGCCTGTTGACAATTAATCATCGGCA	LM56
gD39_galK_r	ATCGGGAGGCTGGGGGGCTGGAACGGGTCCGGTAGGCCCGCTGGATGTGCAGCACTGTCTGCTCCTT	LM56
gD5_galK_f	TTGTCGTCATAGTGGGCTCCATGGGGTCCGCGGCAAATATGCCTTGGCGCCTGTTGACAATTAATCATCGGCA	LM57
gD44-39_11SG_galK_r	AGGCCCGCTGGATGTGGGATCCACCGGAACCAGAGCCACCGCCACTCGATCAGCACTGTCTGCTCCTT	LM57
gB_852_galK_f	CGGTAAACTGCATCGTCGAGGAGGTGGACGCGCGCTCGGTGTACCCGTACCCTGTTGACAATTAATCATCGGCA	LM290
gB_1648_galK_r	TCGCCGAGCATCCGCGCGCTCACCCGCGGCCACGGTGGCCGAGGCGATTCAGCACTGTCTGCTCCTT	LM290

Table 3.3.4 - Primers for knock out of galK cassette and insertion of the final construct. DNA templates for each primers pair were pEA99, which contains the wt gD coding sequence in pcDNA 3.1(-) (165); pSL1180-scFv-PSMA, pMR1-ENV1 and gB D285N A549T respectively.

Primer name	Sequence	HSV-1 BAC
gDup_50mer_f	TAAGCTTCAGCGCGAACGACCAACTACCCCGATCATCAGTTATCCTTAAG	LM55
gDdown_50mer_r	TGTCCACCTTCCCCCTTCCAGACTCGCTTTATATGGAGTTAAGTCCC	LM55
gD5_J591_f	TTGTCGTCATAGTGGGCTCCATGGGGTCCGCGGCAAATATGCCTTGGCGGAGGTGCAGCTGCAGCAGTCAGGACC	LM593
gD39_SG11_r	ATCGGGAGGCTGGGGGGCTGGAACGGGTCCGGTAGGCCCGCTGGATGTGGGATCCACCGGAACCAGAGCCA CCGC	LM593
BAC_LM613_f	TTGTCGTCATAGTGGGCTCCATGGGGTCCGCGGCAAATATGCCTTGGCGCAGGTGAAACTGCAGCAGTCTGG	LM613
BAC_LM613_r	AGGCCCGCTGGATGTGGGATCCACCGGAACCAGAGCCACCGCCACTCGATTGATTCCAGCTTGGTGCCAT CAC	LM613
gB_D285N_Eco93mer_f	TACGGGACGACGGTAAACTGCATCGTCGAGGAGGTGGACGCGCGCTCGGTGTACCCGTACAACGAATTCGTGC TGGC GACTGGCGACTTTGTG	LM291
gB_A549T_87mer_r	GGCCATCACGTCGCCGAGCATCCGCGCGCTCACCCGCGGCCACGGTGGCCGAGGCGATGGTGTGGGGTTC AGCT TGCGGGCCTC	LM291

3.5 Reconstitution of viral progeny from BAC-DNA and virus cultivation

Briefly, the BAC-DNA was extracted from SW102 strain with NucleoBond[®] PC100 (Macherey Nagel) and was quantified by means of Eppendorf Biophotometer. The BAC DNA was transfected into wt-gD-expressing and complementing RGDp6 cells (166); next, a single round of infection was performed in RS cells to remove any virus pseudotyped with wt-gD. Starting from seeds in RS, retargeted viruses were cultivated in cell lines expressing the heterologous receptors: R-LM249 and R-LM291 in SK-OV-3 cells, R-LM113 in J-HER2 cells, R-LM593 in J-PSMA and R-LM613 in J-EGFRvIII and U251EGFRvIII . Infection was monitored by

observation of the cytopathic effect and EGFP fluorescence. Viral stocks were prepared from lysates of infected cells collected at low speed centrifugation (2000 rpm, 10'). Extracellular virions were harvested from infected cell supernatants by ultracentrifugation with 45Ti rotor Beckman (14.000 rpm, 50'). The titer of viral stocks and extracellular virion preparations was determined in SK-OV-3 (HER-2 retargeted viruses) or U251EGFRvIII cells monolayers, overlaid with 1% SeaPlaque Agarose (Lonza) in RPMI 1640 Glutamax-I, supplemented with 6% FBS. For virus retargeted to PSMA the titer was determined by TCID50 in J-PSMA cells overlaid as above mentioned. Viral stock and extracellular virions were stored in aliquots at -80°C.

3.6 Viral yield assay

Cells were seeded in replicate 12-well plates and were infected with different viruses (R-LM5, R-LM249, R-LM291 or R-LM613) at 1 or 0.1 pfu/cell for 90 min at 37°C. Non penetrated extracellular virus was inactivated by means of a pH3 wash (40 mM citric acid, 10 mM KCl, 135 mM NaCl, pH3 (167)) Replicate cultures were frozen at 3, 24, or 48 h after infection, and the viral progeny (cell associated and supernatant) was titrated on SK-OV-3 cells for HER2 recombinant viruses and U251EGFRvIII for R-LM613. R-LM5 was used as control and was titrated on the same cells of recombinant virus titration.

3.7 Infection assay

A number of cell lines in 96-well plates ($\sim 10^5$ cell/well) were infected with recombinant viruses stocks (MOI 5). Infection was monitored as EGFP expression 24 or 48 h later. Digital pictures were taken with a Kodak camera connected to a Zeiss Axioplan fluorescence microscope. For fluorometer measurement, the infection was conducted in the same way, after 24 or 48 h plates were read at 485/528 nm by Synergy HTTR-I fluorometer (Bio-TEK).

3.8 Inhibition of virus infection

SK-OV-3 cells grown in 96-well plates were exposed for 2 h on ice with increasing concentrations of antibodies (R1.302 against nectin-1, Herceptin against HER2, or mouse immunoglobulins) diluted in Dulbecco's modified Eagle medium without serum and then with the viral inoculum at an MOI of 2 PFU/cell (as titrated in SKOV3 cells) for a further 90 min on ice. Following virus adsorption, the unattached virus was removed and the cells were washed twice with ice-cold RPMI Glutamax supplemented with 2.5% fetal bovine serum. The cells were overlaid with medium containing the same concentration of antibodies or immunoglobulin G (IgG), rapidly shifted to 37°C, and incubated for 16 h. Infection was quantified as the EGFP fluorescence intensity by means of a Victor plate reader (Perkin Elmer). The 100% value represented data obtained with cells infected with virus in the absence of antibodies.

3.9 *In vitro* cytotoxicity

3.9.1 Erythrosin B assay

Cells were seeded in 12-well plates, infected the next day after at 3 pfu/cell, or left uninfected. At different time points cells were trypsinized and collected, and the number of viable and nonviable cells was determined by means of the Erythrosin B (Sigma) dye exclusion assay. The number of viable cells (Erythrosin negative) in infected samples was expressed as percentage of viable cells versus the respective uninfected sample.

3.9.2 Alamar Blue Assay

Cells were seeded at 4×10^3 cells /well in 96 multiwell plates. For any virus tested three replicate plates were prepared. Next day, the replicate cultures were infected with escalating doses ranging from MOI 10 to 0,0032 of virus (R-LM291, R-LM613 or R-LM5). The Alamar Blue (10 ul/well, Life Technologies) was added to medium at 24, 48 or 72 hours post infection and incubate 4h at 37°C. Then, plates were read at at 570 and 600 nm with a fluorometer.

The cellular viability was expressed as percentage of difference in reduction of Alamar Blue between infected and uninfected cells, taking into account the fluorescence contribution of the medium. The following formula was used:

$$\frac{[(\epsilon_{ox}) \lambda_2 A \lambda_1 - (\epsilon_{ox}) \lambda_1 A \lambda_2] - [(\epsilon_{ox}) \lambda_2 A^* \lambda_1 - (\epsilon_{ox}) \lambda_1 A^* \lambda_2]}{[(\epsilon_{ox}) \lambda_2 A^\circ \lambda_1 - (\epsilon_{ox}) \lambda_1 A^\circ \lambda_2] - [(\epsilon_{ox}) \lambda_2 A^* \lambda_1 - (\epsilon_{ox}) \lambda_1 A^* \lambda_2]} \times 100$$

where $(\epsilon_{ox})\lambda_2 = 117,216$; $(\epsilon_{ox})\lambda_1 = 80,586$; $A \lambda_1$ and $A \lambda_2$ are the absorbance for infected well at 570 nm and 600 nm; $A^\circ \lambda_1$ and $A^\circ \lambda_2$ are the absorbance for uninfected cells at 570 nm and 600 nm respectively; $A^* \lambda_1$ and $A^* \lambda_2$ are the absorbance of medium at 570 nm and 600 nm respectively.

3.10 *In vivo* experiments

3.10.1 Tumor growth

Athymic Crl:CD1-*Foxn1nu* (referred to as nude) mice were purchased from Charles River, and maintained under sterile conditions. Experiments were authorized by the institutional review board of the University of Bologna, and were performed according to Italian and European guidelines. Groups of individually tagged virgin female nude mice of 6 weeks of age received the s.c. injection of a tumorigenic dose of SK-OV-3 cells (2×10^6 cells) or SJ-Rh4 cells (30×10^6 cells) or BT-474 cells in 0.2 mL PBS. Tumor growth was assessed weekly by measuring with a caliper, tumor volume was calculated as $\pi[\sqrt{(a*b)}]^3/6$, where a is the maximal tumor diameter,

and *b* the tumor diameter perpendicular to *a*. To perform cytofluorometric analysis, tumor samples, washed in PBS, were mechanically and enzymatically dissociated (0.5 mg/mL trypsin, 0.2 mg/mL EDTA; Invitrogen) at 37 °C for 5 min. Cell suspension was filtered across a 70 μ m cell strainer (Falcon Plastics).

3.10.2 *In vivo* infection.

Mice with SK-OV-3 or SJ-RH4 s.c. tumors received an i.t. injection of R-LM249 in 0.2 ml PBS, and were killed 6, 48, and 72 h later. Resected tumors were cut in half and observed under a fluorescent *in vivo* imager (Lighttools Research). Accurate observation of other organs did not reveal any fluorescence.

3.10.3 Antitumor activity.

At 3 days after tumor cell injection or at definite tumor volumes, mice were randomized in groups of 5–10, and R-LM249 injected in 0.2 ml PBS in tumor site or i.t. ‘‘No virus’’ control groups, run in parallel, consisted of mice untreated and treated with PBS only (not statistically different). Latency time corresponded to a tumor mass ≥ 0.03 cm³. Tumor volumes for each group and time were calculated as mean \pm SE, until all mice of the group were alive.

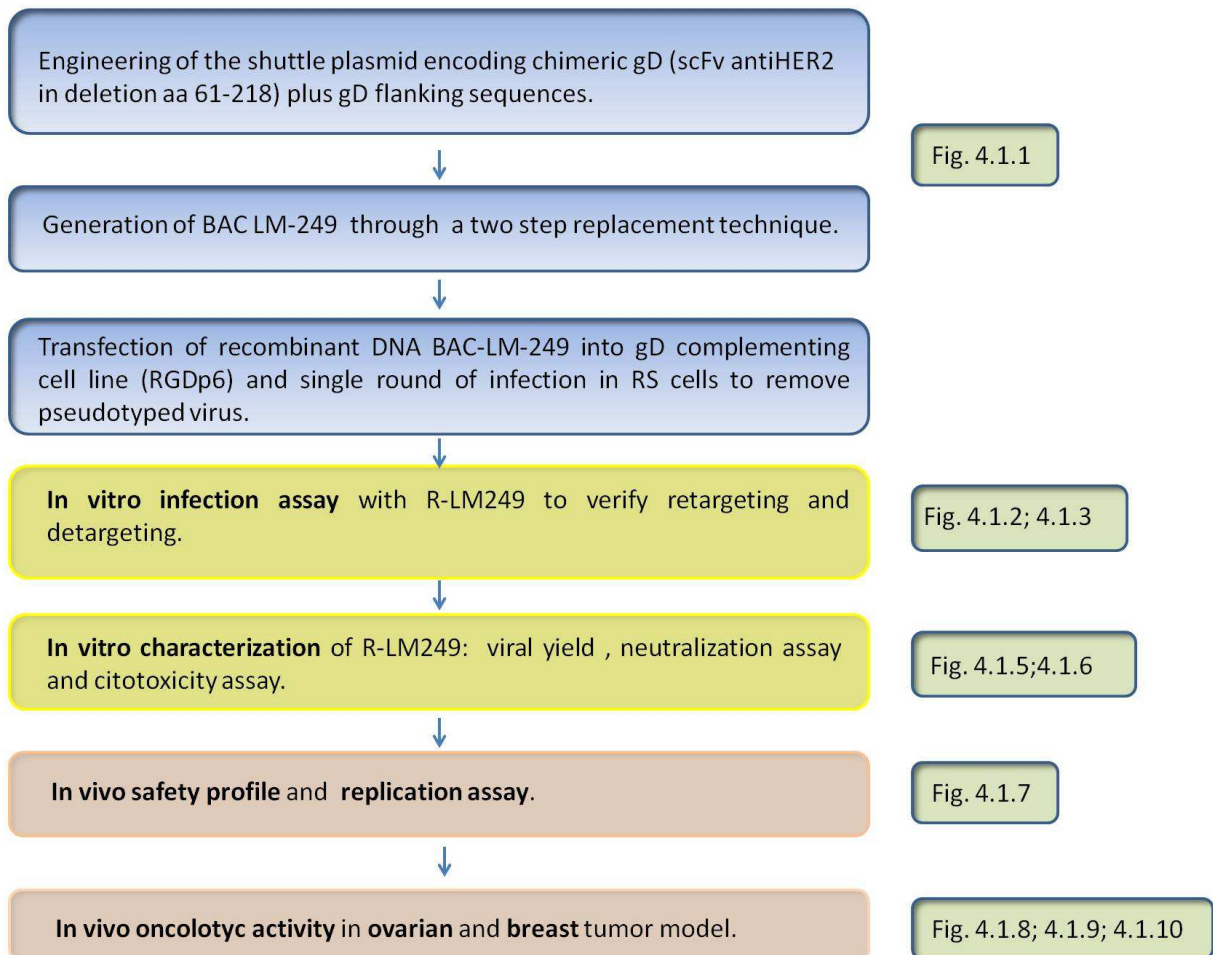
3.10.4 Statistical analysis.

Tumor-free survival curves (Kaplan–Meier) were compared by the Mantel–Haenszel test. Tumor volumes were compared by the Student’s *t* test.

4. Results

4.1 R-LM249

Schematic flow of steps for generation and assay of R-LM249



4.1.1 Genetic engineering of the recombinant HSV-1-BAC R-LM249

Our goal was to generate a oncolytic HSV-1 that at the same time was retargeted to HER2 receptor and detargeted from HSV-1 natural receptors (Nectin-1 and HVEM) through the genetic engineering of gD, the main determinant of HSV-1 tropism. The gD crystal structure showed a natural Ig-folded core (39-41) that was found to serve as a scaffold between the N-terminal and C-terminal of the gD ectodomain (37). We replaced the Ig-folded core (aa 61-218) of gD with a scFv directed to HER2 (sCHER2) (164): sCHER2 sequence was flanked by a short Ser-Gly linker (8 aa) at the N-terminus and a longer Ser-Gly linker (12 aa) at the C-terminus and gD had no mutations at N-terminus sequence. The chimeric gD was introduced in the HSV-1-BAC genome in place of wt gD by means of the two step replacement technique. Briefly, we created the shuttle vector pS249

containing the chimeric gD flanked by the its upstream and downstream sequences and we introduced it in a gD^{EGFP}-HSV-1-BAC that carries □□□EGFP cassette inside BAC sequences between U_L3-U_L4 of HSV-1 (44). Fig.4.1.1 shows the linear map and the crystal structure of gD (Panel 4.4.1B), gD without its Ig-like folded core (gutless gD, Panel 4.4.1C) and the final construct of the protein with the superimposition of the scHER2 crystal (Panel 4.4.1D).

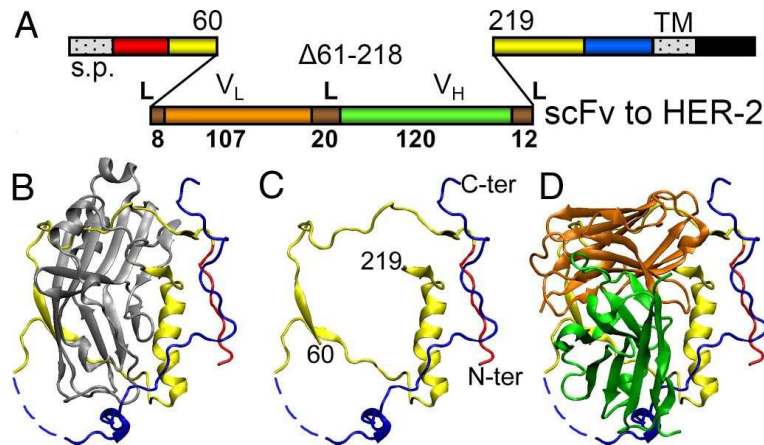


Figure 4.1.15 - Linear and three-dimensional diagrams of gD in R-LM249. **A)** Linear map of gD that shows the scHER2 insertion in deletion aa 61-218 of gD. The size of the scFv insert is drawn to scale. L linker, s.p signal peptide, V_L and V_H: variable light and heavy chains of scFv, TM transmembrane domain and Δ deletion. **B)** Monomeric structure of gD ectodomain (PDB entry 2C6 (40)); color legend: red - gD N-terminus (aa 23-32), blue - C-terminus (aa 257-307), dashed blue line - unresolved residues, gray - gD deletion in R-LM249 (aa 61-218) and yellow as other portions. **C)** gD without aa 61-218. **D)** Structure of gD in R-LM249 with superimposition of scHER2 crystal (PDB entry 1N8Z) drawn to scale. The orientation of two crystals is arbitrary. For crystal graphic creation, visual molecular dynamics (VMD) software was used (168).

4.1.2 R-LM249 is retargeted to HER2 receptor and detargeted from HSV-1 natural receptors

We reconstituted R-LM249 virus in a gD complementing cell line (RGDp6) in order to promote the efficiency of particle assembly and virus spread. Pseudotyped viruses carrying wt-gD were removed by a single round of infection in RS cells. To evaluate the retargeting and detargeting of R-LM249, first we infected a pool of hamster cells transfected to express single receptors and several cell lines from human, murine, simian and rabbit origin. The parental J cells do not express any HSV-1 receptor unlike J-HER2 (expressing HER2 receptor) and therefore they are not susceptible to wt HSV-1 infection. J-Nectin1 and J-HVEM cells express Nectin-1 and HVEM receptors respectively and are infected by wt HSV-1 as all other cells tested. The viral infection was monitored as EGFP fluorescence (Fig. 4.1.2). R-LM249 infected at high levels only J-HER2 and SK-OV-3 cells and did not infect other cells of the pool except for RS and VERO cells where small and sparse plaques occurred. As control, we tried to grow the virus in these two cell lines and EGFP fluorescence and cytopathic effect were lost in few passages. Further to this, the virus was titrated on RS and VERO to quantify the degree of replication and the results showed a range of titer of about 4-5 orders of magnitude lower than in cells permissive to infection as SK-OV-3 cells (data not shown).

Next, we performed the same infection assay measuring the EGFP fluorescence by a fluorometer. R-LM249 showed a high specificity for the heterologous receptor, infecting only HER2 positive cells i.e. J-HER2, SK-OV-3 (high expression) and MCF-7 mammary carcinoma cells (intermediate HER2 expression) (Fig. 4.1.3). These results also demonstrated that R-LM249 needs a high HER2 expression to infect efficiently cells. R-LM249 failed to infect HER2 negative cells as SJ-Rh4 and cells positive for Nectin-1 and HVEM.

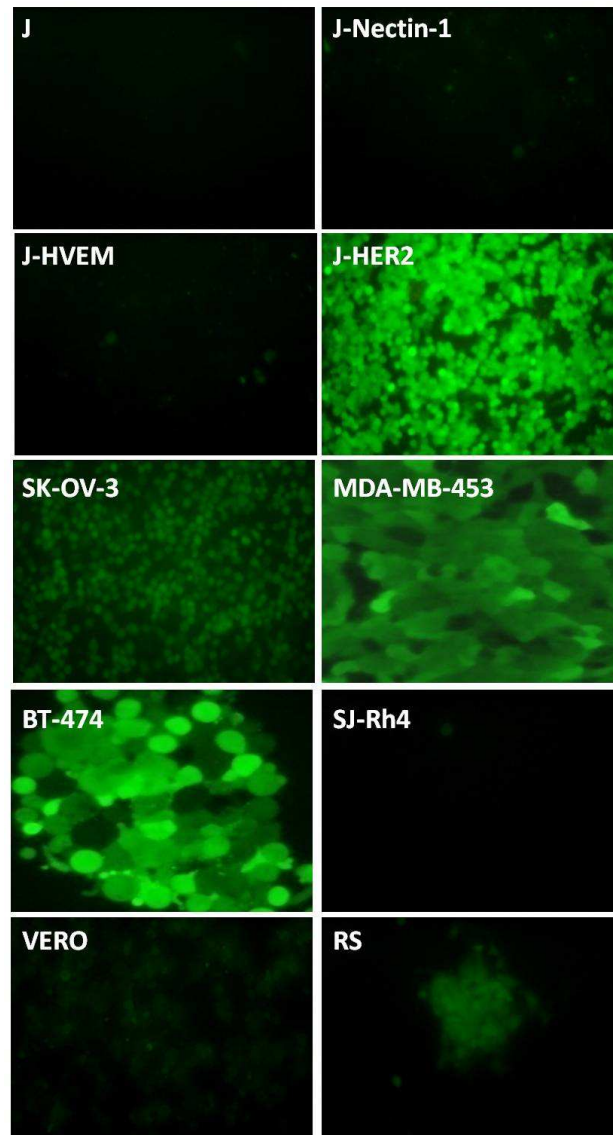


Figure 4.1.16 - R-LM249 infects efficiently HER2 expressing cells. Cell lines were infected at MOI 5 and grown at 37°C for 24 h. The infection was monitored by EGFP fluorescence. Digital pictures were taken with a Kodak camera connected to a Zeiss Axioplan fluorescence microscope.

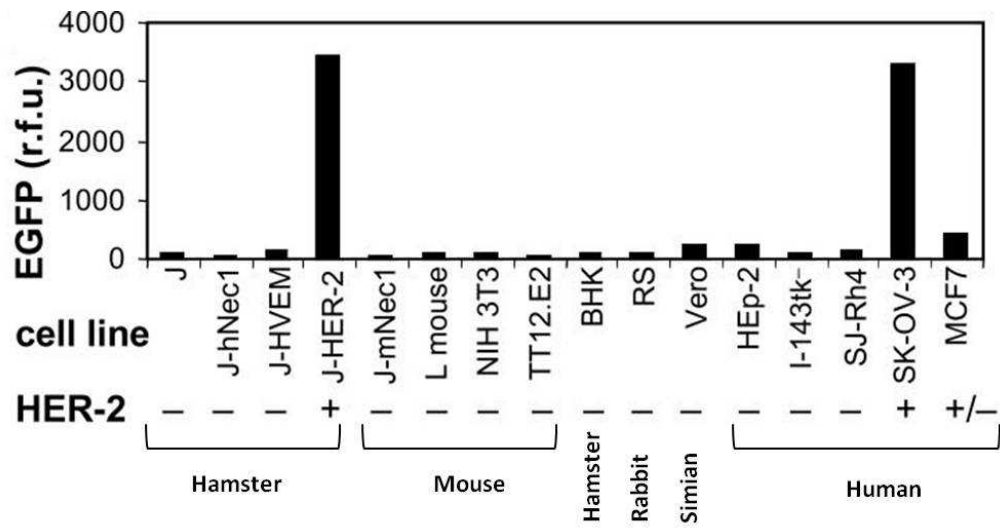


Figure 4.1.17 - R-LM249 infection assay shows effective retargeting to HER2 receptor. Cell lines were infected with R-LM249 and were monitored by EGFP fluorescence 24 hours post infection. Fluorescence emission was measured with a fluorometer (r.f.u. relative fluorescence units). The + and - in the bottom line refer to levels of HER2 expression (44).

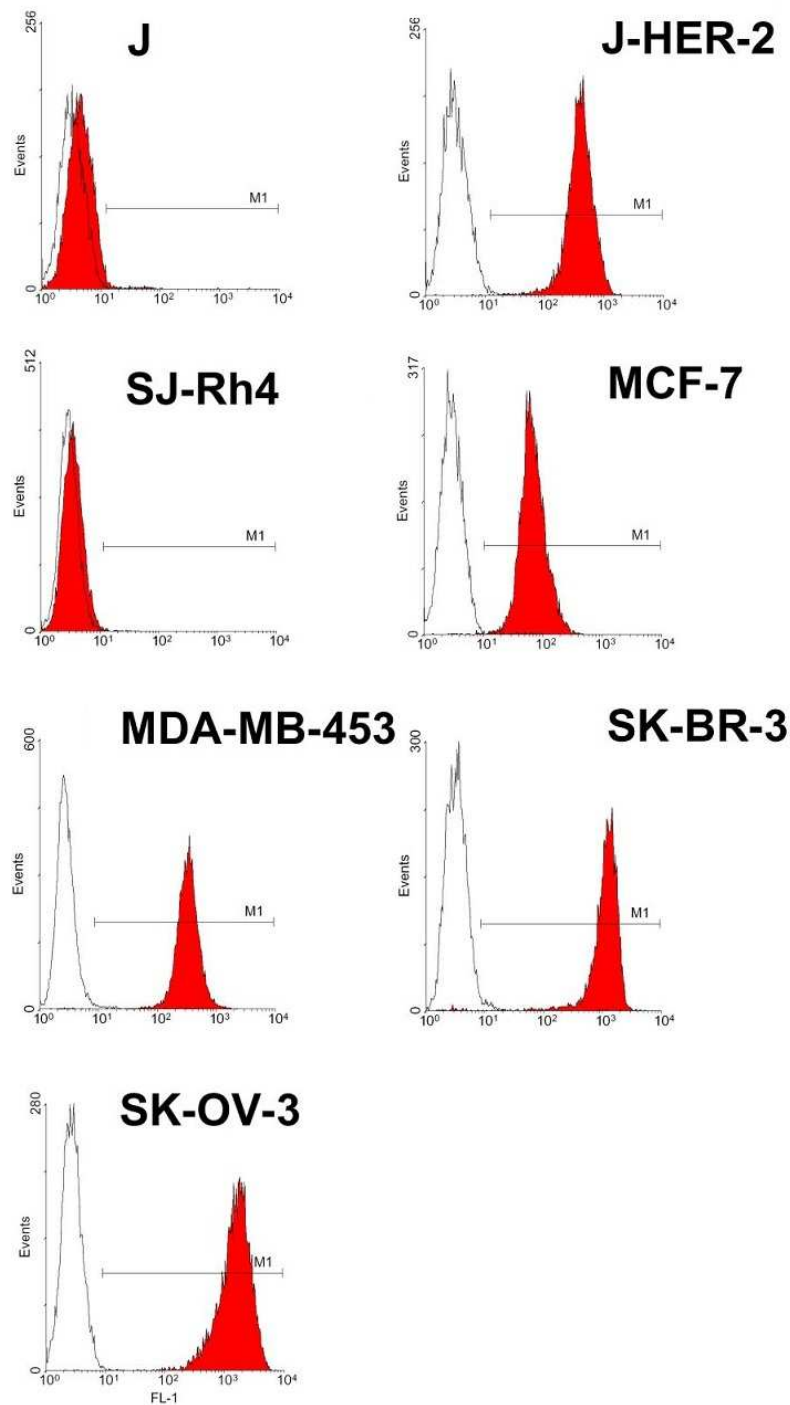


Figure 4.1.18 - HER2 expression levels in different cell lines. The membrane HER-2 expression was evaluated in J, J-HER2, SJ-Rh4, MCF-7, MDA-MB-453, SK-BR-3 and SK-OV-3 cell lines by indirect immunofluorescence with mAb MGR-3 anti HER2 (red curve) or secondary antibody alone (empty curve). HER-2 median fluorescence intensities were: J, 4; J-HER-2, 407; SJ-Rh4, 4; MCF-7, 72; MDA-MB-453, 340; SK-BR-31241; and SK-OV-3, 1655. Cells were analyzed by FACScan flow cytometry (Becton Dickinson) (44).

To confirm the first results about retargeting, viral yield of R-LM249 was compared with that of R-LM5, a HSV-1-BAC carrying EGFP gene within the BAC sequences and wt-gD (80). SK-OV-3 and I143tk⁻ cells, expressing HER2 or not respectively, were infected with two different multiplicities of infection (MOI) and frozen at 3, 24, 48, and 72 hours post infection. This virus replication assay supported and strengthened our preliminary results of cell infections. The viral

titration showed that both viruses were able to grow efficiently in SK-OV-3 cells while R-LM249 failed to replicate in I143tk⁻, exhibiting a titer of 6 logarithms lower than R-LM5 (Fig. 4.1.5).

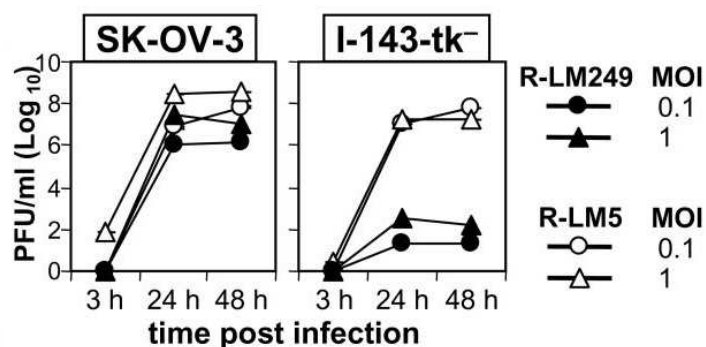


Figure 4.1.19 - R-LM249 and R-LM5 viral yield in SK-OV-3 (HER2 positive) and I143tk⁻ cells (HER2 negative). Cells were infected at 0.1 and 1 multiplicity of infection (MOI, pfu/cell) and harvested at 3, 24, 48, 72 h post infection. Samples were titrated in SK-OV-3 cells (44).

4.1.3 R-LM249 is selective for HER2 receptor usage and cytotoxic to HER2 positive cells

To evaluate the level of specificity through which R-LM249 enters the cells through the binding to HER2 receptor we performed an inhibition of virus infection assay. SK-OV-3 cells were infected with R-LM249 in presence of escalating doses of Herceptin, the humanized monoclonal antibody (mAb) to HER2 used in clinical therapy. As control, infection was measured in presence of mAb R1.302 to nectin-1 or unspecific mouse IgG. The inhibition curve showed that only Herceptin impaired R-LM249 infection in a dose dependent manner (Fig. 4.1.6A) while mAb R1.302 and mouse IgG did not exert any inhibitory effect.

As further proof of R-LM249 specificity we measured its cytolytic activity compared with that of R-LM5 in number of cells expressing HER2 at different degrees. SK-OV-3, SK-BR-3 and MDA-MB-435 cells exhibit an high level of HER-2 expression (Fig. 4.1.4), whereas I-143tk⁻, HEp-2 and SJ-Rh4 cells do not. Cell lysis was estimated by the erithrosin dye exclusion test. R-LM249 was cytotoxic for all HER-2 positive cells, and not cytotoxic for HER-2 negative cells. Conversely, R-LM5 was cytotoxic for all cells tested (Fig. 4.1.6B).

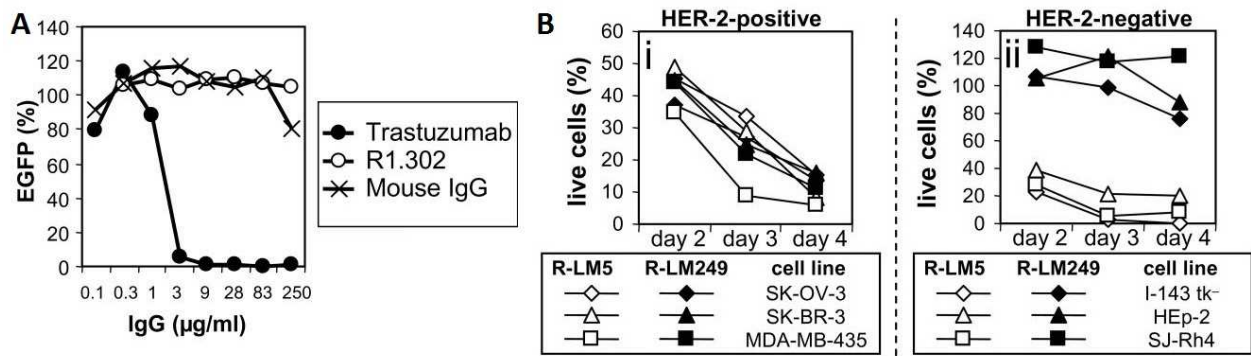


Figure 4.1.20 - The HER2 receptor usage of R-LM249 is specific. **A)** Inhibition of virus infection in presence of escalating doses of Herceptin to HER2, mAb R1.302 to nectin-1 or nonimmune mouse IgG. **B)** Cytotoxicity of R-LM249 and R-LM5 at MOI 3 for HER2 positive (i) or HER2 negative (ii) cells. Cell viability was measured by means of the Erythrosin exclusion assay (44).

These first *in vitro* experiments established that R-LM249 was completely retargeted to HER2 receptor and detargeted from HSV-1 natural receptors and also that the receptor recognition was highly specific and efficient to mediate a cytolytic activity. These results allowed us to move to *in vivo* experiments in mice.

4.1.4 R-LM249 has a high safety profile and is able to replicate *in vivo*

We tested the safety profile of R-LM249 compared with that of R-LM5, by determination of the LD₅₀. Nude mice were intraperitoneally i.p. injected with R-LM249 or R-LM5 doses ranging from 5×10^4 to 5×10^8 pfu/mouse. Mice were kept under examination for the following 21 days and then survivors were sacrificed. The results showed a high safety profile of R-LM249 that caused neither the death nor signs of toxicity of any mouse injected, even those receiving the viral highest dose (5×10^8 pfu). R-LM5 had a pfu/LD₅₀ of about 5×10^4 (Fig. 4.1.7A). To assess the ability of virus to replicate *in vivo* and to exhibit target specificity, R-LM249 was administered through intratumor injection (i.t.) in nude mice bearing subcutaneously HER2 positive or negative tumor masses. After 48 hours post viral inoculation tumors were resected and cut to expose the inner parts. EGFP fluorescence was detected only in HER-2 positive tumor masses demonstrating the ability of virus to infect and spread only in presence of the desired target (Fig 4.1.7B). Indeed, the HER2 negative tumors did not show any sign of infection at any time.

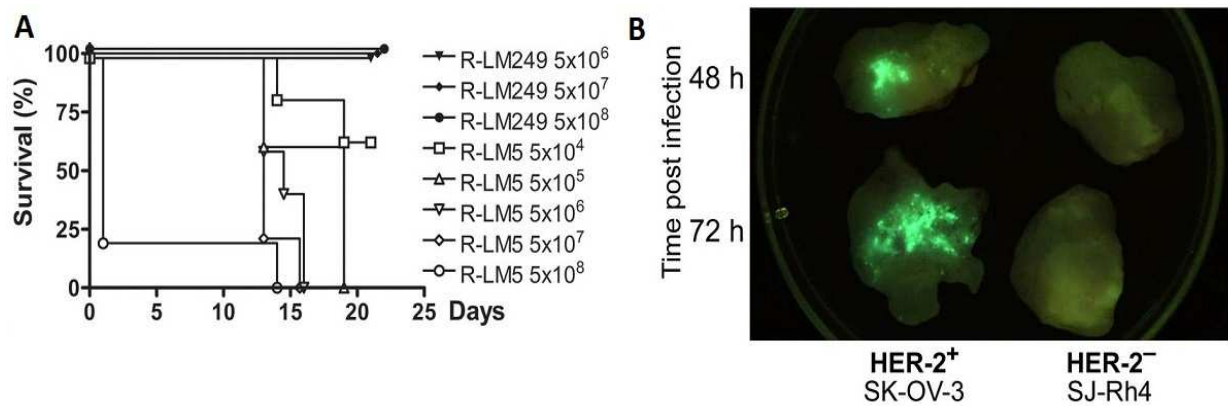


Figure 4.1.7 - R-LM249 safety profile and replication *in vivo*. **A)** Kaplan-Meier survival curve of nude mice injected i.p. with R-LM249 or R-LM5. Five mice were injected for each dose. R-LM249 was injected also at 5×10^4 and 5×10^5 left all mice alive (not reported on the plot). **B)** EGFP fluorescence of HER2 positive (SK-OV-3 cells) and negative (SJ-Rh4 cells) tumor masses. Each tumor sample was obtained from 1 nude mouse at the indicated time after i.t. injection of R-LM249 at 2×10^7 pfu/mouse. The EGFP fluorescence was visualized under a fluorescent *in vivo* imager (44).

4.1.5 R-LM249 is effective and specific in reducing tumor growth of subcutaneous ovarian tumor model

SK-OV-3 cells share with a subset of human breast and ovarian cancer high levels of HER2 receptor expression and the resistance to the mAb Herceptin. For these reasons, we chose this cell line to test the oncolytic activity of R-LM249 *in vivo*. These experiments were conducted in collaboration with Prof. Pier Luigi Lollini's group at the University of Bologna. Nude mice were injected subcutaneously (s.c.) with SK-OV-3 cells and after 3 days they received in the same site a R-LM249 administration ranging from 10^6 to 10^8 pfu/mouse. Treated mice showed an inhibition of the tumor growth at doses higher than 10^6 pfu with the result of 20% of tumor free mice in each group. The most effective doses was 2×10^7 pfu/mouse that strongly slowed tumor growth as showed by masses smaller than 0.3 cm^3 in size for up to 2 months after tumor cell injections (Fig. 4.1.8A). Next, we injected the virus in tumor that had already reach a tumor volume of about $0,2 \text{ cm}^3$. R-LM249 at 2×10^7 pfu/mouse was effective in reducing tumor masses that were maintained under 1 cm^3 up to 2 months after tumor cell inoculation (Fig. 4.1.8B). Subcutaneous tumors observed 15 days after virus treatment showed a visible regression in volume (Fig. 4.1.8C). The experiment was also performed for tumor masses larger than 0.2 cm^3 with no sign of appreciable regression in size (data not shown). The specificity of R-LM249 was also demonstrated by results in mice inoculated with HER2 negative cells (SJ-Rh4) and treated with R-LM249. In these mice, the virus was not able to reduce the tumor mass at both doses tested (2×10^7 and 10^8 pfu/mouse) (Fig. 4.1.8D).

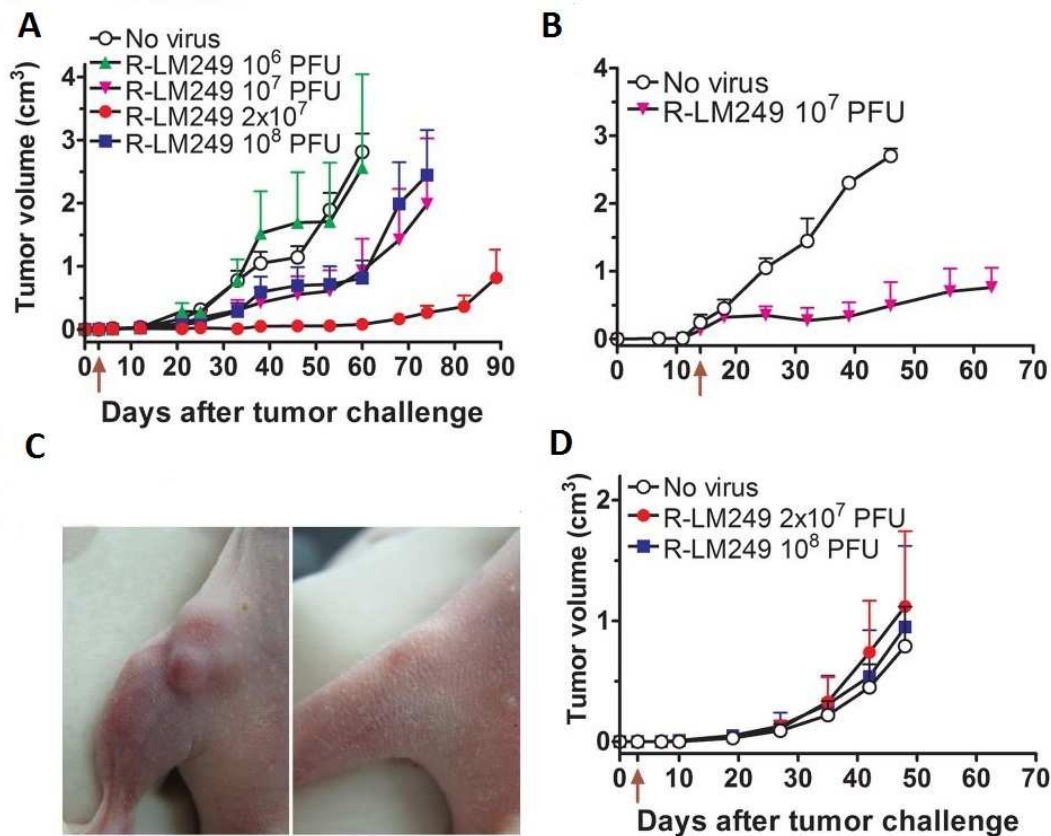


Figure 4.1.21 - Inhibition of tumor growth by R-LM249 *in vivo*. A) R-LM249 was injected at escalating doses in nude mice bearing progressive HER2 positive or negative tumors. Each point represents mean tumor volume \pm SEM of 5 nude mice that received R-LM249 i.t. 3 days after the s.c. injection of SK-OV-3 cells. Statistical significance of difference vs control group “No virus” (Student’s *t* test): 10^6 , not significant; 10^7 and 10^8 , $P < 0.05$ from day 53; 2×10^7 , $P < 0.01$ from day 21. B) Each point represents mean tumor volume \pm SEM of nude mice bearing a SK-OV-3 tumor treated i.t. with R-LM249. C) Mouse bearing a 0.22 cm^3 SK-OV-3 tumor (Left) was treated i.t. with 10^8 pfu R-LM249. (Right) Picture taken 15 days later. D) Kinetics of SJ-Rh4 s.c. tumor appearance in groups of 5–10 nude mice treated with R-LM249 as in A. No significant difference vs. control group (“No virus”) (44).

To assess the ability of R-LM249 to prolong tumor growth inhibition we performed repeated i.t. administrations in nude mice with the most effective dose. Virus was injected at 3, 21, 39 and 63 days after that mice received a subcutaneous inoculation of SK-OV-3 cells. The 2×10^7 pfu/mouse dose of R-LM249 exhibited a lengthening in the inhibition time of tumor growth. In particular, 60% of mice were tumor free up to seven months after the last virus injection (Fig. 4.1.9A). Next, mice were sacrificed and the necroscopic examination did not discover tumor masses at low magnification under white light and at 488 nm (for EGFP expression). The 40% of mice that were not tumor free showed a tumor size under 1 cm^3 up to at least 2 months after the last treatment (Fig. 4.1.9B).

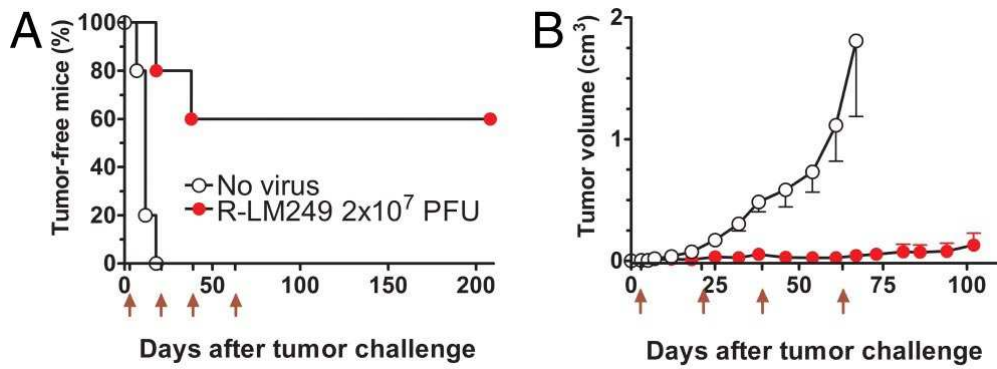


Figure 4.1.22 - R-LM249 oncolytic activity after repeated injections. Groups of 5 nude mice received the s.c. inoculation of HER-2-positive SK-OV-3 cells and were treated with repeated i.t. injections of R-LM249 at days 3, 21, 39, and 63 (red arrows). **A)** Kaplan–Meier analysis of tumor free survival time. Tumor-free survival of R-LM249-treated mice was significantly different from that of control group (“No virus”) ($P < 0.005$ by the Mantel-Haenszel test). **B)** Tumor growth curves, each point represents mean tumor volume \pm SEM of 5 nude mice (including tumor-negative mice). All time points after day 18 were significantly different ($P < 0.01$ by the Student’s t test) (44).

4.1.6 R-LM249 is effective and specific in reducing tumor growth of subcutaneous mammary tumor model

As already shown, BT-474 cells express high level of HER2 receptor (Fig. 4.1.4), and are generally used as model for breast carcinoma (169). After the promising results in a subcutaneous model of ovarian cancer we switched to a subcutaneous mammary tumor model and repeated intratumoral administrations of two doses of R-LM249. The model consisted of nude mice bearing HER2 positive tumors from BT-474 cell line. In Fig. 10A black arrows indicate virus administrations. The result was an inhibition in the growth of human mammary tumors. In particular, 60% of mice were tumor free after approximately 80 days from cells inoculation (Fig. 4.1.10 B), while the remaining 40% showed the size of the tumor drastically reduced (Fig. 4.1.10A). For this experiment, the most effective dose was 10^8 pfu/mouse unlike the ovarian model where it was 2×10^7 pfu/mouse.

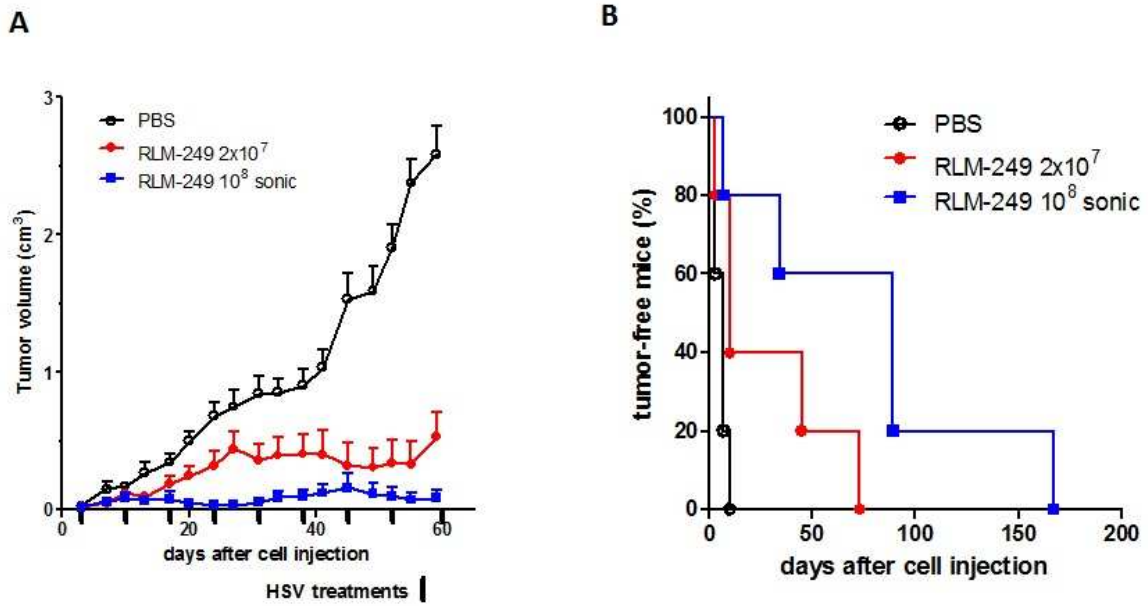
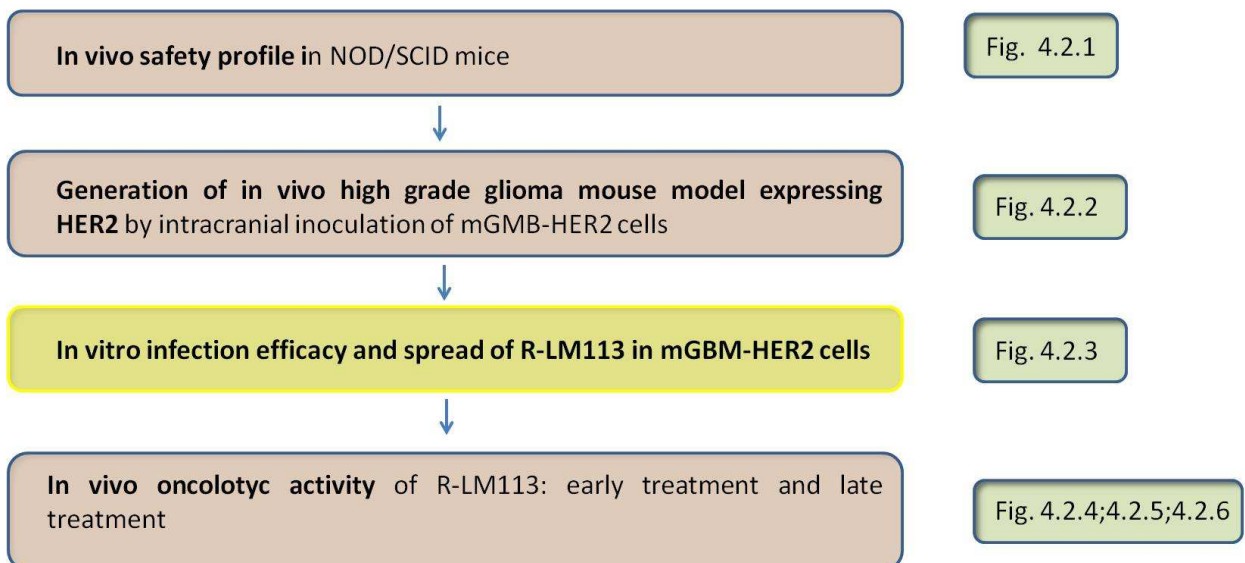


Figure 4.1.23 - Antitumor efficacy of R-LM249 in BT-474 subcutaneous mammary tumor model. Nude mice s.c. inoculated with BT-474 cells, were injected i.t. with 2×10^7 and 1×10^8 pfu/mouse of R-LM249 in ten repeated administration. **A)** Tumor growth curve, each point represents mean tumor volume + SEM. **B)** Kaplan – Meier survival curve for BT-474 tumor masses treated with R-LM249 compared to control mice (PBS).

4.2 R-LM113

Schematic flow of steps for assay of R-LM113

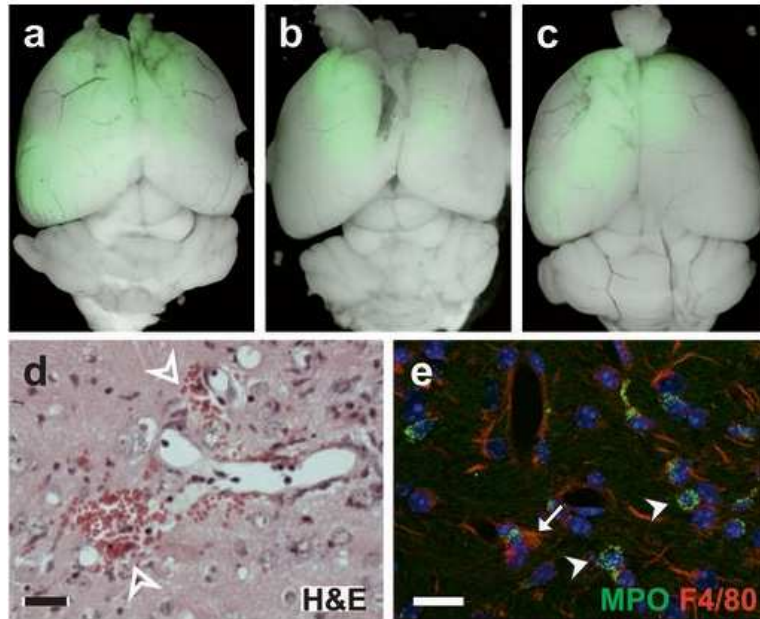


4.2.1 R-LM113 is safe in NOD/SCID mice

R-LM113 is a replication competent HSV-1-BAC fully retargeted to the human HER2 receptor and detargeted from natural HSV-1 receptors (80). The viral tropism was modified through the insertion of the scHER2 in place of amino acids 6-38 deletion in virion envelope glycoprotein gD. The deletion eliminated residues involved in HVEM binding and one of the residues (aa 38) involved in Netin-1 binding. Moreover the size of the heterologous insert was able to mask residues responsible of Nectin-1 recognition (80). Because the HER2 receptor is highly expressed in some forms of glioblastoma, we used this virus in a orthotopic mouse model of this malignant brain tumor. The experiments were performed in NOD/SCID mice strain highly sensitive to HSV-1 infection in collaboration with the group of Dr. Paolo Malatesta (IST-Genoa). First of all, we assessed the safety profile of R-LM113 compared with that of R-LM5. Both viruses carry EGFP as reporter gene inserted into the BAC sequences.

Five mice were injected intracranially with 3×10^5 pfu/mouse of R-LM113. As control the same number of mice received 10^5 pfu/mice of R-LM5. The R-LM113 dose administered was the maximum allowed by the small volumes that can be injected intracranially (i.c.). All mice inoculated with R-LM5 died for lethal encephalitis between 7 to 10 days after viral injection and the explanted brains showed large EGFP positive areas (Fig. 4.2.1 a,b,c). The same brains were sectioned and stained with haematoxylin and eosin and showed an extensive extravasation (Fig. 4.2.1 d). Furthermore the sections resulted positive to granulocytes and macrophages markers by means of myeloperoxidase (MPO) and F4/80 staining to indicate their massive infiltration (Fig. 4.2.1 e). Conversely, mice treated with R-LM113 did not die and were sacrificed 7, 12 and 25 days after virus administration to control the presence of viral spread and neuroinvasiveness. Mice showed neither any sign of EGFP fluorescence nor of extravasation (Fig. 4.2.1 f-i). Moreover there was not macrophages and granulocytes infiltration (Fig. 4.2.1 j). The results indicate that R-LM113 is safe because it is not able to infect normal brain tissue, whereas R-LM5 is lethal even at lower doses than that used for our recombinant virus.

R-LM5



R-LM113

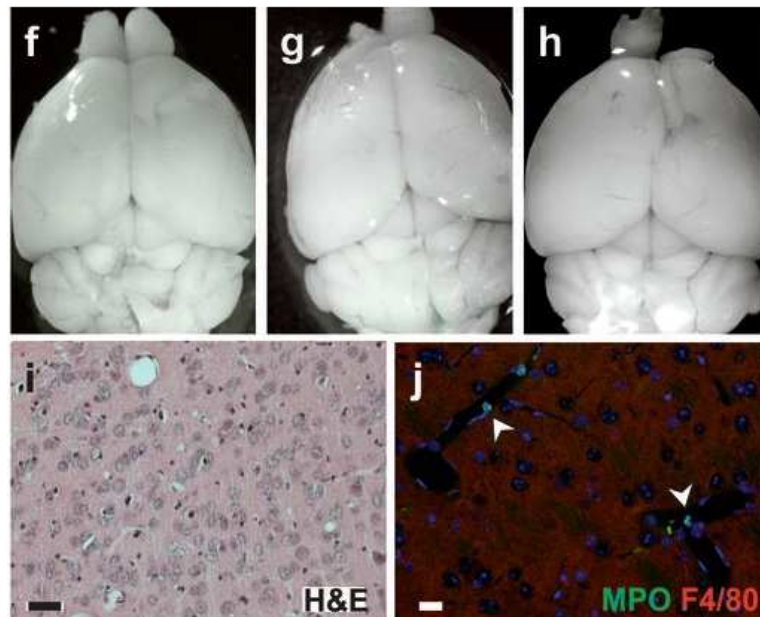


Figure 4.2.1 - R-LM113 in safe *in vivo*. NOD/SCID mouse brains were explanted after injection of 10^5 pfu/mouse of R-LM5 (a-c) or 3×10^5 pfu/mouse of R-LM113 (f-h) and observed in merged fluorescence and brightfield. Viral spread is visualized by EGFP fluorescence. Coronal section of adult NOD/SCID mouse brains after injection of R-LM5 (d,e) or R-LM113 (i,j) stained with heamatoxylin and eosin (d,i) or with antibody for the indicated markers (e,j). Extravasation area areas (empty arrowheads in d), infiltration of granulocytes (arrowheads in e) and macrophages (arrow in e) in the parenchyma are present in R-LM5 injected brains. Conversely, granulocytes are exclusively found inside blood vessels of R-LM113 injected brains (arrowheads in j). Scale bars 20 μm.

4.2.2 Generation of an *in vivo* high grade glioma model expressing HER2

To test R-LM113 oncolytic activity in high grade glioma *in vivo*, we needed to generate a glioma model expressing the HER2 receptor. Murine gliomas cells (mGBM), derived from PDGF-B induced murine gliomas, are able to develop secondary tumors after their orthotopic transplantation in adult mice and emit red fluorescence because they carry and express a transgenic DsRed protein (170, 171). mGBM cells were stably transfected with a plasmid carrying the coding sequence of HER2 receptor. The presence of heterologous receptor in membrane was assessed by indirect immunofluorescence (IFA) (Fig. 4.2.2 a,e). We did not know if the presence of HER2 could impair mGBM cells phenotype or their ability to develop high grade glioma tumors. For this reason mGBM-HER2 and the parental cell line mGBM were stained with several typical gliomas markers in an immunocytochemical analysis (Fig 4.2.2 b,c,d-f,g,h). The results confirmed that the HER2 transfection did not compromise the mGBM cellular profile. In particular we took into account staining for Ng2 (chondroitin sulfate proteoglycan) as a marker of oligodendrocytes; Nestin, a intermediate filament protein express in nerve cells for radial growth of the axons and Oligo2, that is a marker of oligodendrocytes development. Next, mGBM-HER2 cells were transplanted intracranially in adult NOD/SCID mice for the evaluation of their tumorigenic potential. The brains explanted, after two months, showed a broad red fluorescent area (Fig. 4.2.2 k) corresponding to the tumor mass, that had a rather compact structure and wide necrotic areas surrounded by highly proliferating cells forming pseudopalisades. The staining with haematoxylin and eosin as well as MPO and F4/80 revealed signs of extravasation and lymphocytes infiltration (Fig. 4.2.2 i). All results confirmed that the HER2 transfection in mGBM cells did not affect their cellular and tumorigenic properties.

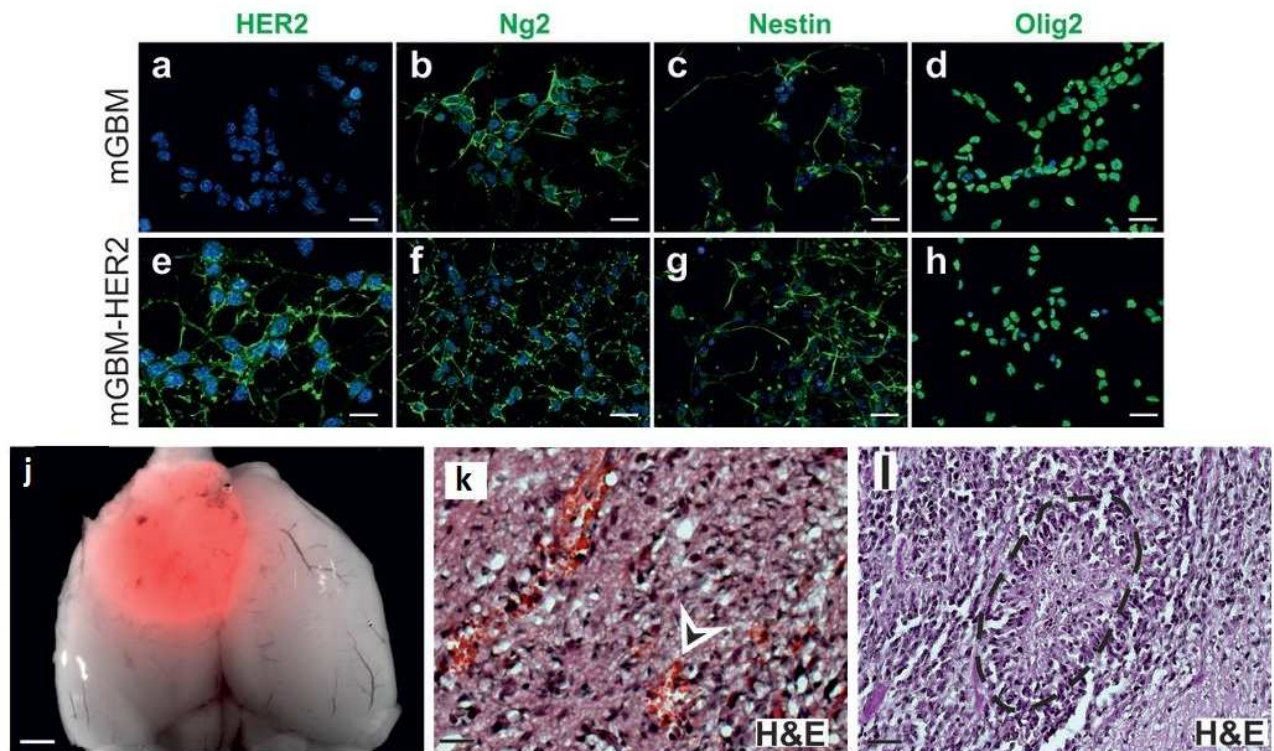


Figure 4.2.2 - mGBM-HER2 cells did not change their biological and tumorigenic potential after HER2 stable transfection. (a-d) Immunostaining of mGBM (a-d) and mGBM-HER2 (e-h) with the markers indicated on each picture. (j) Merged fluorescence and brightfield images in dorsal view of a brain explanted from a mouse injected intracranially with mGBM-HER2. The tumor mass is visible as DsRed fluorescence. (k,l) Haematoxylin and eosin staining of coronal section of tumors derived by mGBM-HER2 cells; dashed lines trace the pseudopalisade boundaries while arrows highlighted the extravasation area. (n-u) Immunostaining of coronal section of tumors derived by mGBM-HER2 cells. The antibody used are indicated on each pictures (green). Arrows indicate macrophages in n, arrowheads indicate granulocytes in n, o. Ds-Red fluorescence is visible in p-u. Nuclei are counterstained in blue with Hoechst 33342 in a-h, n-u. Scale bar, 15 μ m (a,e); 25 μ m (b-d,f-h,k); 12 mm (j); 40 μ m (l).

4.2.3 R-LM113 infects and spreads in mGBM-HER2

Once it was established that the mGBM-HER2 cells were biologically identical to parental mGBM, we verified that they were susceptible and permissive to R-LM113 infection. Replicate cultures of mGBM-HER2 and mGBM cells were exposed to serial dilutions of R-LM113 or R-LM5 as control. The infection was detected after 24h as EGFP fluorescence (Fig. 4.2.3 a-d and a'-d'). In another experiment the efficiency of infection of R-LM113 in mGBM-HER2 was quantified respect to that of R-LM5 with a fluorometer. Two replicas of cells were infected at the same MOI with the two viruses (titrated on SK-OV-3 cells). R-LM113 infected about $11 \pm 3\%$ of mGBM-HER2 cells while R-LM5 infected about $71 \pm 3\%$ of cells (Fig. 4.2.3 e,f).

R-LM113 was also able of cell-to-cell spread in mGBM-HER2 cells as indicated in Fig.4.2.3 (g,h,i). Cells were infected at low MOI (0.025 pfu/cell) and monitored over time for plaques formation.

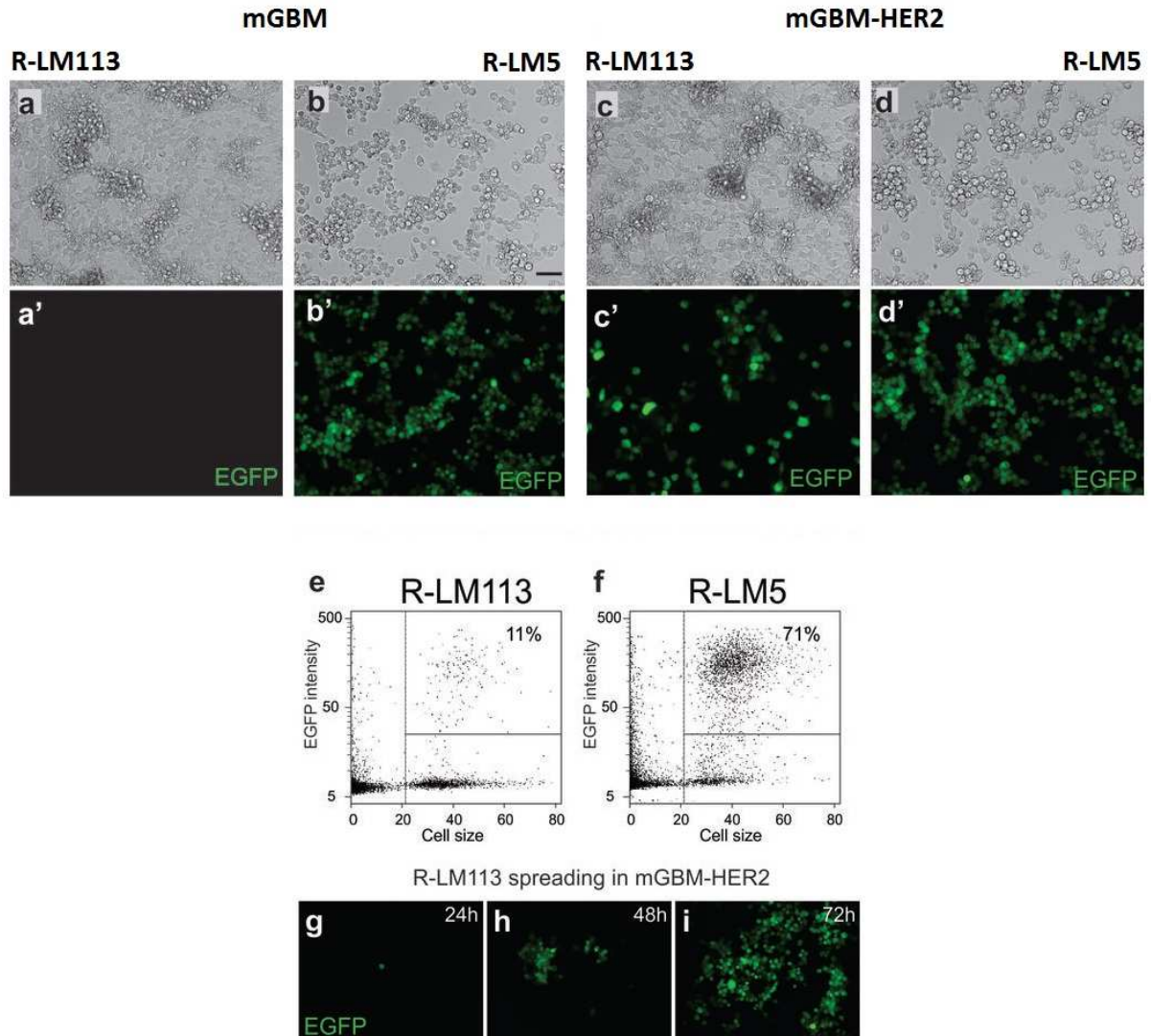


Figure 4.2.3 - Infection efficiency and spread of R-LM113 in mGBM-HER2 cells. (a-d') Pictures of mGBM-HER2 (a,b,a',b') and mGBM (c,d,c',d') cells infected with R-LM113 (a,c) and R-LM5 (b,d). Micrographs were taken in brightfields (a-d) and EGFP fluorescence (a'-d'). (e-f) Representative dot plots of mGBM-HER2 cells infected with R-LM113 and R-LM5 at MOI 5. The percentage of infected cells as EGFP fluorescence is reported on the graph and was evaluated through Image J analysis for the measurements of plot area and fluorescence intensity for each cell. The lines represents the threshold used. (g-i) Cell-to-cell spread of R-LM113 in mGBM-HER2 cells infected at MOI 0,025 and monitored for 72 h. Scale bar, 50 μ m.

4.2.4 Oncolytic activity of R-LM113 *in vivo*

To evaluate R-LM113 oncolytic potential *in vivo* we performed two series of experiments that differed for the time of a administration: I) in the early treatment, a mixture of non-infected and R-LM113 infected mGBM-HER2 cells was inoculated i.c.; II) in the late treatment the virus was injected when the tumor was already developed in the brain. The latter experimental scheme would like to mimic as close as possible the therapeutic application of an oncolytic virus.

Early treatment: for this experiment a pool of 24 NOD/SCID mice were enrolled and in three independent sessions, mice were inoculated intracranially with 2×10^4 mGBM-HER2 cells. In particular, at the same time of uninfected cells inoculation, 12 mice (herein referred to as “R-LM113 early treatment set”) were injected also with 2×10^4 mGBM-HER2 cell previously infected *in vitro* with R-LM113. The other 12 mice were used as control (“early-treatment control set”). Mice were monitored for 160 days.

The results showed that mice belonging to “R-LM113 early-treatment set” had a significant lengthening in median survival time compared to controls (119 days vs 55 days respectively, log-rank test $p < 10^{-4}$) (Fig. 4.2.4 a). All control animals showed neurological symptoms within 69 days and their brain emitted DsRed fluorescence for presence of tumor masses (Fig. 4.2.4 b). Conversely, in the R-LM113 early treatment set, only two mice exhibited neurological symptoms caused by tumor masses. Three mice of the treated set group were sacrificed 66 days after cells transplantation in order to verify the virus infection. No detectable fluorescence was identified at a first macroscopic analysis while, after sectioning, the histological staining showed small cellularized areas with signs of sparse EGFP fluorescent cells as marker of active R-LM113 infection (Fig. 4.2.4 c).

Treated mice that developed neurological symptoms from 69 and 160 days after cells injections (n=5) were analyzed and their brains showed the presence of large DsRed tumor masses, two of which showed EGFP positive areas (Fig. 4.2.5 a).

Two animals of the R-LM113 early treatment set survived until the end of experiment without developing any neurological symptoms. One of them carried a DsRed positive tumor without signs of EGFP fluorescence (Fig 4.2.5 b.b'). The tumor mass was still expressing HER2 suggesting that the virus did not select for HER2 negative tumor cells (Fig. 4.2.5 c). The other mouse bore a very small region of DsRed and EGFP positive cells indicating that R-LM113 was actively hindered tumor growth (Fig. 4.2.5 d-d').

In conclusion the results evidenced that R-LM113 was able to infect, spread and destroy tumor cells *in vivo*, doubling the median survival time of the treatment set compared to control.

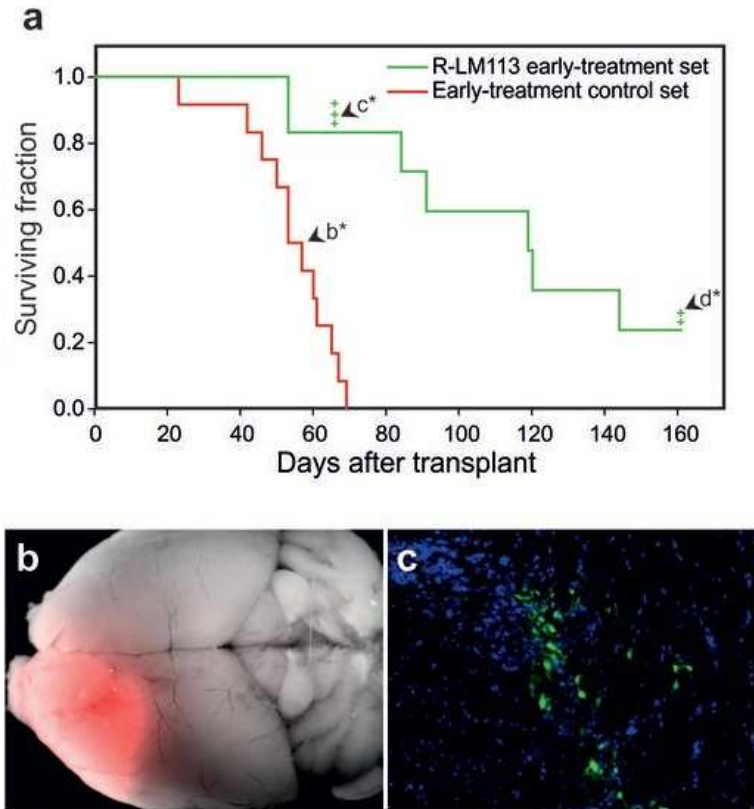


Figure 4.2.4 - R-LM113 counteracts the growth of HER2-expressing gliomas. **a)** Kaplan-Meier plot for animals transplanted with mGBM-HER2 cells alone (red line, Early treatment control set) or together with R-LM113 infected mGBM-HER2 (green line, R-LM113 earlytreatment set). The crosses indicate mice censored for subsequent analysis. **b)** Merged DsRed fluorescence and brightfield image of a brain from a mouse of the control set (arrowhead labeled as b* in a). **c)** Coronal section of the brain from a mouse of the R-LM113 early-treatment set censored 66 days post-transplant (arrowhead labeled as c* in a); in green is shown EGFP expressed from the virus, 23 in blue the nuclei.

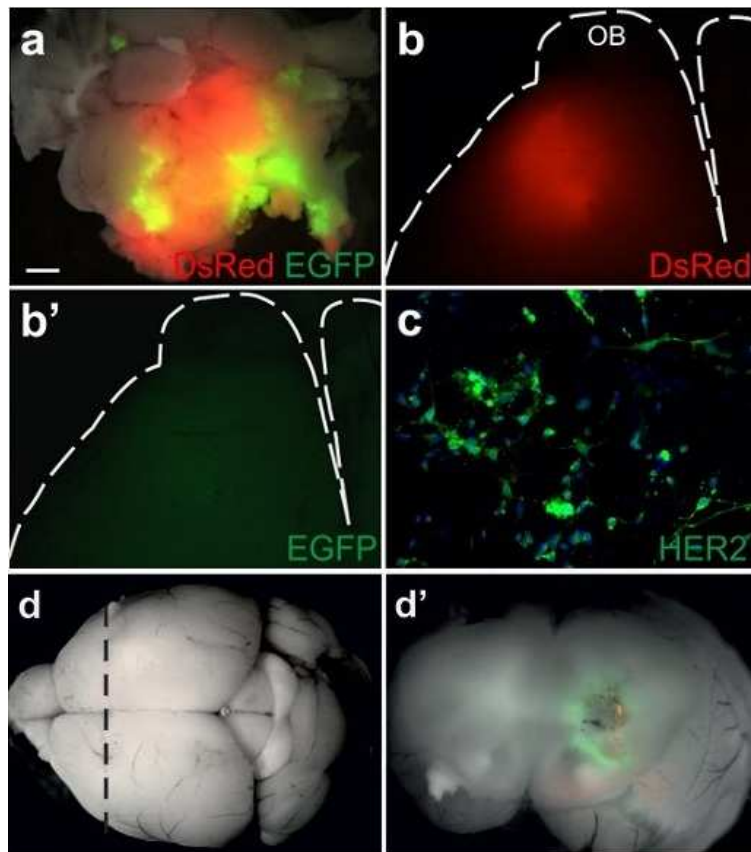


Figure 4.2.5 - R-LM113 counteracts the growth of HER2 expressing gliomas. **a)** Merged red and green fluorescence and brightfield images of the brain from a mouse of the R-LM113 early-treatment set which displayed neurological symptoms 120 days after transplant. To note, the presence of a large DsRed tumor scattered of EGFP-positive areas. **b,b')** Matched fluorescence micrographs of a brain (outlined with dashed line) explanted from a mouse of the early treatment set sacrificed in absence of any neurologic symptom at the end of the planned observation period. To note the presence of a DsRed positive tumor mass (**b**) lacking any detectable EGFP fluorescence (**b'**). **c)** Immunofluorescence staining for HER2 of cells dissociated from the tumor represented in B-B'. OB: olfactory bulb. Scale bar: 1mm in **a**, 0.5mm in **b**, 40 μ m in **c**. **d)** Merged red and green fluorescence and brightfield images of the brain from a mouse of the R-LM113 early-treatment set censored 161 days post-transplant (arrowhead labeled as **d*** in **a**). **d')** Coronal section of the brain shown in **d**, along the dashed line.

Late treatment: 2×10^4 mGBM-HER2 cells were intracranially inoculated in 28 NOD/SCID mice and after 45 days R-LM113 or UV-inactivated R-LM113, as control, were injected in the same stereotaxic coordinates in 20 mice and 8 mice respectively. The time elapsed between two inoculations (cells and virus) was chose because it was 10 days before the median survival time of early control set of the previous experiment. Only mice surviving at least 5 days after virus injection were considered, because the virus had time to replicate and spread and mice had time to recover from intracranial injection.

Mice treated with the virus were called “R-LM113 late treatment set” while control mice were called “UV-R-LM113 late treatment control set”.

The results showed that mice belonging to “R-LM113 late-treatment set” had a significant lengthening in median survival time compared to controls (21 days vs 10 days respectively, $p < 0,003$) (Fig. 4.2.6 a). The first three mice of the treatment set with neurological symptoms had large DsRed tumor masses scattered with EGFP fluorescence indicating that the virus spread inside the tumor (Fig. 4.2.6 b). Likely these gliomas were already too advanced for effective treatment with the virus.

The mouse that survived longer in the late treatment set died 37 days after virus injection. The brain revealed a small Ds-Red tumor mass scattered by EGFP-positive cells (Fig. 4.2.6 c).

In order to assess the viral spread just after R-LM113 injection, the virus was administered to four additional mice which were sacrificed five days after, although they did not show any sign of neurological symptoms. In brains explanted, DsRed tumors scattered by EGFP fluorescence were present. Noteworthy, EGFP fluorescent cells were found in a site distant from which of injection, highlighting the ability of virus to spread into the tumor (Fig. 4.2.6 d).

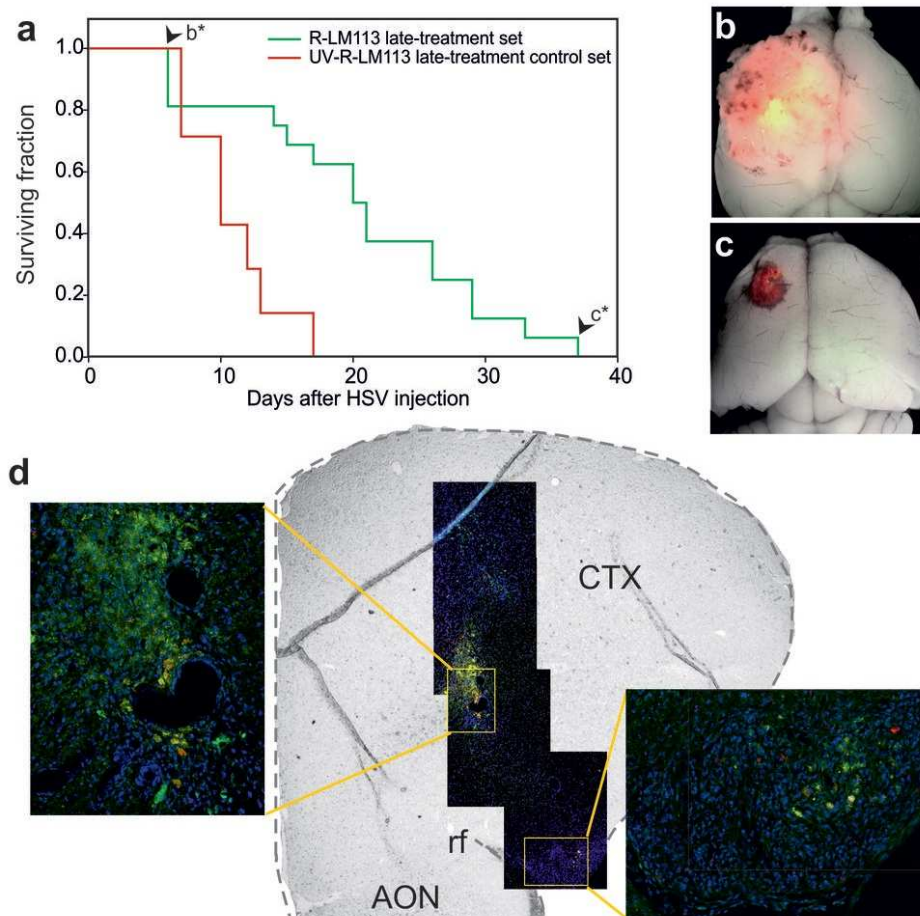
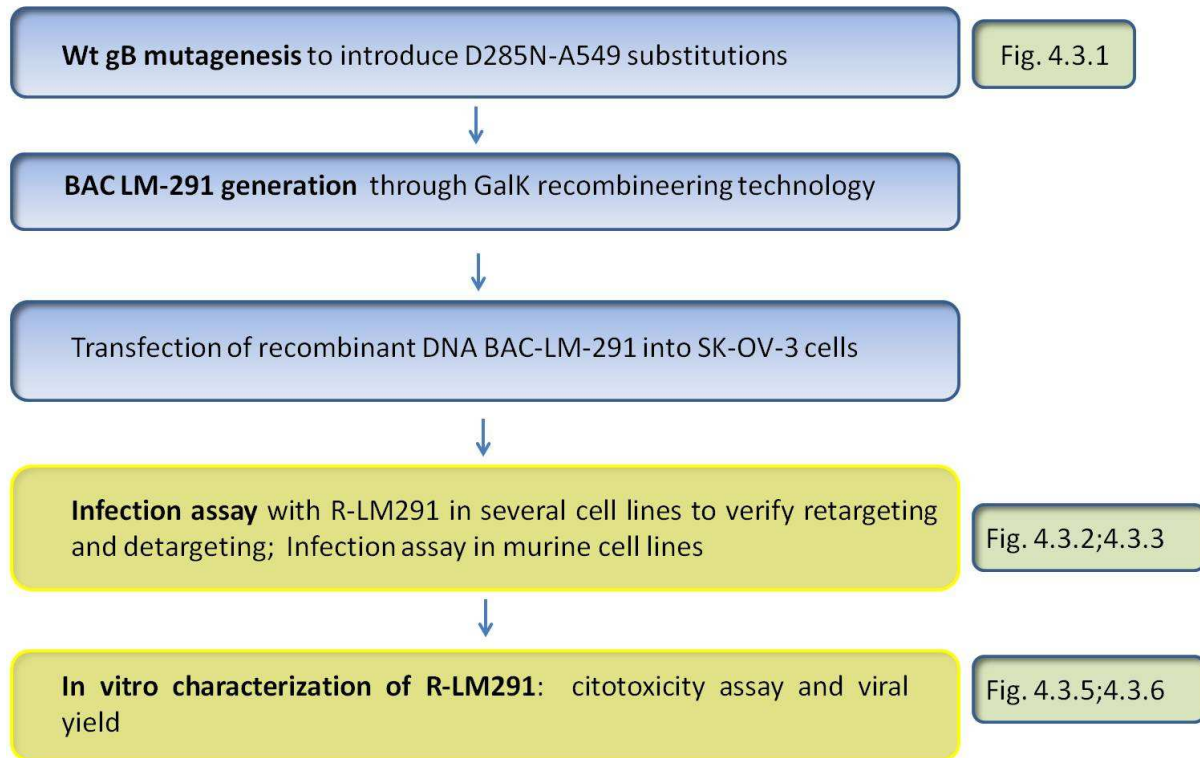


Figure 4.2.6 – R-LM113 improves mouse survival when injected in already established HER2-expressing gliomas. a) Kaplan-Meier plot for mice bearing mGBM-HER2 tumors inoculated with R-LM113 (green line) or with UV-inactivated R-LM113 (red line). (b, c) Merged red and green fluorescence and brightfield images of brains from mice of the R-LM113 late-treatment set died at 6 days (b, arrowhead labeled as b* in panel a) and at 37 days (c, arrowhead labeled as c* in panel a) following R-LM113 inoculation. d) Coronal section of a mGBM-HER2-bearing mouse injected with R-LM113 and sacrificed 5 days post inoculation. In green is shown the virally-expressed EGFP, in red the endogenous fluorescence of DsRed expressed by mGBM-HER2, in blue the nuclei. The right inset shows a magnification of the region distant approximately 1.3mm. AON accessory olfactory nucleus, CTX, cortex; rf, rinal fissure.

4.3 R-LM291

Schematic flow of steps for generation and assay of R-LM291



Glorioso and coworkers reported that HSV expressing a mutant gD whose binding to wt Nectin-1 was severely impaired developed two spontaneous compensatory mutations in gB (D285N-A549T) when it was forced to enter in cells carrying a mutant form of Nectin-1 (56). The hyperactive gB, as it has been named by the authors, was found to increase the rate of entry of the virus even in the absence of receptors for authentic gD or compensate for inefficient gD-receptor interaction. R-LM249 showed promising results in our *in vivo* experiments. Considering that mutations D285N-A549T in gB could increase both virus ability to spread from cell to cell and its oncolytic activity we decided to introduce mutations in gB described by Uchida in R-LM249 genome through galk recombineering technology. The resulting virus was named R-LM291 (Fig. 4.3.1).

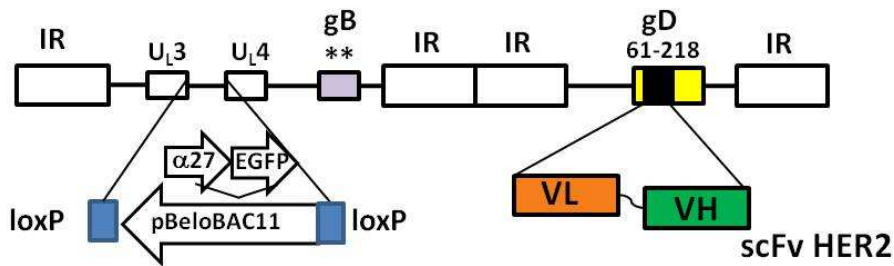


Figure 4.3.1 – Schematic diagram of R-LM291 backbone. The viral HSV-1-BAC backbone is the same of R-LM249 in Fig.1, except for the two mutations in gB (light violet) D285N and A549T (asterisks).

First, we inserted galK cassette between nucleotide 852 and 1648 of gB of R-LM249, generating R-LM290 (Fig 3.3.5 in material and methods). Next, we performed the gB mutagenesis with four mutagenic primers in a plasmid carrying the wt gB coding sequence. The insert was amplified by PCR using the mutated plasmid as template and it was electroporated in galK positive clone of R-LM290. Bacterial colonies carrying R-LM291 were screened by colony PCR and the virus was reconstituted through transfection in SK-OV-3 cells.

4.3.1 R-LM291 infects HER2 positive cells and spreads more efficiently in murine cells.

In order to verify that R-LM291 maintained the retargeted tropism towards HER2-positive cells maintenance we performed an infection assay in several cells lines expressing HER2 receptor or cells lines expressing HSV-1 natural receptors. The infection was monitored as EGFP fluorescence at 48 h post infection. The results showed that R-LM291 was still able to recognize HER2 as the sole receptor for entry in cells. Indeed, it infected efficiently only HER2 positive cells i.e. J-HER2, SK-OV-3 cells. In micrographs of VERO and RS infected cells we noted an increase in fluorescence compared to R-LM249 infection assay (Fig. 4.3.2). The results observed in VERO and RS cells may derive from an acquired ability of R-LM291 to enter through a broader receptor spectrum as reported by Glorioso and coworkers (56). However, the virus was not able to grow in VERO or RS cells, losing EGFP fluorescence and cytopathic effect in few passages. The titration in these cells confirmed titers 4 logs lower than in SK-OV-3 cells.

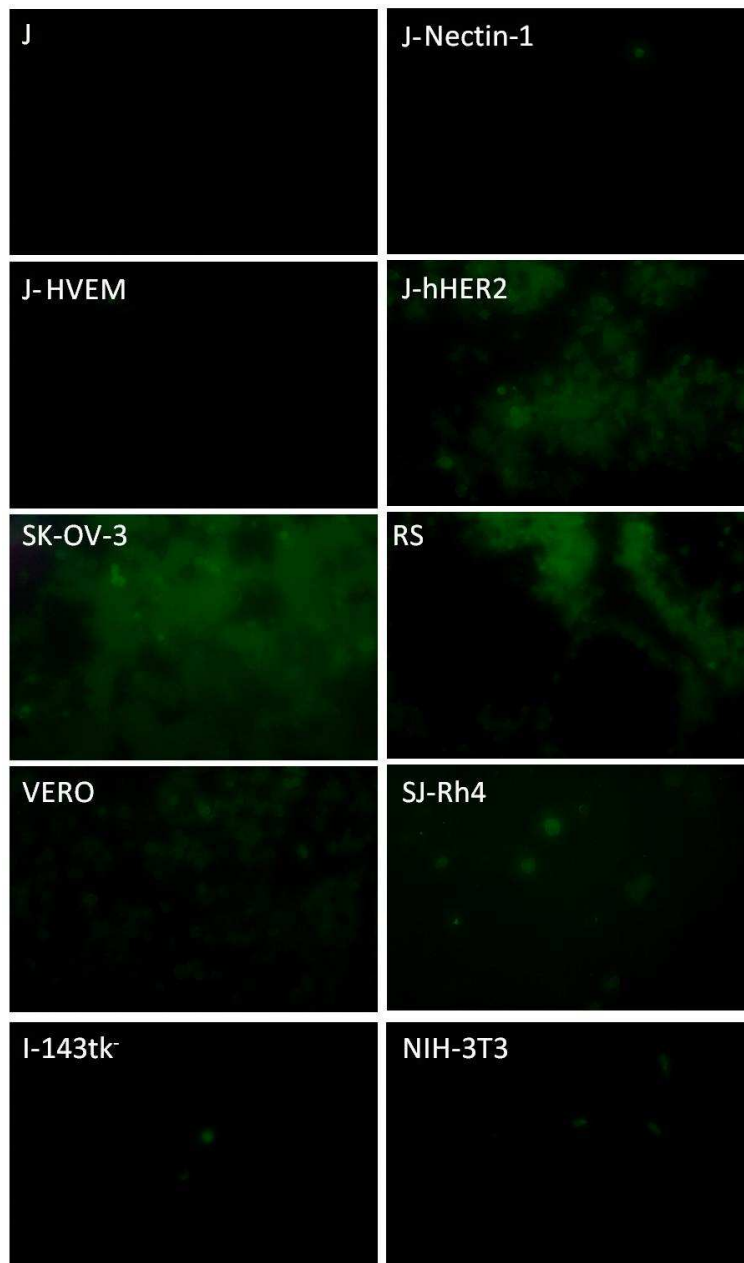


Figure 4.3.2 - R-LM291 infects efficiently HER2 expressing cells. Cell lines were infected at MOI 3 and grown at 37°C for 24 h. The infection was monitored by EGFP fluorescence. Digital pictures were taken with a Kodak camera connected to a Zeiss Axioplan fluorescence microscope.

EGFP fluorescence emission by infected cells was quantified by a fluorometer. The results confirmed the first analysis based on cell infection. J-HER2 and SK-OV-3 were infected efficiently by the virus and VERO and RS cells gave a EGFP signal of detection different from R-LM249 (Fig. 4.1.3 and 4.3.3).

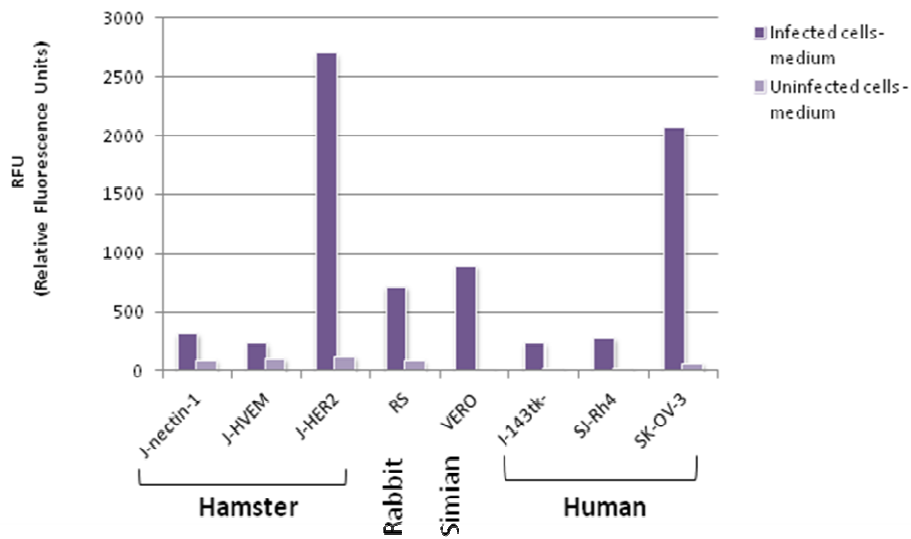


Figure 4.3.3 – R-LM291 infects HER2 positive cells. Cell lines were infected with R-LM291 and monitored by EGFP fluorescence 24 h post infection. The fluorescence value of the medium was subtracted from the infected or uninfected cells values. Fluorescence emission was measured with a fluorometer (r.f.u., relative fluorescence units).

The mutation in gB conferred to R-LM291 the ability to spread more efficiently in murine cells compared to R-LM249. We infected at low MOI three murine mammary cells lines expressing HER2: 1E-huHER2, D2F2/E2-HER2 and FVB 6443.0 explanted from a tumor of a FVB/N HER-2/neu transgenic mouse (Genentech) with R-LM291, R-LM249 and R-LM5 as control. Cells were monitored up to 72 hours post infection through EGFP fluorescence detection. SK-OV-3 cells were infected as control. R-LM291 showed large plaques already at 48 hours of infection in all murine cells tested (Fig 4.3.4). As expected, R-LM5 infected efficiently all cell lines that are susceptible to HSV-1 infection. R-LM249 infected slowly with plaques of small dimension.

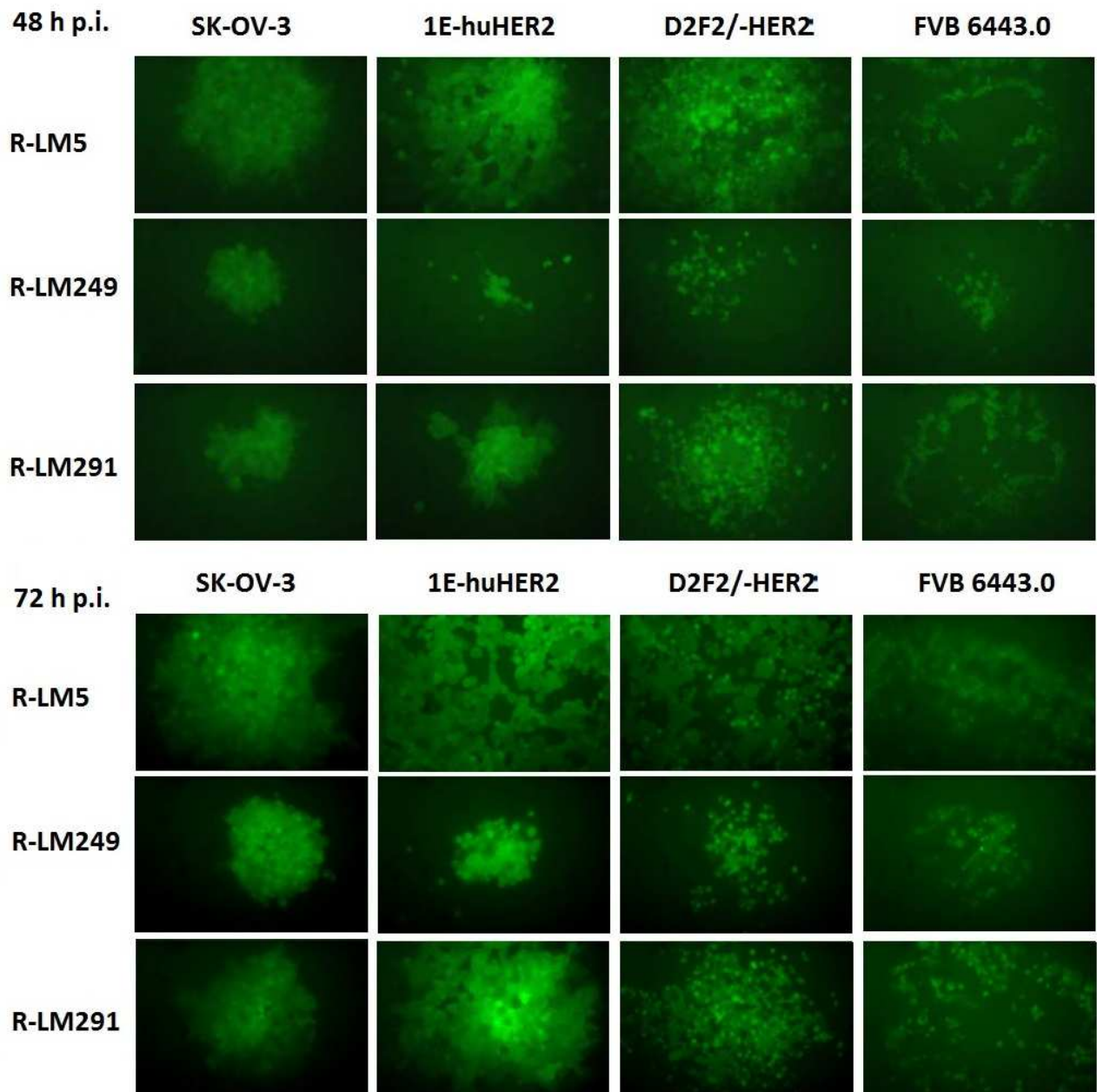


Figure 4.3.4 – R-LM291 infected more efficiently murine cells than R-LM249. Cells were infected with low MOI of R-LM5, R-LM249 and R-LM291. The infection was monitored by EGFP fluorescence over the time (48h and 72h post infection). Digital pictures were taken with a Kodak camera connected to a Zeiss Axioplan fluorescence microscope.

4.3.2 R-LM291 exerts the same cytolytic activity and viral replication as R-LM249 in HER2 positive cells.

Our goal in generating R-LM291 was to increase its oncolytic activity as compared to the parental virus R-LM249. To verify this aspect, we measured R-LM291 cytolytic activity in SJ-Rh4 and SK-OV-3 cells. The latter exhibits high level of HER-2 expression. Cell toxicity was measured over time by the Alamar Blue assay and compared to that of R-LM5 and R-LM249 (Fig. 4.3.5). All three viruses were cytotoxic to SK-OV-3 cells, leaving only 35% of viable cells at highest MOI, at 6 days post infection (Fig. 4.3.5 A). As expected, R-LM249 and R-LM291 exhibited no cytotoxic activity at any doses tested in SJ-Rh4 cells whereas R-LM5 was able to kill 65% of cells 6 days post infection (Fig. 4.3.5 B).

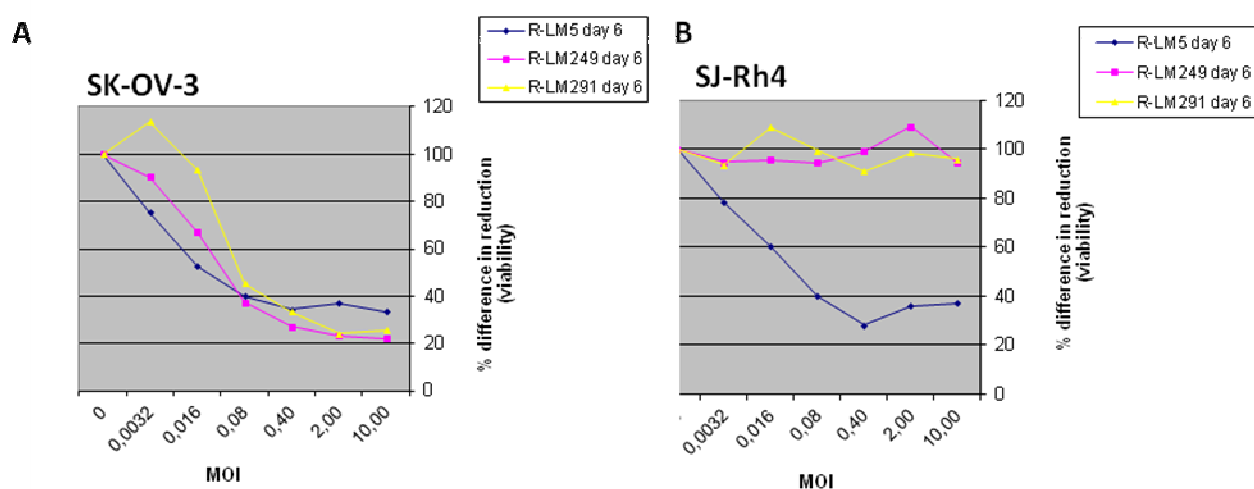


Figure 4.3.5 – R-LM291 and R-LM249 exerted the same cytotoxic activity only in HER2 positive cells. Cytotoxicity of R-LM5, R-LM249 and R-LM291 in HER2 positive (SK-OV-3) (A) or HER2 negative (SJ-Rh4) cells (B). Cell viability was measured by means of the Alamar blue exclusion assay. Cells were seeded in replicated 96 multiwell plates and infected at the MOI indicated in the *x* axis. Every two days cells were assayed for reduction of resazurin to the fluorescent molecule, resorufin and we reported the reading at 6 days post infection. The absorbance was measure at 570/600 nm with a fluorometer.

In addition, we assessed the difference between R-LM291 replication ability compared to that of R-LM249. Thus, we performed a viral yield assay comparing R-LM249, R-LM291 and R-LM5 as control. SK-OV-3 cells and SJ-Rh4 cells were infected at MOI 1 with each virus. The titration was performed in SK-OV-3 cells on samples harvested 3, 24, 48 and 72 h post infection.

The results showed that R-LM291 titration curve was identical to that of R-LM249. Both viruses replicated only in SK-OV-3 cells and failed to replicate in SJ-Rh4 cells (Fig. 4.3.6). As expected, the control virus R-LM5 replicated efficiently in both cell lines tested.

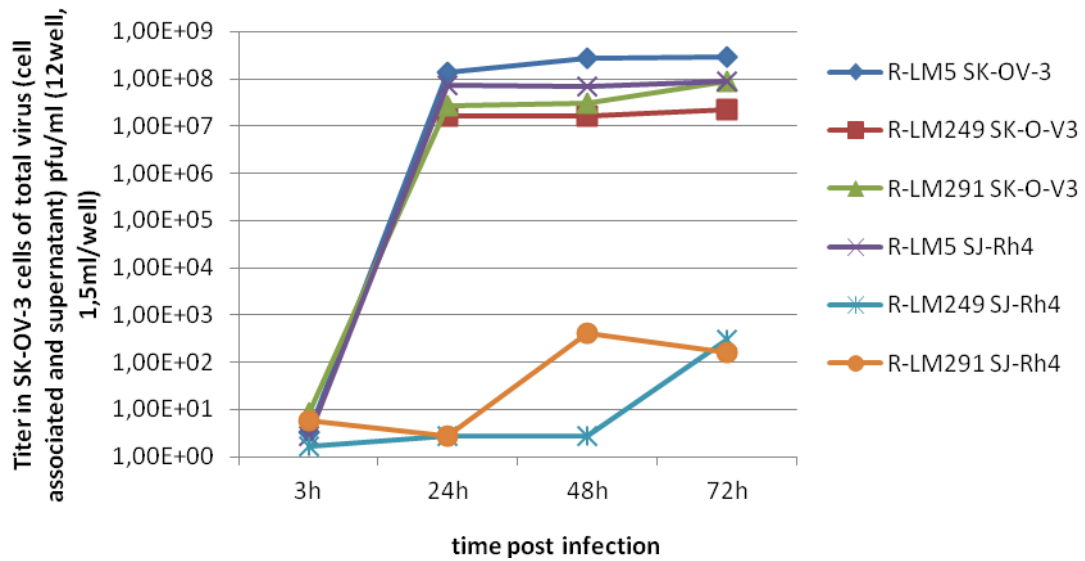
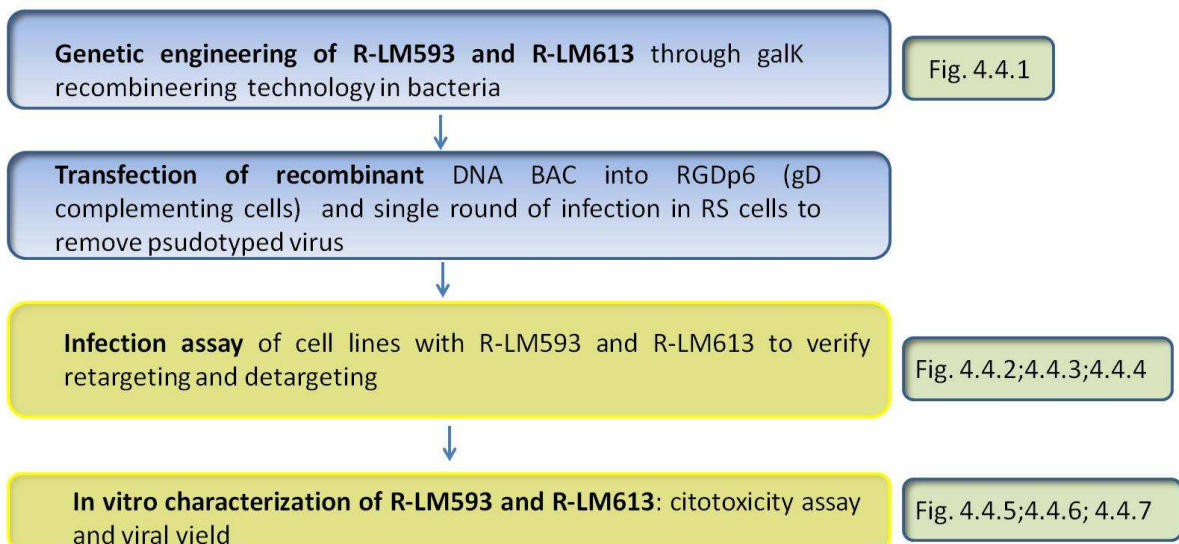


Figure 4.3.6 – R-LM291, R-LM249 and R-LM5 viral yield in SK-OV-3 (HER2 positive) and SJ-Rh4 (HER2 negative) cells. Cells were infected at 1 multiplicity of infection (MOI, pfu/cell) and harvested at 3, 24, 48, 72 h post infection. Samples were titrated in SK-OV-3 cells.

4.4 *o*-HSV retargeted to additional tumor specific receptors (PSMA and EGFRvIII)

Schematic flow of steps for generation and assay of R-LM593 and R-LM613



So far, the focus of my work was viruses retargeted to HER2 receptor. The results proved that the retargeting strategy was effective to drive the recombinant HSV-1, modified with the insertion of a scFv antibody, towards a specific heterologous receptor *in vitro* and on tumor model *in vivo*.

Hence, we took into account additional targets. In particular, we focused on the prostate specific membrane antigen (PSMA) and epidermal growth factor receptor variant III (EGFRvIII) which, as already reported in the introduction, are overexpressed in prostate carcinoma and glioma multiforme, respectively.

Standard therapies demonstrated to be not sufficient for the eradication of these tumors. In particular, prostate cancer treatments place the patients at risk for temporary or permanent impotence, especially those patients who have undergone prostate surgery and radiation therapy. Patients affected by glioma have a median survival time from diagnosis of one year and these statistics have not changed in the past 50 years. Hence, the need to search new and novel therapies is very high.

ScFv antibodies are available for both receptors making the two targets suitable for the generation of new recombinant o-HSVs.

As a first attempt, we introduced the scFv to PSMA and EGFRvIII in the N-terminal position of gD with galK recombinering technology. The resulting viruses were called R-LM593 and R-LM613 (Fig. 4.4.1 A and B). As in R-LM113 the scFvs were followed by a 11 serine glycine linker at C-terminal that was introduced during the recombinering procedures.

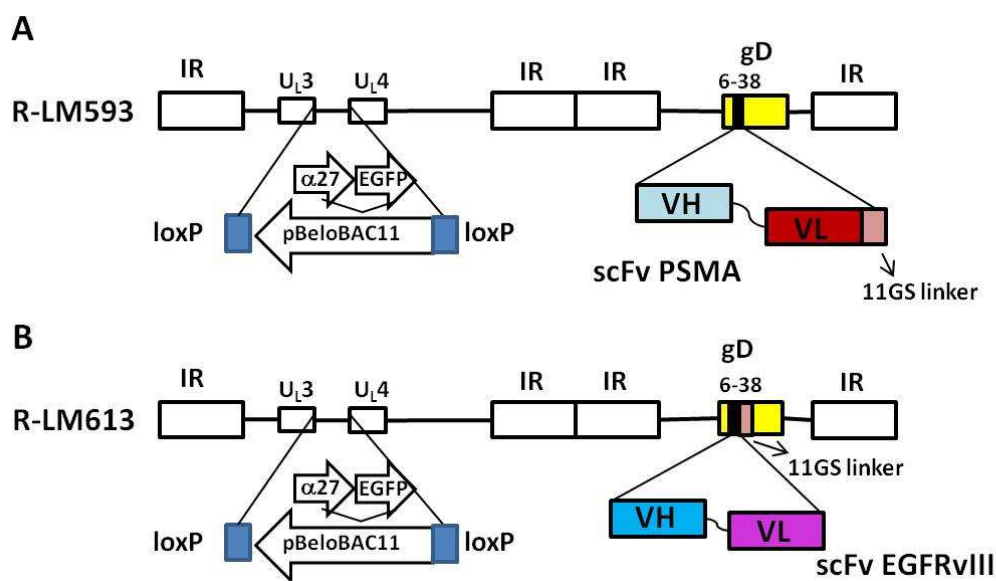


Figure 4.4.1 – A-B Linear maps of R-LM593 and R-LM613 Both scFv were inserted in the deletion of aa6-38 of gD by means of galk recombinering technology. V_L and V_H: variable light and heavy chains of scFv.

4.4.1 R-LM593 and R-LM613 are retargeted to PSMA and EGFRvIII, respectively

As for the other retargeted viruses described so far, first we verified the retargeting to heterologous receptors and the detargeting from HSV-1 natural receptors. We infected several

cells lines (hamster, human, simian and rabbit) monitoring the infection as EGFP fluorescence.

R-LM593 was able to infect J-PSMA cells, that express PSMA and no HSV-1 natural receptor, and LNCaP cells derived from a metastasis of human prostate carcinoma expressing PSMA at high levels and susceptible of wt HSV-1 infection (Fig. 4.4.2). The virus tropism resulted very specific as it infected only PSMA positive cells and did not infect any cell devoid of HSV-1 receptors as J cells or expressing HSV natural receptor J-nectin-1 H-HVEM, I-143-tk⁻ and 293T cells. This indicated that the detargeting/retargeting was effective. However, we found small and sparse plaques in RS and VERO cells. This was a common feature of all our retargeted virus (see also R-LM249 and RLM-291). The plaques remained small in size and the virus cultivated on these cells was lost in few passages.

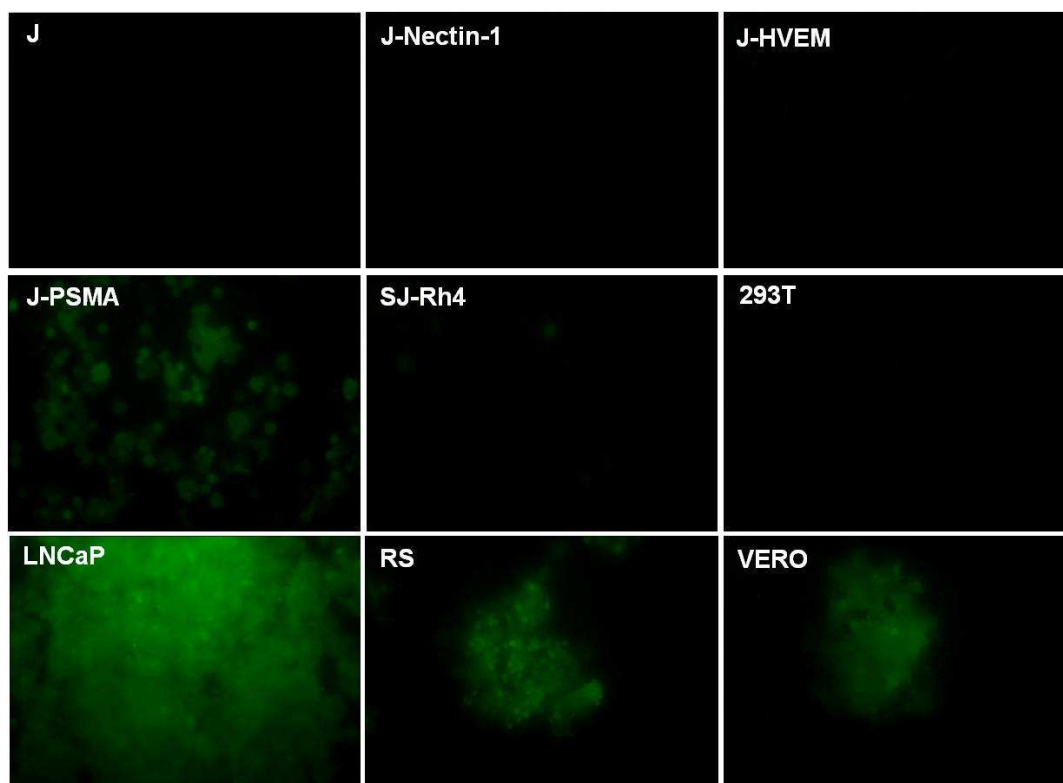


Figure 4.4.2 - R-LM593 infects only PSMA expressing cells. Cell lines were infected at MOI 3 and grown at 37°C for 24 h. The infection was monitored by EGFP fluorescence at 24 h post infection. Digital pictures were taken with a Kodak camera connected to a Zeiss Axioplan fluorescence microscope.

R-LM613 only infected cells expressing EGFRvIII as J-EGFRvIII and U251EGFRvIII, proving that its tropism has been redirected to the receptor target (Fig. 4.4.3). In addition, the virus was detargeted from HSV-1 natural receptors as evidenced by the absence of positive-fluorescent cells in J, J-Nectin-1, J-HVEM, I-143-tk⁻ and 293T cells. Noteworthy, the virus did not infect J-EGFR, expressing the wt form of the receptor. This result indicated that the scFv EGFRvIII

allows to discriminate between the native form of the receptor and the mutant one. Also in this case RS and VERO gave a background infection.

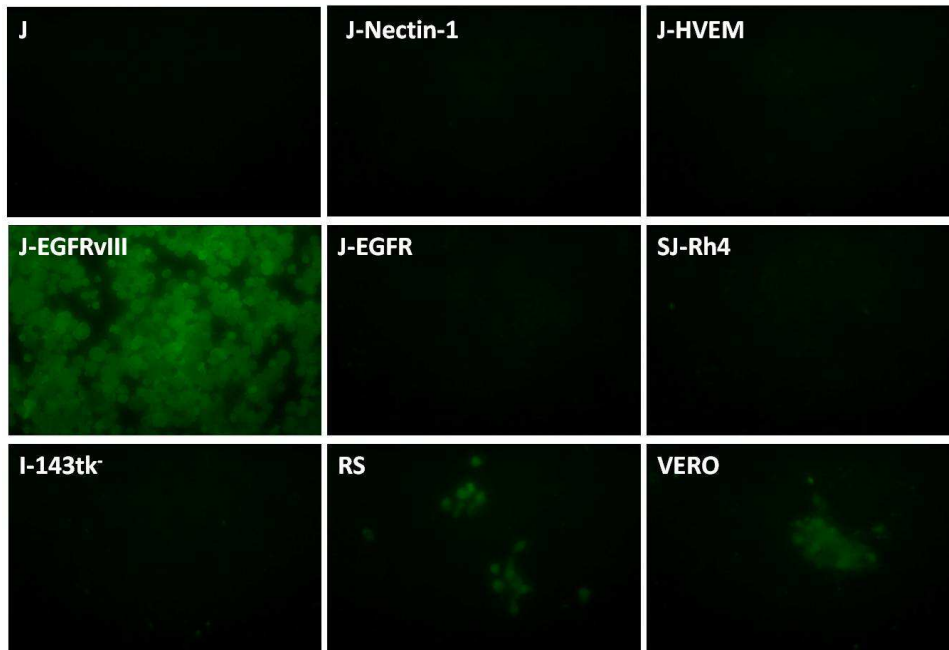


Figure 4.4.3 - R-LM613 infects only EGFRvIII expressing cells. Cell lines were infected at MOI 3 and grown at 37°C for 24 h. The infection was monitored by EGFP fluorescence at 24 h post infection. Digital pictures were taken with a Kodak camera connected to a Zeiss Axioplan fluorescence microscope.

The results of infection assays were confirmed for both viruses by fluorometer reading of the EGFP signal in infected cells (Fig. 4.4.4 A and B).

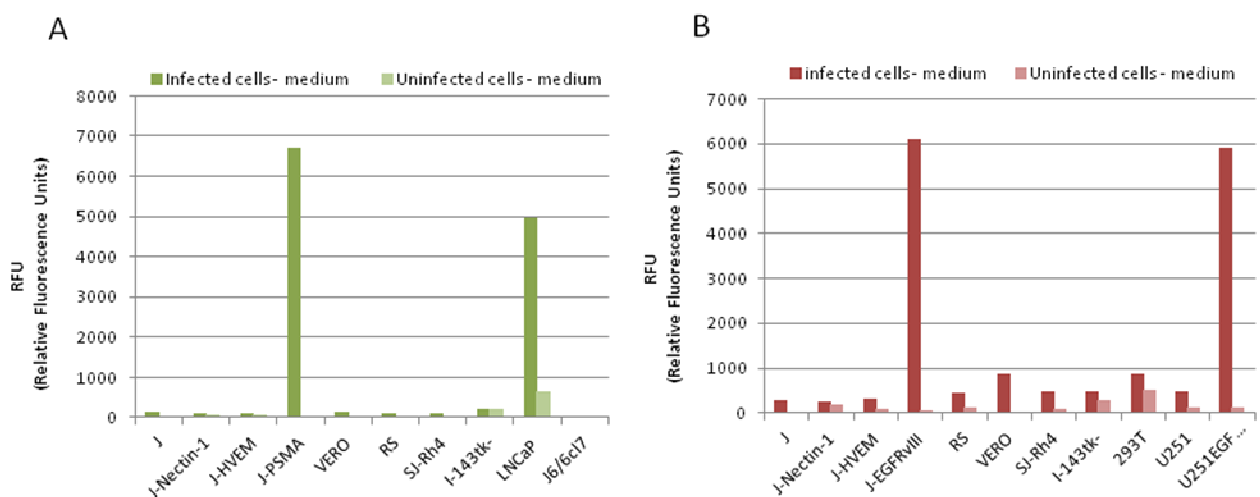


Figure 4.4.4 – R-LM593 and R-LM613 infect only cell expressing their target receptors. A) R-LM593 infection. B) R-LM613 infection. Cell lines were infected with R-LM593 or R-LM613 and monitored by EGFP fluorescence 48 h post infection. The fluorescence value of the medium was subtracted from the infected or uninfected cells values. Fluorescence emission was measured with a fluorometer (r.f.u., relative fluorescence units).

4.4.2 R-LM593 and R-LM613 specifically kill the cells expressing the targeted receptors

To assess ability of the recombinant viruses to kill cells expressing the target receptors and to further strengthen evidence for their specificity, we measured R-LM593 and R-LM613 cytotoxicity by means of Alamar Blue assay. For R-LM593 the assay was performed with escalating MOI in four cell lines: two were PSMA positive (LNCaP and J-PSMA) and two were PSMA negative (J-nectin1 and SJ-Rh4). R-LM5 was used as control in the same cell lines. R-LM593 was cytotoxic only in LNCaP and J-PSMA cells, lowering, at the highest doses, the percentage of viable cells to about 40% in 6 days for LNCaP cells and 60% in 4 days for J-PSMA (Fig 4.4.5 A,C). By contrast, R-LM593 did not exert a cytotoxic activity in PSMA negative cells after 6 day for SJ-Rh4 and 4 days for J-Nectin1 (Fig 4.4.5 B,D). J nectin-1 cells showed a recovery of viability when infected with R-LM5 at low MOI. This was due likely to a small pool of J-Nectin1 cells that became resistant to the HSV infection and started to replicate. The results further demonstrated that R-LM593 was effectively retargeted to PSMA receptor and detargeted from HSV-1 natural receptors. R-LM5 as expected was cytotoxic in all cell lines except for cells not expressing HSV-1 receptor i.e. J-PSMA.

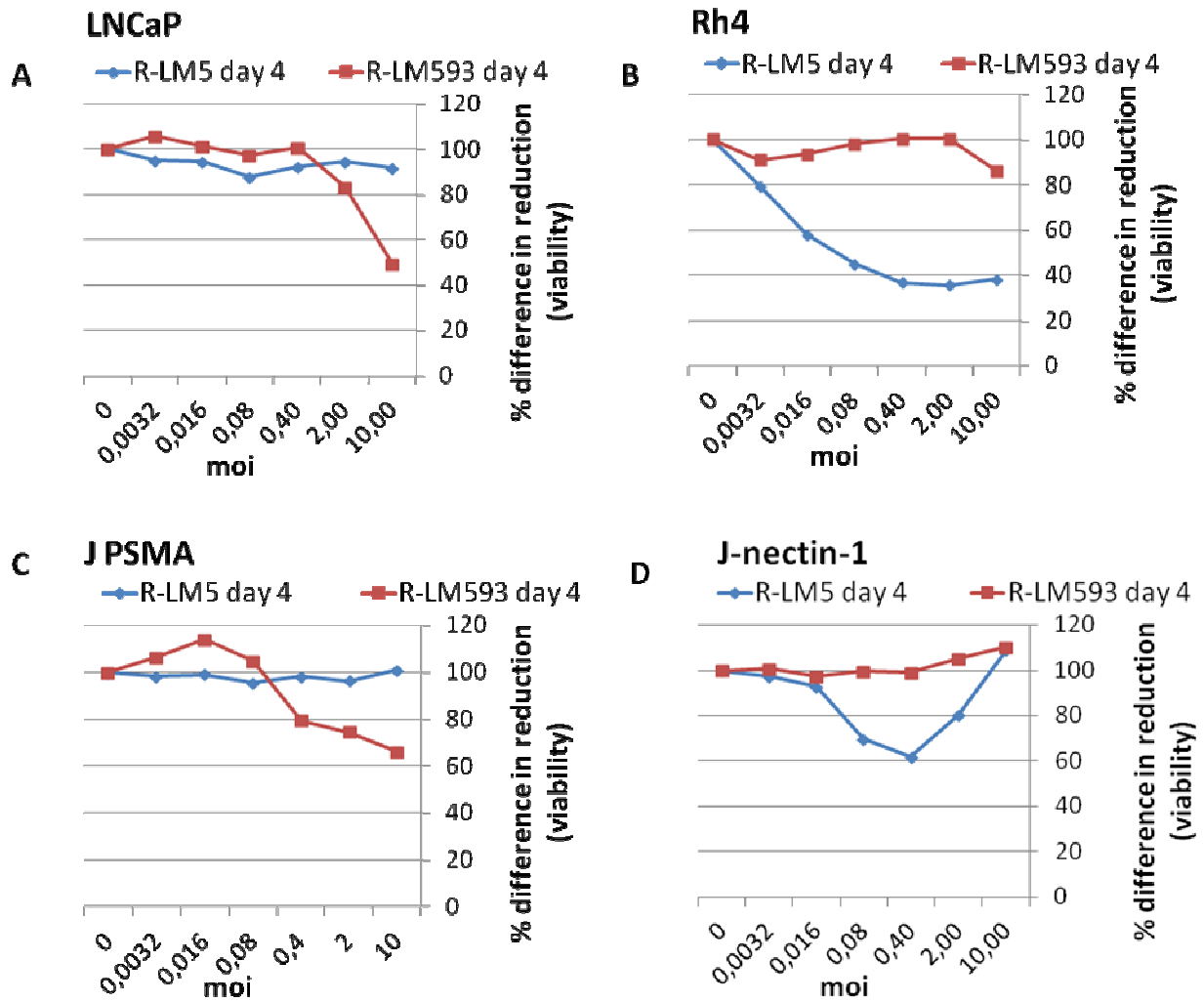


Figure 4.4.5 - R-LM593 is cytotoxic for cell lines expressing PSMA. Cytotoxicity of R-LM5 and R-LM593 was tested in PSMA positive (A,C - LNCaP, J-PSMA) or PSMA negative (B,D J-nectin-1, SJ-Rh4) cells. Cell viability was measured by means of the Alamar blue exclusion assay. Cells were seeded in replicated 96 multiwell plates and infected at the MOI indicated in the x axis. Every two days cells were assayed for reduction of resazurin to the fluorescent molecule resorufin. We reported the reading at 6 days post infection. The reduction in J-PSMA and J-nectin1 was measured until 4 days after infection because they died completely at day 6. The absorbance was measured at 570/600 nm with a fluorometer.

The cytotoxic activity of R-LM613 was assessed in two glioblastoma cell lines: U251EGFRvIII that express the target receptor EGFRvIII and the U251 that does not express EGFRvIII. Both cell lines were permissive and susceptible to wt HSV-1 infection. The results showed that R-LM613 did not exhibit any cytotoxic activity in U251 (Fig. 4.4.6 A) while it was highly cytotoxic for U251 EGFRvIII cells carrying the cell viability to 40 % at the highest dose (MOI 10) in 6 days (Fig. 4.4.6 B). The control virus R-LM5, as expected, was cytotoxic for both cell lines.

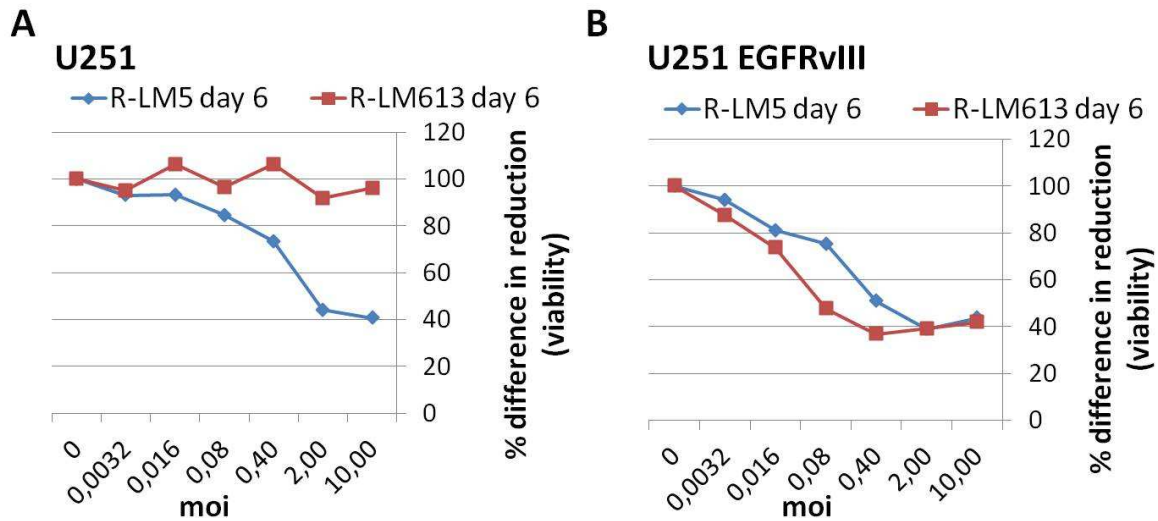


Figure 4.4.6 - R-LM613 is cytotoxic only in EGFRvIII expressing cells. Cytotoxicity of R-LM5 and R-LM613 was tested in EGFRvIII negative (A- U251) or EGFRvIII positive (B - U251EGFRvIII) cells. Cell viability was measured by means of the Alamar blue exclusion assay. Cells were seeded in replicated 96 multiwell plates and infected at escalating MOI. Every two days cells were assayed for reduction of resazurin to the fluorescent molecule, resorufin. The absorbance was measure at 570/600 nm with a fluorometer.

4.4.3 R-LM613 grows efficiently in U251EGFRvIII and J-EGFRvIII cell

To further validate our results about R-LM613 we carried out a virus yield assay infecting EGFRvIII positive cell lines i.e. U251EGFRvIII and J-EGFRvIII, or cells negative for the same receptor but expressing HSV-1 natural receptors J, J-Nectin-1, JHVEM and U251. The same cells were infected with R-LM5 as control. R-LM613 replicated efficiently in U251EGFRvIII and J-EGFRvIII indicating that it was able to recognize the target receptor in a specific fashion. Conversely, the R-LM613 titer was nearly equal to 0 in J derived cells while in U251 cells it reached 10^4 pfu/ml even if with an efficiency 100 times lower than in U251EGFRvIII (Fig. 4.4.7).

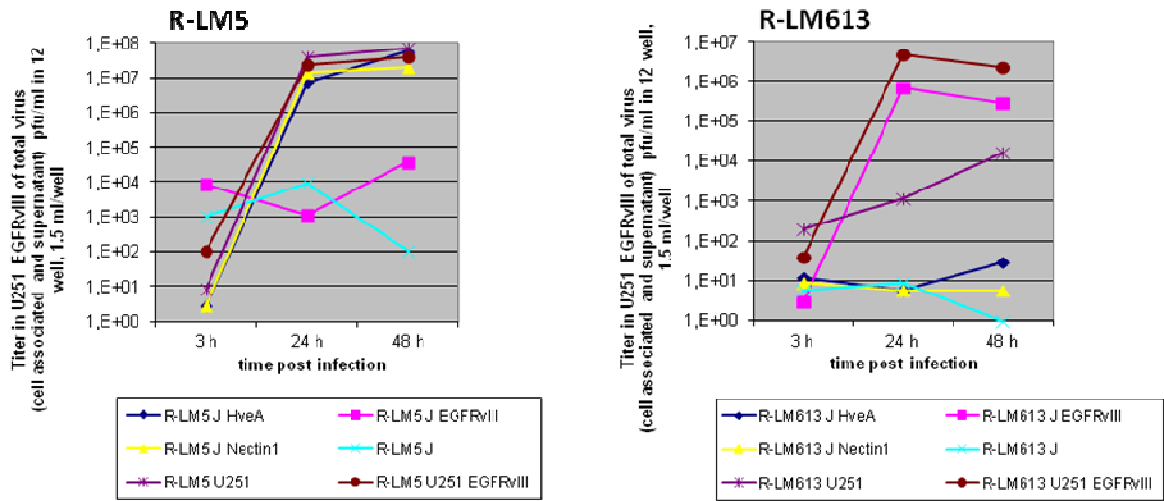


Figure 4.4.7 - Viral yield of R-LM613 and R-LM5 in cell expressing EGFRvIII receptors and cell expressing or not HSV-1 natural receptors. Cell were infected at 1 MOI (pfu/cell) and harvested at 3,24, 48h post infection. Samples were titrated in U251EGFRvIII cells.

5. Discussion

Tumors are still one of the major causes of human mortality. Despite numerous advances made for their treatment (surgical resection, chemotherapy, radiotherapy or a combination of these), some aggressive types of cancer cannot be treated effectively. Furthermore chemotherapy is very invasive as it kills indiscriminately healthy cells and tumor cells, with considerable side effects to the patients.

Oncolytic virotherapy is a promising therapeutic approach against cancer. Some viruses exert cytolytic activity on infected cells in order to ensure a fast and effective viral progeny spread to the surrounding tissues. This feature can be exploited to kill tumor cells selectively, sparing healthy ones. Furthermore these viruses are able to replicate within cells, unlike drugs that have in addition, a limiting half-life.

HSV arises as a promising oncolytic vector for several reasons: it has a genome size that can accommodate large transgenes (up to 30 kbp) and it is amenable to genetic engineering; it is a mild human pathogen against which effective anti virals exist (e.g. acyclovir). Moreover, some attenuated oncolytic HSV are already in clinical trials (130, 131). A side effect related to the attenuation strategy is that it affects virus potency. In fact, these viruses are highly safe but characterized by lower viral replication, as compared to wt HSV.

Based on these observations, the objective of this thesis was to construct replication-competent recombinant HSV retargeted to tumor specific receptors and simultaneously detargeted from the natural HSV-1 receptor, HVEM and Nectin-1.

Three tumor specific receptors were selected for the retargeting approach: HER2, which is over-expressed in 25-30% of breast and ovarian cancer and glioma multiforme; PSMA, which is over-expressed in prostate cancer and in neovasculature of solid tumors; and EGFR variant III, which is expressed in gliomas.

The general strategy for retargeting was based on the availability of single chain antibodies (scFv) to the target receptors. The scFvs are smaller than the full chain antibodies and offer a high binding specificity. The host spectrum of HSV-1 has been modified by the insertion of scFv in the envelope glycoprotein gD. Indeed, gD determines the HSV natural tropism by binding to HVEM, Nectin-1 and 3-O-sulfate heparan sulfate. Upon binding to the receptor, gD triggers fusion by recruiting the glycoproteins gB, gH, and gL. The results of this thesis show the successful construction of chimeric forms of gD (gD-scFv) that render HSV-1 able to interact only with tumor specific receptors and no longer with the natural receptors. The genetic manipulations of viruses were performed using a BAC-HSV-1 genome (162).

o-HSVs retargeted to HER2 receptor

The HER2 receptor was the first receptor targeted in our studies. This target is clinically relevant because of its high expression in breast and ovary tumors, as well as in gliomas. The mAb trastuzumab, represented the first HER2-specific therapy available, becomes ineffective within a year from the beginning of the therapy, and cannot be used against brain tumors because mAbs fail to cross the blood brain barrier (172).

We have generated three HER2-retargeted viruses: (i) R-LM113 (80), which carries the scFv to

HER2 in the deletion of aa 6-38 of gD; (ii) R-LM249, which carries the insertion of scFv in place of aa 61-218, which were deleted (80); (iii) R-LM291, a derivative of R-LM249 carrying two mutations in gB known to increase the rate of entry of HSV (56); these mutations should better the ability of R-LM249 to enter cells (56).

R-LM113 was preliminarily characterized *in vitro* (80). The results of the experiments showed that the virus is fully detargeted from the HSV-1 receptors HVEM and Nectin-1, since it is unable to grow to titers higher than 10^3 - 10^4 pfu/ml in J-nectin-1, J-HVEM, I-143tk- and Hep2 cells. Conversely, R-LM113 was able to infect and spread in HER2 positive cells such as J-HER2 and SK-OV-3.

The rationale of RLM113 engineering was to locate the scFv to HER2 in a frontal position relative to the contact surface between gD and Nectin-1 and eliminate the portion of the protein involved in binding to HVEM and Nectin-1. The deletion also encompasses aa 38 later found to be important for the binding to Nectin-1 (41).

The HER2 receptor is expressed in a significant number of high grade gliomas, where it induces an increase of anaplasia correlated to a poor prognosis (173).

In this thesis, the virus has been tested for the safety profile and employed in an *in vivo* model of HER2-expressing gliomas (171, 173). The murine glioblastoma (GMB) cells were based on the over-expression of platelet derived growth factor B (PDGF-B) (171, 174). The experiments were conducted in collaboration with Dr. Paolo Malatesta's group (IST institute of Genoa).

LM113 showed a high safety profile after intracranial injections, as compared to wt HSV-1 R-LM5 in NOD/SCID mice. Animals inoculated with the virus did not show any sign of virus spread in the brain, while the wt virus was lethal even at lower doses. The oncolytic activity *in vivo* was evaluated with two different approaches: the virus was administered at the same time as tumor cells (early treatment set), or after 45 days following cell inoculation (late treatment set). The treatments with R-LM113 improved the survival time of mice in both experiments. The best effect was observed in the early treatment group where mice showed no signs of encephalitis, confirming the safety of the virus. The analysis of brains with established tumors (late treatment set) in the period immediately following virus administration has shown the ability of R-LM113 to spread away from the injection site. This result is important in view of clinical application on glioma that are a highly invasive and infiltrating tumors.

This is the first report on the efficacy of a non-attenuated, replication competent, and retargeted o-HSV-1 in a model of intracranial glioblastoma.

R-LM249 was designed following the observations by Zhou and Roizman that the gD fragment from aa 61 to 218 does not carry out any function required for the virus entry into cells (37). It was speculated that this portion of gD, which coincides almost completely with the Ig-folded domain, serves as a link between the N-terminal domain and the profusion domain of gD. The scFv to HER2 was inserted in place of the Ig-folded domain by means of a two-step replacement technique. R-LM249 is at the same time retargeted to HER2 receptor and detargeted from HSV-1 natural receptors. In fact it was able to infect only HER2 positive cells such as J-HER2, SK-OV-3, MDA-MB-453 and BT-474, and failed to infect J cells that express no HSV-1 receptor. Moreover, the receptor usage was specific since the infection was inhibited only by antibodies

against HER2 receptor.

Although we do not have any direct evidence we assume that the detargeting from both receptors is the result of a conformational change in gD due to the size of the insert and the deletion of some residues essential to binding to Nectin-1 (e.g. aa 215) and HVEM.

We were able to grow the virus to 10^9 pfu/roller bottle and to evaluate the virus oncolytic activity *in vivo*.

The latter study provided two important results: i) the virus exhibited a high safety profile documented by a high LD₅₀ compared to wt HSV-1 ii) R-LM249 was able to inhibit the growth of HER2 human tumors cells. The virus was tested in a subcutaneous ovarian tumor model and in a subcutaneous breast tumor model in nude mice. In the ovarian cancer model, a single administration resulted in a significant and lasting therapeutic effect (weeks after treatment) in HER2-positive tumors up to 0.2 cm³. The repeated injections led to a high percentage of tumor free mice up to five months after the last treatment, while the remaining mice showed strongly delayed and reduced tumor growth. The most effective dose was 2×10^7 pfu/mouse. These doses are in accordance with those used for other o-HSVs in mice (129). It is unclear why a higher dose was less effective. One likely explanation is, the virion aggregates reduced the effect; in alternative it caused massive apoptosis of target cells by reducing the reservoir of cells in which the virus could replicate and spread.

Glorioso and coworkers recently reported the identification of two mutations in gB D285N/A549T, selected by repeated passage of an HSV mutant gD defective in Nectin-1 binding (56), which increases the virus' rate of entry into cells. This discovery was the basis for the genetic engineering of R-LM291, that maintains the same backbone of R-LM249 with the addition of mutations in gB. So far, the virus has been characterized in cell cultures. R-LM291 has maintained the retargeting to HER2 receptor and the inability to use HVEM and Nectin-1 as receptors for entry. The viral yield shows that there is no substantial increase in the virus replication in HER2 positive cells, as compared to R-LM249. The important feature is that the virus exhibited an improved cell-to-cell spread in murine cells, as compared to the progenitor R-LM249.

o-HSV retargeted to PSMA and EGFRvIII receptors.

The viruses R-LM593 and R-LM613 are retargeted to PSMA and EGFRvIII receptors, respectively. These viruses were generated only in the last year of my thesis, and they have not yet been characterized as far as *in vivo* anti-tumor efficacy is concerned. The rationale for their generation is as follows:

Prostate cancer is the leading cause of death in males in the eastern part of the world. In America it is the second leading cause of death with 186,000 new cases per year. Effective therapies are not available for local and advanced cancer state (148). This tumor is a promising candidate for oncolytic virotherapy because the site of the primary tumor is easily accessible to a loco-regional virus administration.

The PSMA receptor is a membrane glycoprotein expressed in highly localized or metastatic prostate tumors. It is being employed as a target for imaging-based diagnosis and for the

immunotherapy of the tumor (175). In the R-LM593 virus, the anti-PSMA scFv was engineered at the amino terminal portion of gD (delta 6-38). The *in vitro* characterization showed that the retargeting and detargeting have been successfully achieved, since the virus is able to infect only cells which express the target receptor, such as J-PSMA and LNCaP. In addition, the cytotoxic activity is exerted only towards PSMA positive cells.

Glioblastomas account for approximately 20% of all brain tumors. The disease has a poor prognosis in almost all cases because the tumors are resistant to conventional therapies. The average survival time from diagnosis is one year. Since these statistics have not changed in the last 50 years, glioblastomas are among tumors most suitable to test the efficacy of oncolytic HSV. The virus can be inoculated with stereotactic intra-tumoral injections or during surgery. The brain compartments affected by the treatment are excluded from the immune system and make these tumors suitable to oncolytic virus administration, regardless of the serostatus of the patient.

The EGFRvIII receptor is over-expressed in gliomas and is a mutant form of EGFR. It is generated by a deletion of exons from 2 to 7 of wt gene which leads to a deletion of 267 amino acids in the extracellular domain of the receptor. Therefore, EGFRvIII is unable to bind ligands and is constitutively active (152). The virus R-LM613 was engineered to carry the scFv anti-EGFRvIII in the N-terminal portion of gD. Infection assays *in vivo* have shown that the virus is able to infect only cells expressing EGFRvIII, such as J-EGFRvIII and U251EGFRvIII, on which it exerts a specific cytotoxic activity that is not found in cells expressing the HSV-1 natural receptors. The yield of R-LM613 confirmed that the virus can replicate only in EGFRvIII-expressing cells.

5.1 General considerations and perspectives

A most remarkable aspect of our results is that gD can tolerate dramatic genetic modifications, yet viruses carrying such extensively modified forms of gD are viable. My studies show that gD can tolerate the deletion of the Ig-folded core and its replacement with a heterologous fragment, or the insertion of the scFv at the N-terminus of the molecule; in this case gD had a relatively small deletion. Overall, gD can tolerate the insertion of heterologous sequences almost as large as the gD ectodomain itself. This extreme plasticity of gD has enabled the construction of a number of candidate α -HSVs retargeted to three different cancer-specific receptors.

In light of the results, we can state that two privileged positions in gD were identified, in which an scFv to tumor-specific receptor can be inserted. The first position is located at the N-terminus of gD (deletion from aa 6 to 38); and the second is a replacement of the Ig-folded core of the protein (from aa 61 to 218) (44, 80). It is noteworthy that the insertion of scFvs at the two positions did not affect the ability of the the scFvs to interact with their cognate receptors, and this property was transferred to gD. In turn, gD was still capable (i) of adopting the proper conformation, and undergoing structural changes required for the subsequent steps in virus entry. Moreover (ii) the retargeted viruses grew to yields just one order of magnitude lower than those achieved by viruses carrying wt gD, indicating that overall gD was still capable of carrying out its major functions, i.e. receptor recognition, and signaling to downstream virion glycoproteins

gH/gL and gB.

The retargeting strategies similar to the ones performed in my studies have been attempted with two other enveloped viruses, measles virus (161, 176) and VSV (177), which have been retargeted towards a number of receptors (CEA, CD20, CD38, PSMA, EGFR, EGFRvIII and HER2). These viruses are being tested with promising results in models of intraperitoneal and subcutaneous tumors, doubling the survival of treated animals. Probably, the most promising results are those obtained with measles virus retargeted to EGFR or EGFRvIII, when applied in an orthotopic xenografts glioma model in immunodeficient mice (178) these viruses caused a significant increase of survival time. These examples strengthen the feasibility of the retargeting strategy.

Concerning *in vivo* studies, it remains to determine (i) the oncolytic efficacy of the retargeted viruses in models of immunocompetent mice and (ii) a route of administration other to intratumoral.

The immune system could facilitate the clearance of the tumor but on the other side it could also decrease virus efficacy. HSV-1 is a common human pathogen and general population carries antibody against the virus. Studies in prior HSV-immunized mice demonstrate that immune response does not significantly interfere with therapeutic efficacy (179). In a clinical trial phase I study the initial intratumoral injection reliably induced a strong anti-HSV immune response in HSV seronegative patients, evidenced by increase in antibody titer. However, this does not appear to affect the extent of the other clinical responses (130). One of our future objectives will be to evaluate the effect of preexisting immunity on the efficacy of our oncolytic HSV redirected to HER2. Moreover, we want to test HER2 retargeted viruses in an immunocompetent mouse model that leads to the appearance of HER2 positive tumors based on a transgenic mouse produced by Genentech.

So far, our studies have assessed the efficacy of the loco-regional route of administration. Local administration results effective for tumors that can easily be reached through intra-tumoral injections or for tissue adjacent to resected tumors. Clearly, the ideal type of administration of o-HSV is by a systemic route (intraperitoneal for intraperitoneal tumors, or intravenous for metastases).

The currently available HER-2-retargeted o-HSV needs to be optimized in order to be suitable for systemic delivery. We plan to introduce the following modifications: HSV glycoproteins gC and gB carry heparan sulphate binding sites which mediate virus attachment to a variety of cells, including cells negative for HSV receptors. We also plan to delete the heparan sulphate binding site, and eventually replace them with scFv to HER-2, so that the final virus will bind with increased strength to the target tumor cells.

In conclusion, up to now the studies carried out have shown that i) the o-HSV retargeting is a feasible strategy and that ii) viruses retarget to HER2 receptor (R-LM113 and R-LM249) cause a target-specific inhibition of human tumor growth. The use of scFv potentially allows for targeting any cellular receptor and the strategy can be applied for retargeted HSV to a wide spectrum of receptor families for which a single chain antibody is available.

6. Bibliography

1. Roizman B & Whitley RJ (2001) The nine ages of herpes simplex virus. *Herpes* 8(1):23-27.
2. Roizman B & Pellet PE (2001) The family *Herpesviridae*: a brief introduction. *Fields Virology*, eds Knipe DM, Howley P, Griffin D, Lamb R, Martin M, Roizman B, & S. S (Lippincott Williams & Wilkins, Philadelphia), 4rd Ed Vol 2, pp 2381-2397.
3. Roizman B, Whitley R, & Lopez C (1993) *The Human herpesviruses*, (Raven Press Ltd., 1185 Avenue of the Americas, New York), Vol 1.
4. Roizman B (1996) *Herpesviridae. Virology*, eds Fields BN, Knipe DM, Howley P, Chanock RM, Hirsch MS, Melnick JL, Monath TP, & Roizman B (Raven Press, New York, N.Y.), 3rd Ed, pp 2221-2230.
5. Roizman B (2011) The checkpoints of viral gene expression in productive and latent infection: the role of the HDAC/CoREST/LSD1/REST repressor complex. *J Virol* 85(15):7474-7482.
6. Whitley RJ & Roizman B (2001) Herpes simplex virus infections. *Lancet* 357(9267):1513-1518.
7. Bloom DC, Giordani NV, & Kwiatkowski DL (2010) Epigenetic regulation of latent HSV-1 gene expression. *Biochim Biophys Acta* 1799(3-4):246-256.
8. Watanabe D (2010) Medical application of herpes simplex virus. *Journal of Dermatological Science* 57:75-82.
9. Roizman B, Knipe DM, & Whitley RJ (2007) Herpes simplex viruses. *Fields Virology*, eds Knipe DM, Howley PM, Griffin DE, Lamb RA, Martin MA, Roizman B, & Straus SE (Lippincott Williams & Wilkins, New York, N.Y.), 5th Ed Vol 2, pp 2501-2601.
10. Grunewald K, *et al.* (2003) Three-dimensional structure of herpes simplex virus from cryo-electron tomography. *Science* 302(5649):1396-1398.
11. Schrag JD, Prasad BV, Rixon FJ, & Chiu W (1989) Three-dimensional structure of the HSV1 nucleocapsid. *Cell* 56(4):651-660.
12. van Genderen IL, Brandimarti R, Torrisi MR, Campadelli G, & van Meer G (1994) The phospholipid composition of extracellular herpes simplex virions differs from that of host cell nuclei. *Virology* 200(2):831-836.
13. Spear PG, Eisenberg RJ, & Cohen GH (2000) Three classes of cell surface receptors for alphaherpesvirus entry. *Virology* 275(1):1-8.
14. Ren Y, Bell S, Zenner HL, Lau SY, & Crump CM (2012) Glycoprotein M is important for the efficient incorporation of glycoprotein H-L into herpes simplex virus type 1 particles. *J Gen Virol* 93(Pt 2):319-329.
15. Poffenberger KL & Roizman B (1985) A noninverting genome of a viable herpes simplex virus 1: presence of head-to-tail linkages in packaged genomes and requirements for circularization after infection. *J Virol* 53(2):587-595.
16. Deshmane SL, Raengsakulrach B, Berson JF, & Fraser NW (1995) The replicating intermediates of herpes simplex virus type 1 DNA are relatively short. *J Neurovirol* 1(2):165-176.
17. Sandri-Goldin RM (2003) Replication of the herpes simplex virus genome: does it really go around in circles? *Proc Natl Acad Sci U S A* 100(13):7428-7429.
18. Roizman B & Sears AE (1996) Herpes simplex viruses and their replication. *Virology*, eds Fields BN, Knipe DM, Howley P, Chanock RM, Hirsch MS, Melnick JL, Monath TP, & Roizman B (Raven Press, New York, N.Y.), 3rd Ed, pp 2231-2295.

19. Umbach JL, Nagel MA, Cohrs RJ, Gilden DH, & Cullen BR (2009) Analysis of human alphaherpesvirus microRNA expression in latently infected human trigeminal ganglia. *J Virol* 83(20):10677-10683.
20. Roizman B, Zhou G, & Du T (2011) Checkpoints in productive and latent infections with herpes simplex virus 1: conceptualization of the issues. *J Neurovirol*.
21. Nicola AV, McEvoy AM, & Straus SE (2003) Roles for endocytosis and low pH in herpes simplex virus entry into HeLa and Chinese hamster ovary cells. *J Virol* 77(9):5324-5332.
22. Gianni T, Campadelli-Fiume G, & Menotti L (2004) Entry of Herpes Simplex Virus Mediated by Chimeric Forms of Nectin1 Retargeted to Endosomes or to Lipid Rafts Occurs through Acidic Endosomes. *J Virol* 78(22):12268-12276.
23. Maillet S, *et al.* (2006) Herpes simplex virus type 1 latently infected neurons differentially express latency-associated and ICP0 transcripts. *J Virol* 80(18):9310-9321.
24. Shen Y & Nemunaitis J (2006) Herpes simplex virus 1 (HSV-1) for cancer treatment. *Cancer Gene Ther* 13(11):975-992.
25. Campadelli-Fiume G, *et al.* (2007) The multipartite system that mediates entry of herpes simplex virus into the cell. *Rev Med Virol* 17(5):313-326.
26. Gianni T, *et al.* (2010) Herpes simplex virus glycoproteins H/L bind to cells independently of α V β 3 integrin and inhibit virus entry, and their constitutive expression restricts infection. *J Virol* 84(8):4013-4025.
27. Herold BC, WuDunn D, Soltys N, & Spear PG (1991) Glycoprotein C of herpes simplex virus type 1 plays a principal role in the adsorption of virus to cells and in infectivity. *J Virol* 65(3):1090-1098.
28. Spear PG (1992) Membrane fusion induced by herpes simplex virus. *Viral Fusion Mechanism*, ed Bentz J (CRC Press, Boca Raton), pp 201-232.
29. Krummenacher C, *et al.* (1998) Herpes simplex virus glycoprotein D can bind to poliovirus receptor-related protein 1 or herpesvirus entry mediator, two structurally unrelated mediators of virus entry. *J Virol* 72(9):7064-7074.
30. Campadelli-Fiume G & Menotti L (2007) Entry of alphaherpesviruses into the cell. *Human Herpesviruses Biology, Therapy, and Immunoprophylaxis*, eds Arvin A, Campadelli-Fiume G, Mocarski E, Moore PS, Roizman B, Whitley R, & Yamanishi K (Cambridge University Press, Cambridge, UK), pp 93-111.
31. Chowdary TK, *et al.* (2010) Crystal structure of the conserved herpesvirus fusion regulator complex gH-gL. *Nat Struct Mol Biol* 17(7):882-888.
32. Heldwein EE, *et al.* (2006) Crystal structure of glycoprotein B from herpes simplex virus 1. *Science* 313(5784):217-220.
33. Dolter KE, Goins WF, Levine M, & Glorioso JC (1992) Genetic analysis of type-specific antigenic determinants of herpes simplex virus glycoprotein C. *J Virol* 66(8):4864-4873.
34. Trybala E, *et al.* (1993) Herpes simplex virus type 1-induced hemagglutination: glycoprotein C mediates virus binding to erythrocyte surface heparan sulfate. *J Virol* 67(3):1278-1285.
35. Ruyechan WT, Morse LS, Knipe DM, & Roizman B (1979) Molecular genetics of herpes simplex virus. II. Mapping of the major viral glycoproteins and of the genetic loci specifying the social behavior of infected cells. *J Virol* 29(2):677-697.
36. Eisenberg RJ, *et al.* (1987) Complement component C3b binds directly to purified glycoprotein C of herpes simplex virus types 1 and 2. *Microb Pathog* 3(6):423-435.
37. Zhou G & Roizman B (2007) Separation of receptor binding and pro-fusogenic domains of glycoprotein D of herpes simplex virus 1 into distinct interacting proteins. *Proc Natl Acad Sci U S A* 104(10):4142-4146.
38. Stiles KM & Krummenacher C (2010) Glycoprotein D actively induces rapid internalization of two nectin-1 isoforms during herpes simplex virus entry. *Virology* 399(1):109-119.

39. Carfi A, *et al.* (2001) Herpes simplex virus glycoprotein D bound to the human receptor HveA. *Mol Cell* 8(1):169-179.
40. Krummenacher C, *et al.* (2005) Structure of unliganded HSV gD reveals a mechanism for receptor-mediated activation of virus entry. *Embo J* 24(23):4144-4153.
41. Di Giovine P, *et al.* (2011) Structure of herpes simplex virus glycoprotein d bound to the human receptor nectin-1. *PLoS Pathog* 7(9):e1002277.
42. Watson RJ, Weis JH, Salstrom JS, & Enquist LW (1982) Herpes simplex virus type-1 glycoprotein D gene: nucleotide sequence and expression in Escherichia coli. *Science* 218(4570):381-384.
43. Yoon M, Zago A, Shukla D, & Spear PG (2003) Mutations in the N termini of herpes simplex virus type 1 and 2 gDs alter functional interactions with the entry/fusion receptors HVEM, nectin-2, and 3-O-sulfated heparan sulfate but not with nectin-1. *J Virol* 77(17):9221-9231.
44. Menotti L, *et al.* (2009) Inhibition of human tumor growth in mice by an oncolytic herpes simplex virus designed to target solely HER-2-positive cells. *Proc Natl Acad Sci USA* 106(22):9039-9044.
45. Cocchi F, Menotti L, Di Ninni V, Lopez M, & Campadelli-Fiume G (2004) The herpes simplex virus JMP mutant enters receptor-negative J cells through a novel pathway independent of the known receptors nectin1, HveA, and nectin2. *J Virol* 78(9):4720-4729.
46. Ace CI, Dalrymple MA, Ramsay FH, Preston VG, & Preston CM (1988) Mutational analysis of the herpes simplex virus type 1 trans-inducing factor Vmw65. *J Gen Virol* 69 (Pt 10):2595-2605.
47. Bender FC, Whitbeck JC, Lou H, Cohen GH, & Eisenberg RJ (2005) Herpes simplex virus glycoprotein B binds to cell surfaces independently of heparan sulfate and blocks virus entry. *J Virol* 79(18):11588-11597.
48. Suenaga T, *et al.* (2010) Myelin-associated glycoprotein mediates membrane fusion and entry of neurotropic herpesviruses. *Proc Natl Acad Sci USA* 107:866-871.
49. Satoh T, *et al.* (2008) PILRalpha is a herpes simplex virus-1 entry coreceptor that associates with glycoprotein B. *Cell* 132(6):935-944.
50. Arii J, *et al.* (2010) Non-muscle myosin IIA is a functional entry receptor for herpes simplex virus-1. *Nature* 467(7317):859-862.
51. Beitia Ortiz de Zarate I, Kaelin K, & Rozenberg F (2004) Effects of mutations in the cytoplasmic domain of herpes simplex virus type 1 glycoprotein B on intracellular transport and infectivity. *J Virol* 78(3):1540-1551.
52. Bzik DJ, Fox BA, DeLuca NA, & Person S (1984) Nucleotide sequence of a region of the herpes simplex virus type 1 gB glycoprotein gene: mutations affecting rate of virus entry and cell fusion. *Virology* 137(1):185-190.
53. Roche S, Bressanelli S, Rey FA, & Gaudin Y (2006) Crystal structure of the low-pH form of the vesicular stomatitis virus glycoprotein G. *Science* 313(5784):187-191.
54. Rey FA (2006) Molecular gymnastics at the herpesvirus surface. *EMBO Rep* 7(10):1000-1005.
55. Highlander SL, Cai WH, Person S, Levine M, & Glorioso JC (1988) Monoclonal antibodies define a domain on herpes simplex virus glycoprotein B involved in virus penetration. *J Virol* 62(6):1881-1888.
56. Uchida H, *et al.* (2010) A double mutation in glycoprotein gB compensates for ineffective gD-dependent initiation of herpes simplex virus type 1 infection. *J Virol* 84(23):12200-12209.
57. Fuller AO, Santos RE, & Spear PG (1989) Neutralizing antibodies specific for glycoprotein H of herpes simplex virus permit viral attachment to cells but prevent penetration. *J Virol* 63(8):3435-3443.
58. Parry C, Bell S, Minson T, & Browne H (2005) Herpes simplex virus type 1 glycoprotein

- H binds to alphavbeta3 integrins. *J Gen Virol* 86(Pt 1):7-10.
59. Takai Y, Irie K, Shimizu K, Sakisaka T, & Ikeda W (2003) Nectins and nectin-like molecules: roles in cell adhesion, migration, and polarization. *Cancer Sci* 94(8):655-667.
 60. Takai Y, Miyoshi J, Ikeda W, & Ogita H (2008) Nectins and nectin-like molecules: roles in contact inhibition of cell movement and proliferation. *Nat Rev Mol Cell Biol* 9(8):603-615.
 61. Cocchi F, Menotti L, Mirandola P, Lopez M, & Campadelli-Fiume G (1998) The ectodomain of a novel member of the immunoglobulin subfamily related to the poliovirus receptor has the attributes of a bona fide receptor for herpes simplex virus types 1 and 2 in human cells. *J Virol* 72(12):9992-10002.
 62. Locksley RM, Killeen N, & Leonardo MJ (2001) The TNF and TNFR receptors superfamilies: Integrating mammalian biology. *Cell* 104:487-501.
 63. Montgomery RI, Warner MS, Lum BJ, & Spear PG (1996) Herpes simplex virus-1 entry into cells mediated by a novel member of the TNF/NGF receptor family. *Cell* 87(3):427-436.
 64. Harrop JA, *et al.* (1998) Antibodies to TR2 (herpesvirus entry mediator), a new member of the TNF receptor superfamily, block T cell proliferation, expression of activation markers, and production of cytokines. *J Immunol* 161(4):1786-1794.
 65. Connolly SA, *et al.* (2003) Structure-based mutagenesis of herpes simplex virus glycoprotein D defines three critical regions at the gD-HveA/HVEM binding interface. *J Virol* 77(14):8127-8140.
 66. Whitbeck JC, *et al.* (2001) Localization of the gD-binding region of the human herpes simplex virus receptor, HveA. *J Virol* 75(1):171-180.
 67. Geraghty RJ, Krummenacher C, Cohen GH, Eisenberg RJ, & Spear PG (1998) Entry of alphaherpesviruses mediated by poliovirus receptor-related protein 1 and poliovirus receptor. *Science* 280(5369):1618-1620.
 68. Shukla D, *et al.* (1999) A novel role for 3-O-sulfated heparan sulfate in herpes simplex virus 1 entry. *Cell* 99(1):13-22.
 69. Spear PG (2004) Herpes simplex virus: receptors and ligands for cell entry. *Cell Microbiol* 6(5):401-410.
 70. Guo ZS, Thorne SH, & Bartlett DL (2008) Oncolytic virotherapy: molecular targets in tumor-selective replication and carrier cell-mediated delivery of oncolytic viruses. *Biochim Biophys Acta* 1785(2):217-231.
 71. Dock G (1904) The influence of complicating diseases upon leukemia. *American Journal of the Medical Sciences*.
 72. Pelner L (1958) Effects of concurrent infections and their toxins on the course of leukemia. *Acta Medica Scandinavica Supp* 338:1-47.
 73. Campadelli-Fiume G, *et al.* (2011) Rethinking herpes simplex virus: the way to oncolytic agents. *Rev Med Virol* 21(4):213-226.
 74. Parker JN, *et al.* (2000) Engineered herpes simplex virus expressing IL-12 in the treatment of experimental murine brain tumors. *Proc Natl Acad Sci U S A* 97(5):2208-2213.
 75. Cattaneo R, Miest T, Shashkova EV, & Barry MA (2008) Reprogrammed viruses as cancer therapeutics: targeted, armed and shielded. *Nat Rev Microbiol* 6(7):529-540.
 76. Schneider U, Bullough F, Vongpunsawad S, Russell SJ, & Cattaneo R (2000) Recombinant measles viruses efficiently entering cells through targeted receptors. *J Virol* 74(21):9928-9936.
 77. Allen C, *et al.* (2006) Retargeted oncolytic measles strains entering via the EGFRvIII receptor maintain significant antitumor activity against gliomas with increased tumor specificity. *Cancer Res* 66(24):11840-11850.
 78. Frentzen A, *et al.* (2009) Anti-VEGF single-chain antibody GLAF-1 encoded by

- oncolytic vaccinia virus significantly enhances antitumor therapy. *Proc Natl Acad Sci U S A* 106(31):12915-12920.
79. Menotti L, Cerretani A, & Campadelli-Fiume G (2006) A herpes simplex virus recombinant that exhibits a single-chain antibody to HER2/neu enters cells through the mammary tumor receptor, independently of the gD receptors. *J Virol* 80(11):5531-5539.
 80. Menotti L, Cerretani A, Hengel H, & Campadelli-Fiume G (2008) Construction of a fully retargeted herpes simplex virus 1 recombinant capable of entering cells solely via human epidermal growth factor receptor 2. *J Virol* 20(October):10153-10161.
 81. Muhlebach MD (2010) Liver cancer protease activity profiles support therapeutic options with matrix metalloproteinase - Activatable Oncolytic measles virus. *Cancer Res* 70:7620-7629.
 82. Springfield C, *et al.* (2006) Oncolytic efficacy and enhanced safety of measles virus activated by tumor-secreted matrix metalloproteinases. *Cancer Res* 66(15):7694-7700.
 83. Matsubara S, *et al.* (2001) A conditional replication-competent adenoviral vector, Ad-OC-E1a, to cotarget prostate cancer and bone stroma in an experimental model of androgen-independent prostate cancer bone metastasis. *Cancer Res* 61(16):6012-6019.
 84. Parker JN, Bauer DF, Cody JJ, & Markert JM (2009) Oncolytic viral therapy of malignant glioma. *Neurotherapeutics* 6(3):558-569.
 85. Bischoff JR, *et al.* (1996) An adenovirus mutant that replicates selectively in p53-deficient human tumor cells. *Science* 274(5286):373-376.
 86. Reid T, *et al.* (2002) Hepatic arterial infusion of a replication-selective oncolytic adenovirus (dl1520): phase II viral, immunologic, and clinical endpoints. *Cancer Res* 62(21):6070-6079.
 87. Jiang H, Gomez-Manzano C, Lang FF, Alemany R, & Fueyo J (2009) Oncolytic adenovirus: preclinical and clinical studies in patients with human malignant gliomas. *Curr Gene Ther* 9(5):422-427.
 88. Breitbach CJ, *et al.* (2011) Intravenous delivery of a multi-mechanistic cancer-targeted oncolytic poxvirus in humans. *Nature* 477(7362):99-102.
 89. Qiao J, *et al.* (2008) Cyclophosphamide facilitates antitumor efficacy against subcutaneous tumors following intravenous delivery of reovirus. *Clin Cancer Res* 14(1):259-269.
 90. Willmon C, *et al.* (2011) Vesicular stomatitis virus-induced immune suppressor cells generate antagonism between intratumoral oncolytic virus and cyclophosphamide. *Mol Ther* 19(1):140-149.
 91. Eto Y, Yoshioka Y, Mukai Y, Okada N, & Nakagawa S (2008) Development of PEGylated adenovirus vector with targeting ligand. *Int J Pharm* 354(1-2):3-8.
 92. Fujiwara S, *et al.* (2011) Carrier cell-based delivery of replication-competent HSV-1 mutants enhances antitumor effect for ovarian cancer. *Cancer Gene Ther* 18(2):77-86.
 93. Markert JM, *et al.* (2000) Conditionally replicating herpes simplex virus mutant, G207 for the treatment of malignant glioma: results of a phase I trial. *Gene Ther* 7(10):867-874.
 94. Zhou G & Roizman B (2005) Characterization of a recombinant herpes simplex virus 1 designed to enter cells via the IL13Ralpha2 receptor of malignant glioma cells. *J Virol* 79(9):5272-5277.
 95. Shenk T (2001) *Adenoviridae: The viruses and their replication.*
 96. Martuza RL, Malick A, Markert JM, Ruffner KL, & Coen DM (1991) Experimental therapy of human glioma by means of a genetically engineered virus mutant. *Science* 252(5007):854-856.
 97. Varghese S & Rabkin SD (2002) Oncolytic herpes simplex virus vectors for cancer virotherapy. *Cancer Gene Ther* 9(12):967-978.
 98. Chou J, Kern ER, Whitley RJ, & Roizman B (1990) Mapping of herpes simplex virus-1 neurovirulence to gamma 134.5, a gene nonessential for growth in culture. *Science*

- 250(4985):1262-1266.
99. MacLean AR, ul-Fareed M, Robertson L, Harland J, & Brown SM (1991) Herpes simplex virus type 1 deletion variants 1714 and 1716 pinpoint neurovirulence-related sequences in Glasgow strain 17+ between immediate early gene 1 and the 'a' sequence. *J Gen Virol* 72 (Pt 3):631-639.
 100. Mace AT, Ganly I, Soutar DS, & Brown SM (2008) Potential for efficacy of the oncolytic Herpes simplex virus 1716 in patients with oral squamous cell carcinoma. *Head Neck* 30(8):1045-1051.
 101. Fong Y, *et al.* (2009) A herpes oncolytic virus can be delivered via the vasculature to produce biologic changes in human colorectal cancer. *Mol Ther* 17(2):389-394.
 102. Geevarghese SK, *et al.* (2010) Phase I/II study of oncolytic herpes simplex virus NV1020 in patients with extensively pretreated refractory colorectal cancer metastatic to the liver. *Hum Gene Ther* 21(9):1119-1128.
 103. Passer BJ, Wu CL, Wu S, Rabkin SD, & Martuza RL (2009) Analysis of genetically engineered oncolytic herpes simplex viruses in human prostate cancer organotypic cultures. *Gene Ther* 16(12):1477-1482.
 104. Todo T (2008) "Armed" oncolytic herpes simplex viruses for brain tumor therapy. *Cell Adh Migr* 2(3):208-213.
 105. Markert JM, *et al.* (2009) Phase Ib trial of mutant herpes simplex virus G207 inoculated pre-and post-tumor resection for recurrent GBM. *Mol Ther* 17(1):199-207.
 106. Todo T, Martuza RL, Rabkin SD, & Johnson PA (2001) Oncolytic herpes simplex virus vector with enhanced MHC class I presentation and tumor cell killing. *Proc Natl Acad Sci U S A* 98(11):6396-6401.
 107. Kanai R, *et al.* (2012) Oncolytic virus-mediated manipulation of DNA damage responses: synergy with chemotherapy in killing glioblastoma stem cells. *J Natl Cancer Inst* 104(1):42-55.
 108. Wang J, Hu P, Zeng M, Rabkin SD, & Liu R (2012) Oncolytic herpes simplex virus treatment of metastatic breast cancer. *Int J Oncol* 40(3):757-763.
 109. Veerapong J, *et al.* (2007) Systemic delivery of (gamma1)34.5-deleted herpes simplex virus-1 selectively targets and treats distant human xenograft tumors that express high MEK activity. *Cancer Res* 67(17):8301-8306.
 110. Shah AC, Parker JN, Shimamura M, & Cassady KA (2009) Spontaneous and Engineered Compensatory HSV Mutants that Counteract the Host Antiviral PKR Response. *Viruses* 1(3):510-522.
 111. Andreansky S, *et al.* (1998) Treatment of intracranial gliomas in immunocompetent mice using herpes simplex viruses that express murine interleukins. *Gene Ther* 5(1):121-130.
 112. Wong RJ, *et al.* (2001) Cytokine gene transfer enhances herpes oncolytic therapy in murine squamous cell carcinoma. *Hum Gene Ther* 12(3):253-265.
 113. Varghese S, *et al.* (2007) Systemic therapy of spontaneous prostate cancer in transgenic mice with oncolytic herpes simplex viruses. *Cancer Res* 67(19):9371-9379.
 114. Varghese S, *et al.* (2006) Enhanced therapeutic efficacy of IL-12, but not GM-CSF, expressing oncolytic herpes simplex virus for transgenic mouse derived prostate cancers. *Cancer Gene Ther* 13(3):253-265.
 115. Bennett JJ, *et al.* (2001) Interleukin 12 secretion enhances antitumor efficacy of oncolytic herpes simplex viral therapy for colorectal cancer. *Ann Surg* 233(6):819-826.
 116. Disis ML, *et al.* (1996) Granulocyte-macrophage colony-stimulating factor: an effective adjuvant for protein and peptide-based vaccines. *Blood* 88(1):202-210.
 117. Liu BL, *et al.* (2003) ICP34.5 deleted herpes simplex virus with enhanced oncolytic, immune stimulating, and anti-tumour properties. *Gene Ther* 10(4):292-303.
 118. Senzer NN, *et al.* (2009) Phase II clinical trial with a second generation, GM-CSF encoding, oncolytic herpesvirus in unresectable metastatic melanoma. *J Clin Oncol*

- (*ASCO Meeting Abstract*) 27(15s):9035.
119. Zhou G, Ye GJ, Debinski W, & Roizman B (2002) Engineered herpes simplex virus 1 is dependent on IL13Ralpha2 receptor for cell entry and independent of glycoprotein D receptor interaction. *Proc. Natl. Acad. Sci. U.S.A.* 99(23):15124-15129.
 120. Laquerre S, Anderson DB, Stolz DB, & Glorioso JC (1998) Recombinant herpes simplex virus type 1 engineered for targeted binding to erythropoietin receptor-bearing cells. *J Virol* 72(12):9683-9697.
 121. Manservigi R, Argnani R, & Marconi P (2010) HSV Recombinant Vectors for Gene Therapy. *Open Virol J* 4:123-156.
 122. Zhou G & Roizman B (2006) Construction and properties of a herpes simplex virus 1 designed to enter cells solely via the IL-13alpha2 receptor. *Proc Natl Acad Sci U S A* 103(14):5508-5513.
 123. Menotti L, Cerretani A, & Campadelli-Fiume G (2006) A HSV recombinant exhibiting a single chain antibody to HER2/neu enters cells through the mammary tumor receptor, independently of the gD receptors. *The 31st International Herpesvirus Workshop*.
 124. Harrow S, *et al.* (2004) HSV1716 injection into the brain adjacent to tumour following surgical resection of high-grade glioma: safety data and long-term survival. *Gene Ther* 11(22):1648-1658.
 125. MacKie RM, Stewart B, & Brown SM (2001) Intralesional injection of herpes simplex virus 1716 in metastatic melanoma. *Lancet* 357(9255):525-526.
 126. Watanabe I, *et al.* (2008) Effects of tumor selective replication-competent herpes viruses in combination with gemcitabine on pancreatic cancer. *Cancer Chemother Pharmacol* 61(5):875-882.
 127. Kemeny N, *et al.* (2006) Phase I, open-label, dose-escalating study of a genetically engineered herpes simplex virus, NV1020, in subjects with metastatic colorectal carcinoma to the liver. *Hum Gene Ther* 17(12):1214-1224.
 128. Karrasch M, *et al.* (2009) Treatment of recurrent malignant glioma with G207, a genetically engineered herpes simplex virus-1, followed by irradiation: Phase I results. *J Clin Oncol (ASCO Meeting Abstract)* 27(15s):2042.
 129. Markert JM, *et al.* (2012) Preclinical Evaluation of a Genetically Engineered Herpes Simplex Virus Expressing Il-12. *J Virol*.
 130. Hu JC, *et al.* (2006) A phase I study of OncoVEXGM-CSF, a second-generation oncolytic herpes simplex virus expressing granulocyte macrophage colony-stimulating factor. *Clin Cancer Res* 12(22):6737-6747.
 131. Harrington KJ, *et al.* (2010) Phase I/II study of oncolytic HSV GM-CSF in combination with radiotherapy and cisplatin in untreated stage III/IV squamous cell cancer of the head and neck. *Clin Cancer Res* 16(15):4005-4015.
 132. Kaufman HL & Bines SD (2010) OPTIM trial: a Phase III trial of an oncolytic herpes virus encoding GM-CSF for unresectable stage III or IV melanoma. *Future Oncol* 6(6):941-949.
 133. Citri A & Yarden Y (2006) EGF-ERBB signalling: towards the systems level. *Nat Rev Mol Cell Biol* 7(7):505-516.
 134. Gutierrez C & Schiff R (2011) HER2: biology, detection, and clinical implications. *Arch Pathol Lab Med* 135(1):55-62.
 135. Callahan R & Hurvitz S (2011) Human epidermal growth factor receptor-2-positive breast cancer: Current management of early, advanced, and recurrent disease. *Curr Opin Obstet Gynecol* 23(1):37-43.
 136. Hynes NE & Lane HA (2005) ERBB receptors and cancer: the complexity of targeted inhibitors. *Nat Rev Cancer* 5(5):341-354.
 137. Baselga J & Swain SM (2009) Novel anticancer targets: revisiting ERBB2 and discovering ERBB3. *Nat Rev Cancer* 9(7):463-475.

138. Blackwell KL, *et al.* (2010) Randomized study of Lapatinib alone or in combination with trastuzumab in women with ErbB2-positive, trastuzumab-refractory metastatic breast cancer. *J Clin Oncol* 28(7):1124-1130.
139. Cao Y, *et al.* (2012) Single-chain antibody-based immunotoxins targeting Her2/neu: design optimization and impact of affinity on antitumor efficacy and off-target toxicity. *Mol Cancer Ther* 11(1):143-153.
140. Ghosh A & Heston WD (2004) Tumor target prostate specific membrane antigen (PSMA) and its regulation in prostate cancer. *J Cell Biochem* 91(3):528-539.
141. Rajasekaran AK, Anilkumar G, & Christiansen JJ (2005) Is prostate-specific membrane antigen a multifunctional protein? *Am J Physiol Cell Physiol* 288(5):C975-981.
142. Gong MC, Chang SS, Sadelain M, Bander NH, & Heston WD (1999) Prostate-specific membrane antigen (PSMA)-specific monoclonal antibodies in the treatment of prostate and other cancers. *Cancer Metastasis Rev* 18(4):483-490.
143. Wang X, *et al.* (2007) Targeted treatment of prostate cancer. *J Cell Biochem* 102(3):571-579.
144. Wernicke AG, *et al.* (2011) Prostate-specific membrane antigen as a potential novel vascular target for treatment of glioblastoma multiforme. *Arch Pathol Lab Med* 135(11):1486-1489.
145. Israeli RS, Powell CT, Corr JG, Fair WR, & Heston WD (1994) Expression of the prostate-specific membrane antigen. *Cancer Res* 54(7):1807-1811.
146. Fracasso G, *et al.* (2002) Anti-tumor effects of toxins targeted to the prostate specific membrane antigen. *Prostate* 53(1):9-23.
147. Bander NH, *et al.* (2003) Targeting metastatic prostate cancer with radiolabeled monoclonal antibody J591 to the extracellular domain of prostate specific membrane antigen. *J Urol* 170(5):1717-1721.
148. Msaouel P, *et al.* (2009) Engineered measles virus as a novel oncolytic therapy against prostate cancer. *Prostate* 69(1):82-91.
149. Kuroda K, *et al.* (2010) Saporin toxin-conjugated monoclonal antibody targeting prostate-specific membrane antigen has potent anticancer activity. *Prostate* 70(12):1286-1294.
150. Bander NH, *et al.* (2005) Phase I trial of 177lutetium-labeled J591, a monoclonal antibody to prostate-specific membrane antigen, in patients with androgen-independent prostate cancer. *J Clin Oncol* 23(21):4591-4601.
151. Barwe SP, *et al.* (2007) Preferential association of prostate cancer cells expressing prostate specific membrane antigen to bone marrow matrix. *Int J Oncol* 30(4):899-904.
152. Hatanpaa KJ, Burma S, Zhao D, & Habib AA (2010) Epidermal growth factor receptor in glioma: signal transduction, neuropathology, imaging, and radioresistance. *Neoplasia* 12(9):675-684.
153. Sugawa N, Ekstrand AJ, James CD, & Collins VP (1990) Identical splicing of aberrant epidermal growth factor receptor transcripts from amplified rearranged genes in human glioblastomas. *Proc Natl Acad Sci U S A* 87(21):8602-8606.
154. Grandi P, *et al.* (2010) Targeting HSV-1 virions for specific binding to epidermal growth factor receptor-vIII-bearing tumor cells. *Cancer Gene Ther* 17(9):655-663.
155. Gan HK, Kaye AH, & Luwor RB (2009) The EGFRvIII variant in glioblastoma multiforme. *J Clin Neurosci* 16(6):748-754.
156. Lollini PL, Menotti L, De Giovanni C, Campadelli-Fiume G, & Nanni P (2009) Oncolytic herpes virus retargeted to HER-2. *Cell Cycle* 8(18):2859-2860.
157. Bacchetti S & Graham FL (1977) Transfer of the gene for thymidine kinase to thymidine kinase-deficient human cells by purified herpes simplex viral DNA. *Proc Natl Acad Sci U S A* 74(4):1590-1594.
158. Warming S, Costantino N, Court DL, Jenkins NA, & Copeland NG (2005) Simple and

- highly efficient BAC recombineering using galK selection. *Nucleic Acids Res* 33(4):e36.
159. Lorimer IA & Lavictoire SJ (2000) Targeting retrovirus to cancer cells expressing a mutant EGF receptor by insertion of a single chain antibody variable domain in the envelope glycoprotein receptor binding lobe. *J Immunol Methods* 237(1-2):147-157.
 160. Gong MC, *et al.* (1999) Cancer patient T cells genetically targeted to prostate-specific membrane antigen specifically lyse prostate cancer cells and release cytokines in response to prostate-specific membrane antigen. *Neoplasia* 1(2):123-127.
 161. Nakamura T, *et al.* (2005) Rescue and propagation of fully retargeted oncolytic measles viruses. *Nat Biotechnol* 23(2):209-214.
 162. Tanaka M, Kagawa H, Yamanashi Y, Sata T, & Kawaguchi Y (2003) Construction of an excisable bacterial artificial chromosome containing a full-length infectious clone of herpes simplex virus type 1: viruses reconstituted from the clone exhibit wild-type properties *in vitro* and *in vivo*. *J Virol* 77(2):1382-1391.
 163. Borst EM, Hahn G, Koszinowski UH, & Messerle M (1999) Cloning of the human cytomegalovirus (HCMV) genome as an infectious bacterial artificial chromosome in *Escherichia coli*: a new approach for construction of HCMV mutants. *J Virol* 73(10):8320-8329.
 164. Sidhu SS, *et al.* (2004) Phage-displayed antibody libraries of synthetic heavy chain complementarity determining regions. *J Mol Biol* 338(2):299-310.
 165. Menotti L, *et al.* (2000) The murine homolog of human-Nectin1 δ serves as a species non-specific mediator for entry of human and animal α herpesviruses in a pathway independent of a detectable binding to gD. *Proc Natl Acad Sci U S A* 97(9):4867-4872.
 166. Zhou G, Galvan V, Campadelli-Fiume G, & Roizman B (2000) Glycoprotein D or J delivered in trans blocks apoptosis in SK-N-SH cells induced by a herpes simplex virus 1 mutant lacking intact genes expressing both glycoproteins. *J Virol* 74(24):11782-11791.
 167. Brunetti CR, *et al.* (1995) Role of mannose-6-phosphate receptors in herpes simplex virus entry into cells and cell-to-cell transmission. *J Virol* 69(6):3517-3528.
 168. Humphrey W, Dalke A, & Schulten K (1996) VMD: visual molecular dynamics. *J Mol Graph* 14(1):33-38, 27-38.
 169. Liu X, Abdelrahim M, Abudayyeh A, Lei P, & Safe S (2009) The nonsteroidal anti-inflammatory drug tolfenamic acid inhibits BT474 and SKBR3 breast cancer cell and tumor growth by repressing erbB2 expression. *Mol Cancer Ther* 8(5):1207-1217.
 170. Calzolari F, *et al.* (2008) Tumor progression and oncogene addiction in a PDGF-B-induced model of gliomagenesis. *Neoplasia* 10(12):1373-1382, following 1382.
 171. Appolloni I, *et al.* (2009) PDGF-B induces a homogeneous class of oligodendrogliomas from embryonic neural progenitors. *Int J Cancer* 124(10):2251-2259.
 172. Lampson LA (2010) Monoclonal antibodies in neuro-oncology: Getting past the blood brain barrier. *mAbs* 3(2):153-160.
 173. Gambini E, *et al.* (2012) Replication-competent Herpes Simplex Virus Retargeted to HER2 as Therapy for High-grade Glioma. *Mol Ther*.
 174. Terrile M, *et al.* (2010) PDGF-B-driven gliomagenesis can occur in the absence of the proteoglycan NG2. *BMC Cancer* 10:550.
 175. Baccala A, Sercia L, Li J, Heston W, & Zhou M (2007) Expression of prostate-specific membrane antigen in tumor-associated neovasculature of renal neoplasms. *Urology* 70(2):385-390.
 176. Liu C, Hasegawa K, Russell SJ, Sadelain M, & Peng KW (2009) Prostate-specific membrane antigen retargeted measles virotherapy for the treatment of prostate cancer. *Prostate* 69(10):1128-1141.
 177. Gao Y, Whitaker-Dowling P, Griffin JA, Barmada MA, & Bergman I (2008) Recombinant vesicular stomatitis virus targeted to Her2/neu combined with anti-CTLA4 antibody eliminates implanted mammary tumors. *Cancer Gene Ther*.

178. Paraskevakou G, *et al.* (2007) Epidermal growth factor receptor (EGFR)-retargeted measles virus strains effectively target EGFR- or EGFRvIII expressing gliomas. *Mol Ther* 15(4):677-686.
179. Lambright ES, *et al.* (2000) Effect of preexisting anti-herpes immunity on the efficacy of herpes simplex viral therapy in a murine intraperitoneal tumor model. *Mol Ther* 2(4):387-393.